

2023/06/27

Underground Science - Day 3

Jodi Cooley

Executive Director | SNOLAB

Professor of Physics | Queen's University

Adjunct Research Professor | SMU

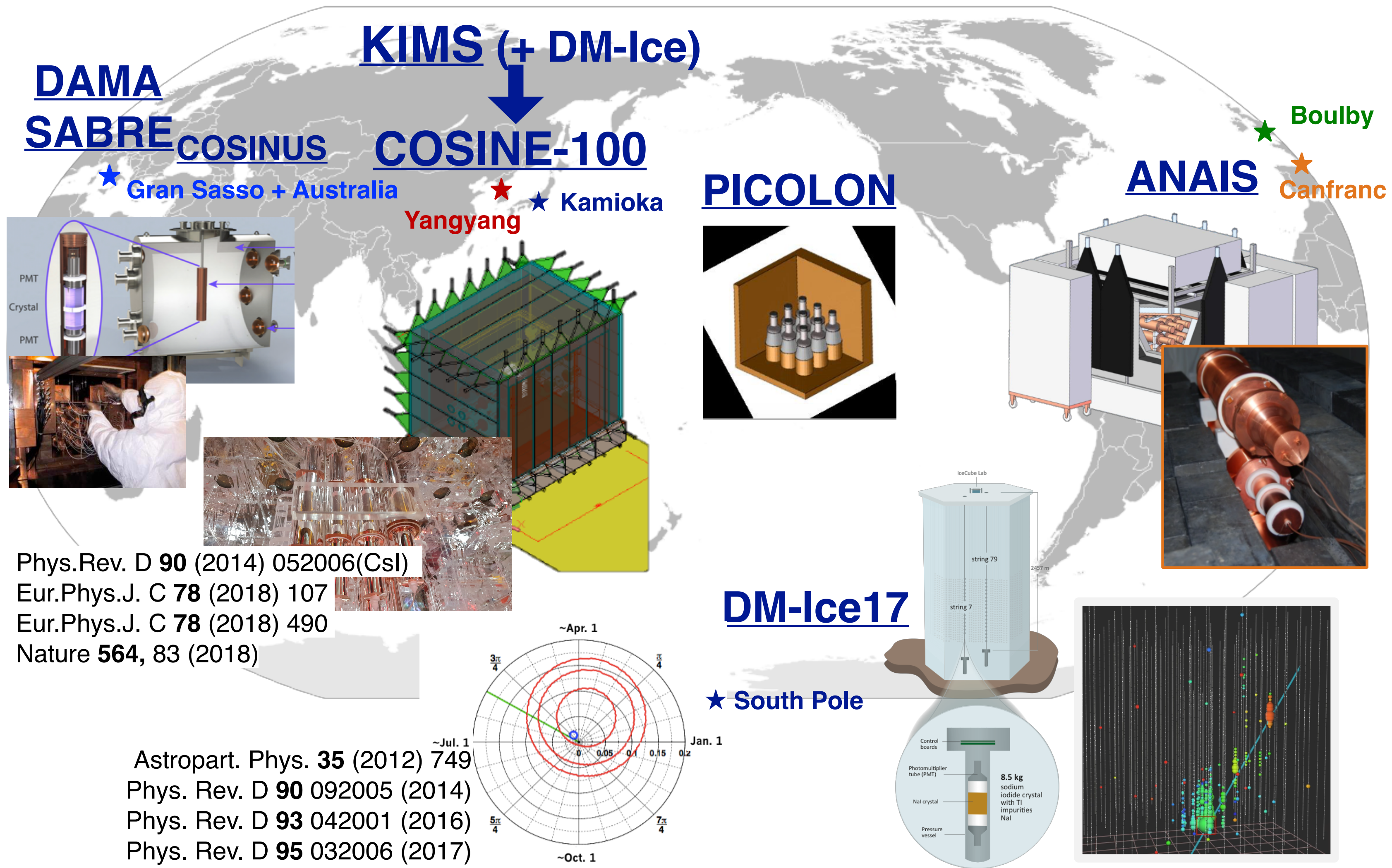


Last Time:



- Discussed the different backgrounds that come into play in underground physics and the tools and techniques used to understand, mitigate and characterize those backgrounds.
- Discussed the DAMA/LIBRA excess, possible interpretations and their pitfalls.

Worldwide Effort to Test DAMA/Libra



COSINE-100

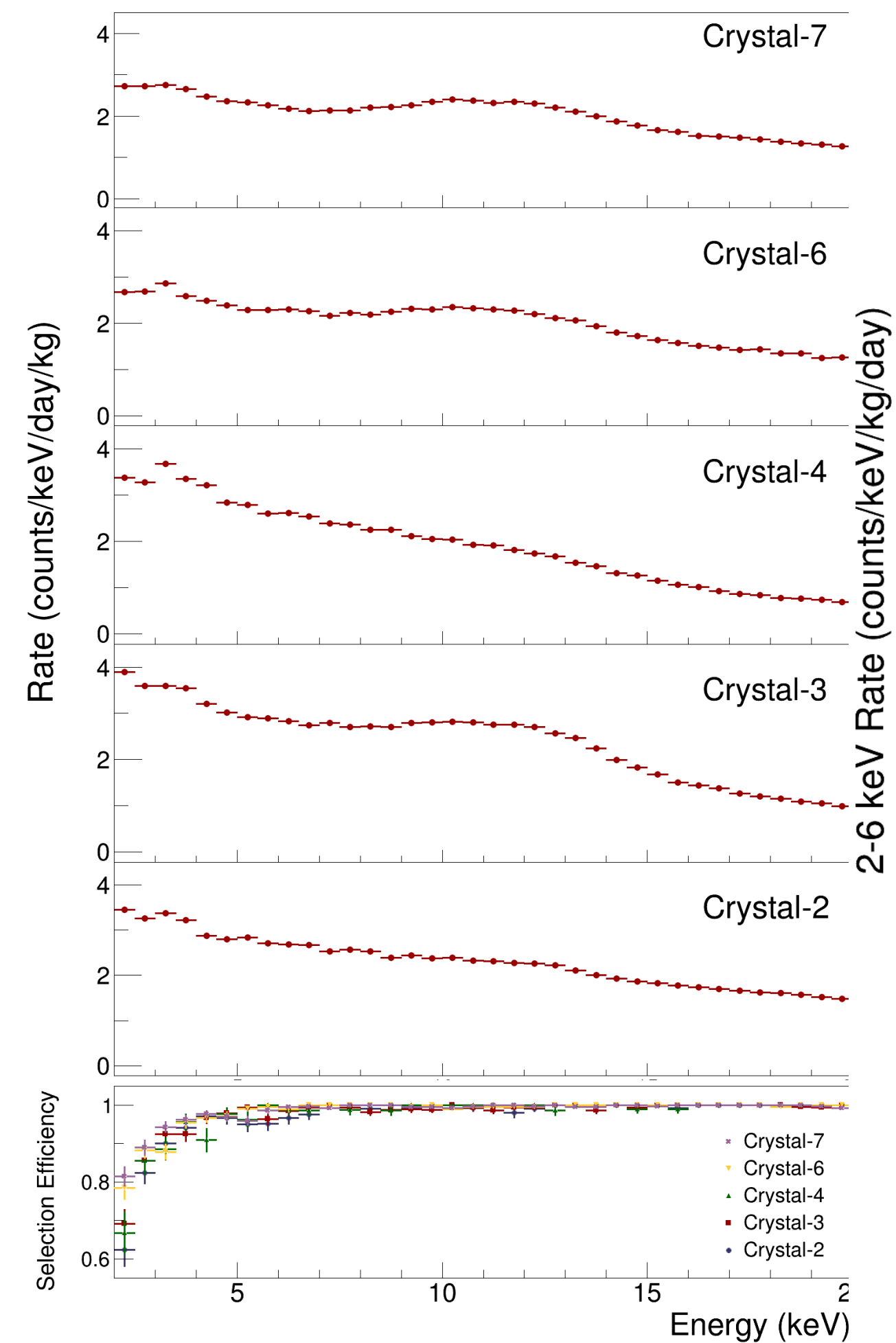


- Located in Yangyang Laboratory, South Korea
- 8 copper encapsulated NaI(Tl) crystals
 - 106 kg total
- Two 3-inch PMTs per crystal
 - trigger at ~ 0.2 p.e. threshold
- Calibration via sources through tubes
- Total Background: 2 - 4 x DAMA/LIBRA avg. (2.7 cpd/kg/keV on average in 2 - 6 keV ROI)
- U/Th/K below DAMA, ^{210}Po very close
- High light yield

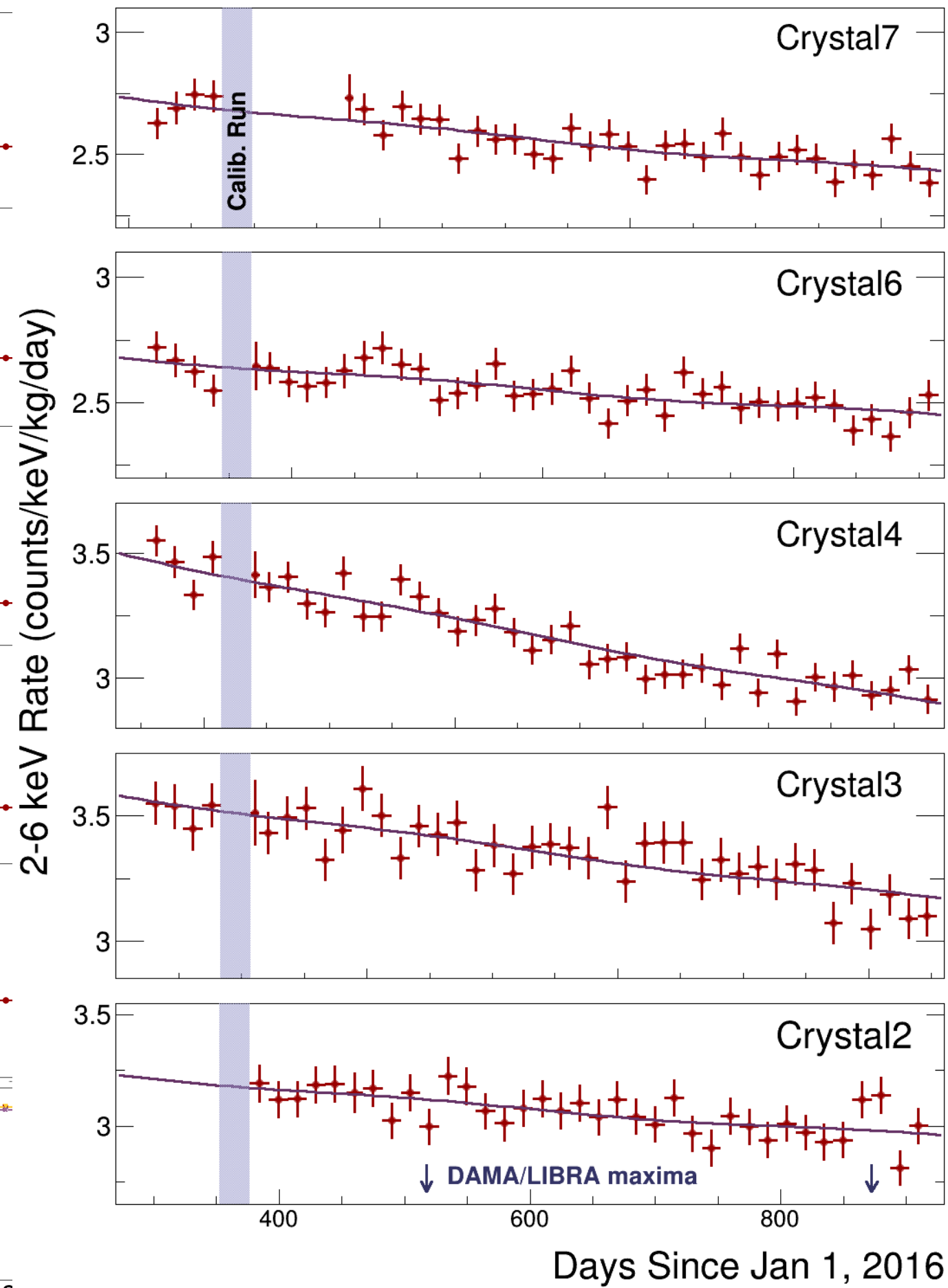
| Crystal | Mass (kg) | Powder | Alpha rate (mBq/kg) | ^{40}K (ppb) | ^{238}U (ppt) | ^{232}Th (ppt) | Light yield (p.e./keV) |
|-----------|-----------|-----------|---------------------|-----------------------|------------------------|-------------------------|------------------------|
| Crystal 1 | 8.3 | AS-B | 3.20 ± 0.08 | 43.4 ± 13.7 | < 0.02 | 1.31 ± 0.35 | 14.88 ± 1.49 |
| Crystal 2 | 9.2 | AS-C | 2.06 ± 0.06 | 82.7 ± 12.7 | < 0.12 | < 0.63 | 14.61 ± 1.45 |
| Crystal 3 | 9.2 | AS-WS II | 0.76 ± 0.02 | 41.1 ± 6.8 | < 0.04 | 0.44 ± 0.19 | 15.50 ± 1.64 |
| Crystal 4 | 18.0 | AS-WS II | 0.74 ± 0.02 | 39.5 ± 8.3 | | < 0.3 | 14.86 ± 1.50 |
| Crystal 5 | 18.0 | AS-C | 2.06 ± 0.05 | 86.8 ± 10.8 | | 2.35 ± 0.31 | 7.33 ± 0.70 |
| Crystal 6 | 12.5 | AS-WS III | 1.52 ± 0.04 | 12.2 ± 4.5 | < 0.018 | 0.56 ± 0.19 | 14.56 ± 1.45 |
| Crystal 7 | 12.5 | AS-WS III | 1.54 ± 0.04 | 18.8 ± 5.3 | | < 0.6 | 13.97 ± 1.41 |
| Crystal 8 | 18.3 | AS-C | 2.05 ± 0.05 | 56.15 ± 8.1 | | < 1.4 | 3.50 ± 0.33 |
| DAMA | | | < 0.5 | < 20 | 0.7 - 10 | 0.5 - 7.5 | 5.5 - 7.5 |

COSINE-100 Modulation Search

- 1.7 years (97.7 kg x years) exposure
- Global fit using cosmogenic and sinusoidal components simultaneously for crystals
- Crystal 1, 5, and 8 excluded in this analysis due to low light yield and excessive PMT noise
- Sideband events decrease exponentially, agrees with known cosmogenic components

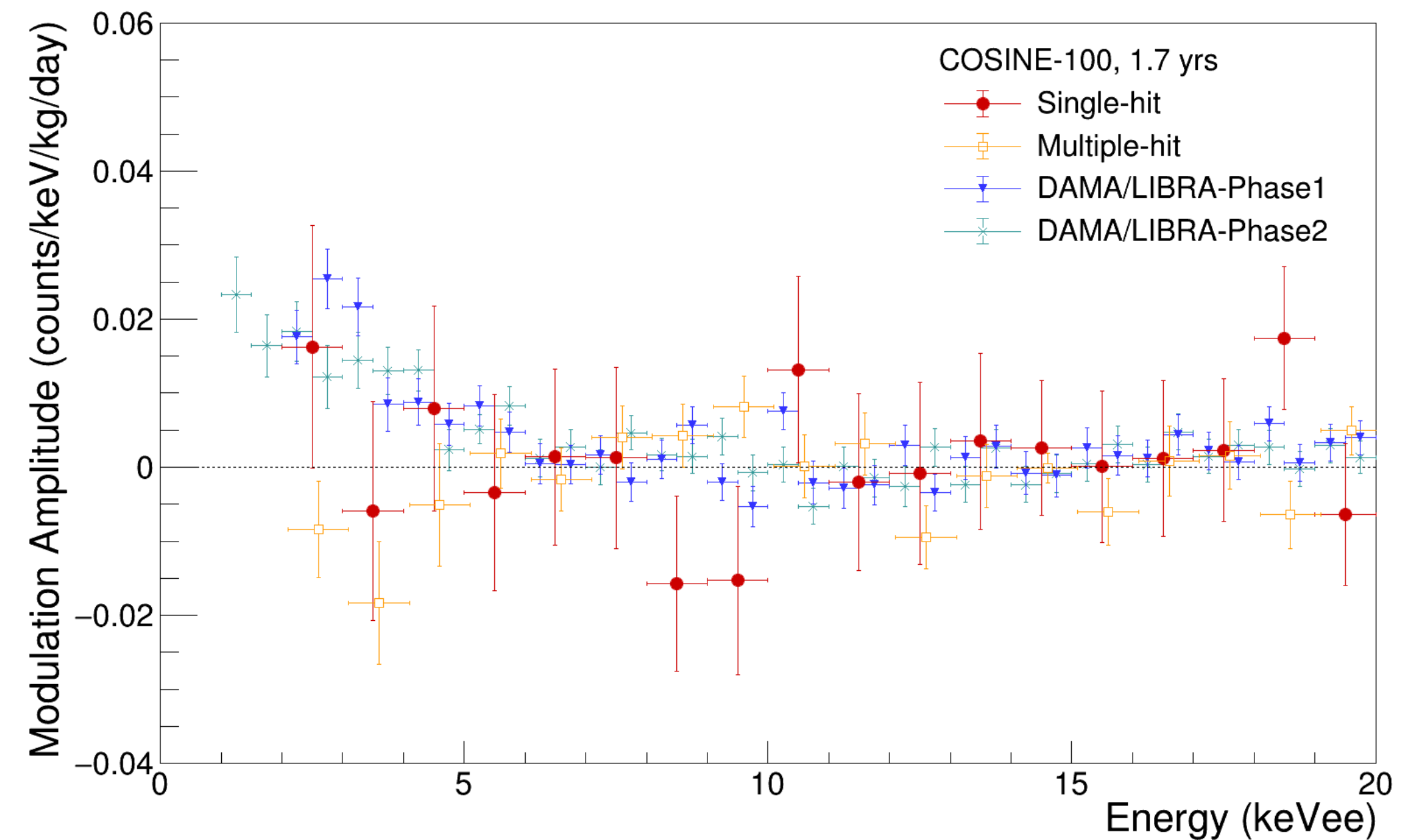
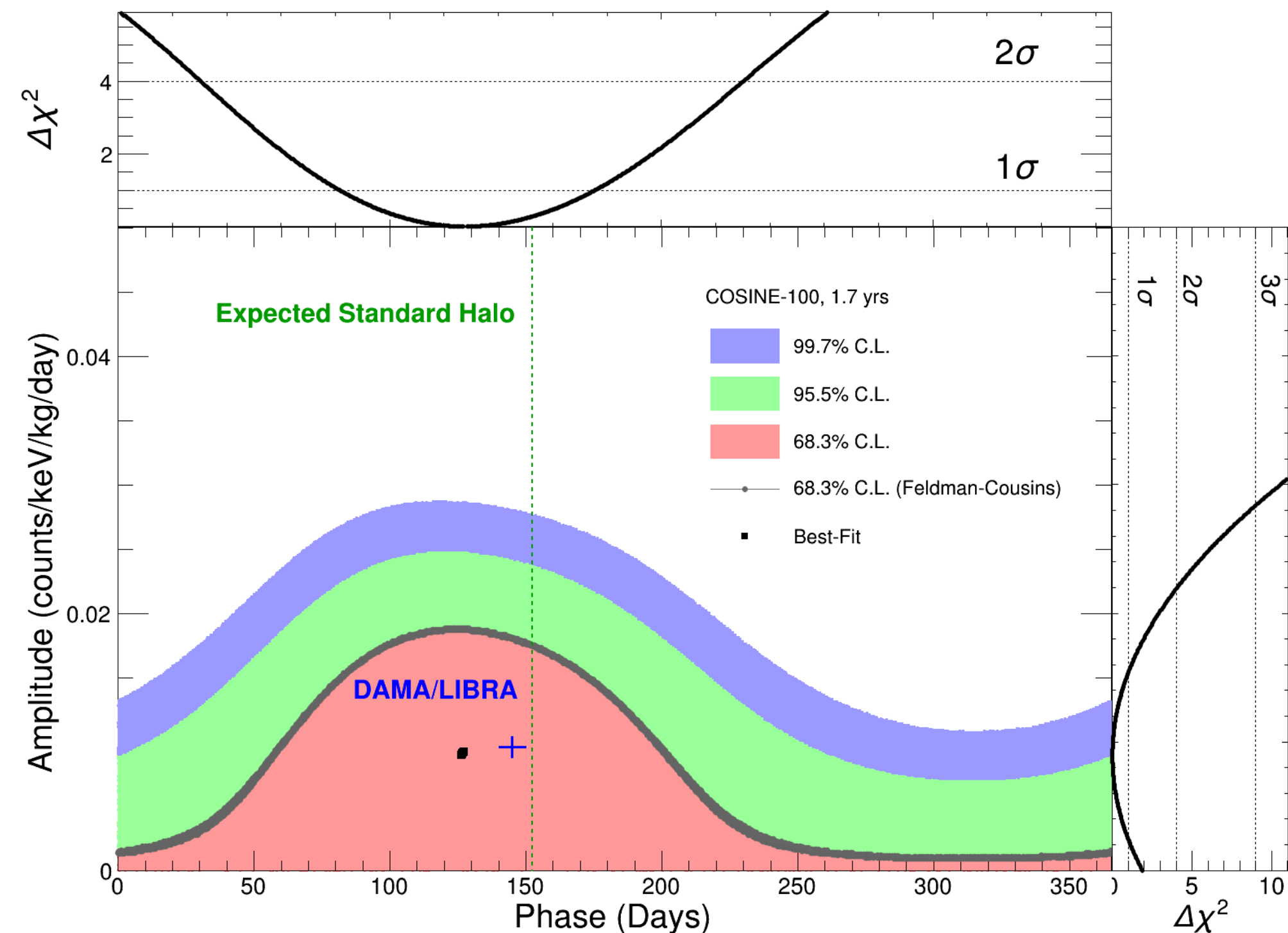


Energy spectra between 2 - 20 keV and signal efficiency using ^{60}Co source



Rate vs time for the 2-6 keV ROI

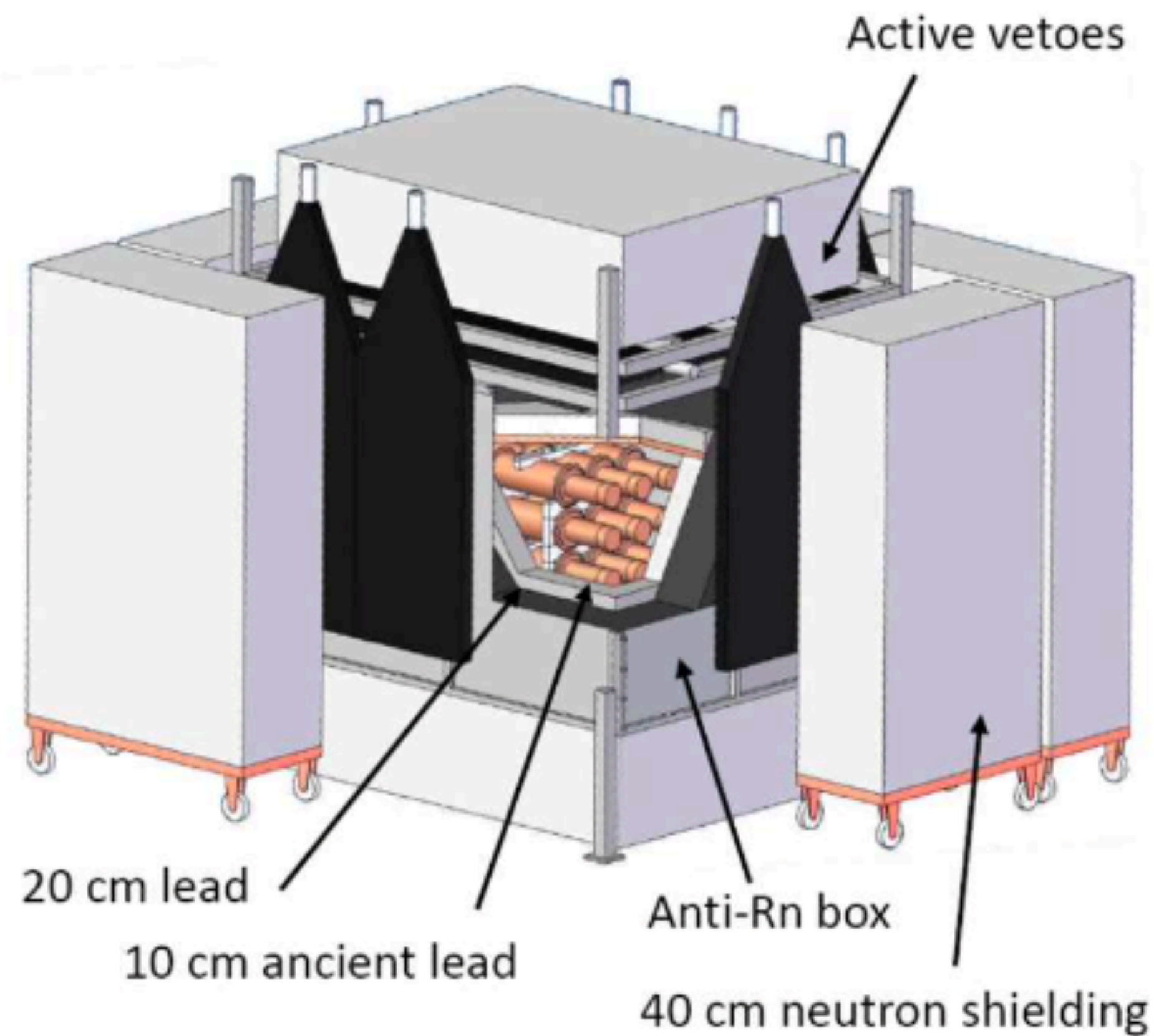
COSINE-100 Results



- Best fit amplitude and phase for 2 - 6 keV
 - 0.0092 ± 0.0067 cpd/kg/keV
 - 127.2 ± 45.9 days
- The result is consistent with both the null hypothesis and DAMA/LIBRA's best fit value
- Expect 3σ coverage of DAMA region within 5 years of data exposure
- Future analyses will utilize at least a 1 keV threshold and improved event selection to reduce the exposure required for 3σ coverage.

| Configuration | χ^2 | <i>d.o.f.</i> | p-value | Amplitude (counts/keV/kg/day) | Phase (Days) |
|----------------------------|----------|---------------|---------|-------------------------------|------------------|
| COSINE-100 | 175.3 | 174 | 0.457 | 0.0092 ± 0.0067 | 127.2 ± 45.9 |
| DAMA/LIBRA (Phase1+Phase2) | - | - | - | 0.0096 ± 0.0008 | 145 ± 5 |
| COSINE-100 | 175.6 | 175 | 0.473 | 0.0083 ± 0.0068 | 152.5 (fixed) |
| COSINE-100 (Without LS) | 194.7 | 175 | 0.143 | 0.0024 ± 0.0071 | 152.5 (fixed) |
| ANAIS-112 | 48.0 | 53 | 0.67 | -0.0044 ± 0.0058 | 152.5 (fixed) |
| DAMA/LIBRA (Phase1+Phase2) | 71.8 | 101 | 0.988 | 0.0095 ± 0.0008 | 152.5 (fixed) |

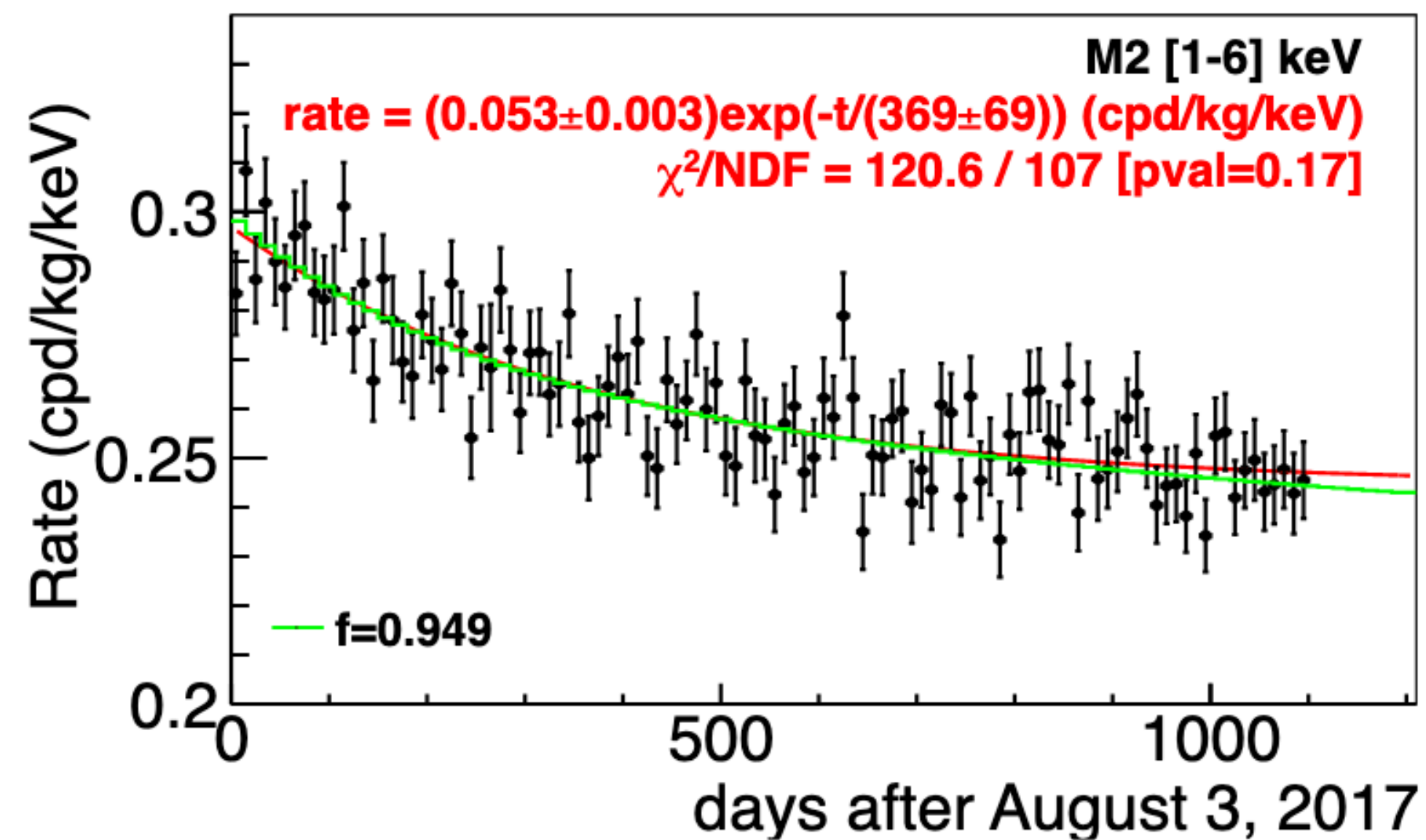
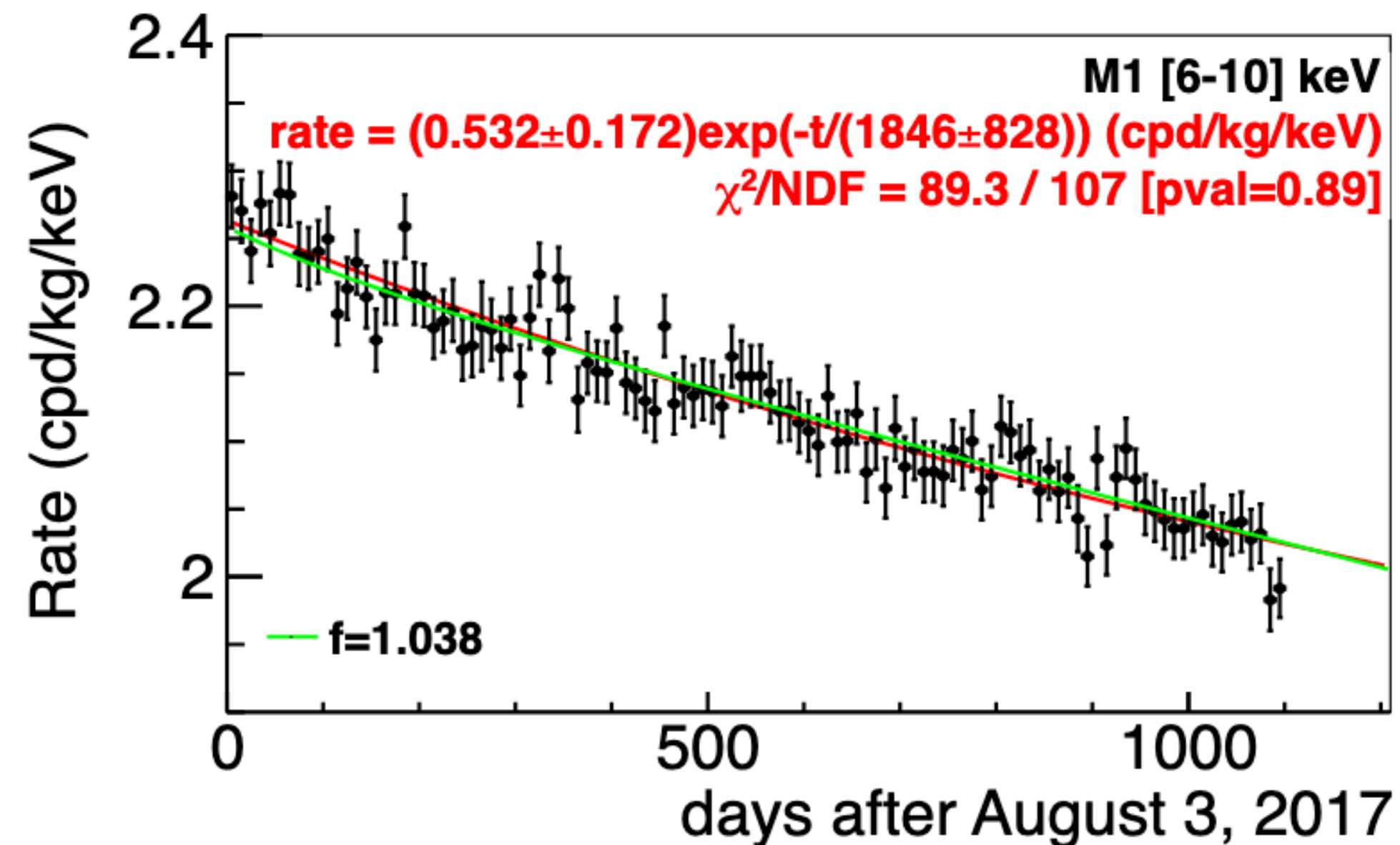
ANAIS 112



- Located in Hall B at the Canfranc Laboratory (2450 mwe).
- NaI(Tl) crystals (12.5 kg each) grown from ultra pure NaI powder and housed in OFE copper.
- 112.5 kg of NaI(Tl), distributed in a 3×3 array of modules.
- Mylar window for low energy calibration
- Two Hamamatsu R12669SEL2 photomultipliers
- Low background, high quantum efficiency.



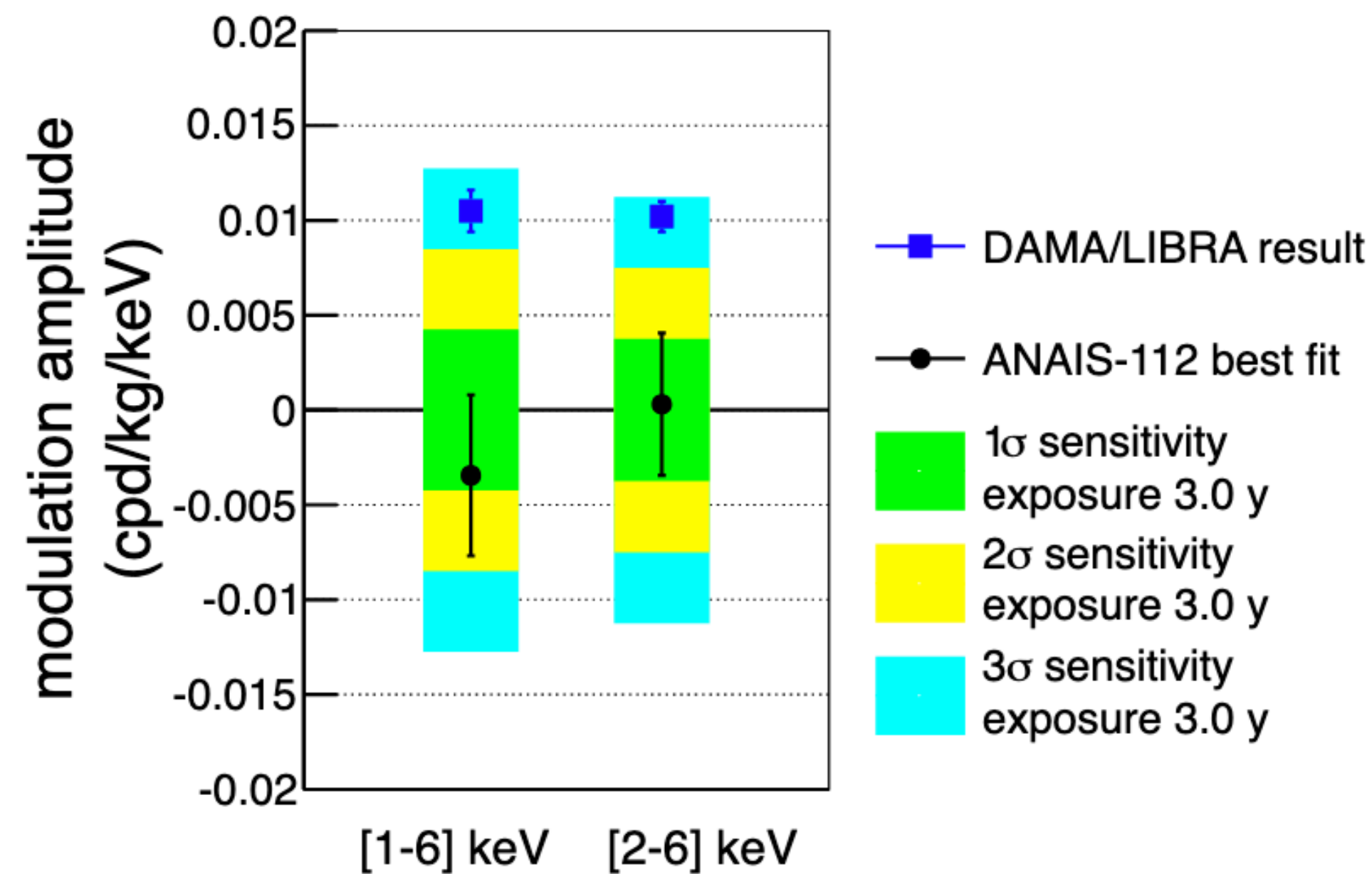
ANAIS 112: 3-Year Background Models



- Three independent background modeling procedures:
 - Exponentially decaying background
 - Probability distribution function derived from background model
 - Probability distribution function for every detector to account for possible systematic effects related with the different backgrounds and efficiencies of the different modules.

ANAIS 112: 3 Year Results

| Energy region | Model | χ^2 /NDF null hyp | nuisance params | S_m cpd/kg/keV | p-value mod | p-value null |
|---------------|-------|---------------------------|--------------------|----------------------|-------------|--------------|
| [1-6] keV | 1 | 132 / 107 | 3 | -0.0045 ± 0.0044 | 0.051 | 0.051 |
| | 2 | 143.1 / 108 | 2 | -0.0036 ± 0.0044 | 0.012 | 0.013 |
| | 3 | 1076 / 972 | 18 | -0.0034 ± 0.0042 | 0.011 | 0.011 |
| [2-6] keV | 1 | 115.7 / 107 | 3 | -0.0008 ± 0.0039 | 0.25 | 0.27 |
| | 2 | 120.8 / 108 | 2 | 0.0004 ± 0.0039 | 0.17 | 0.19 |
| | 3 | 1018 / 972 | 18 | 0.0003 ± 0.0037 | 0.14 | 0.15 |



- Data support the absence of modulation in both energy region and three background models.
- Best fits are incompatible with DAMA/LIBRA at 3.3 σ in the [1-6] keV region and 2.6 σ in the [2-6]keV region

Liquid Noble Experiments

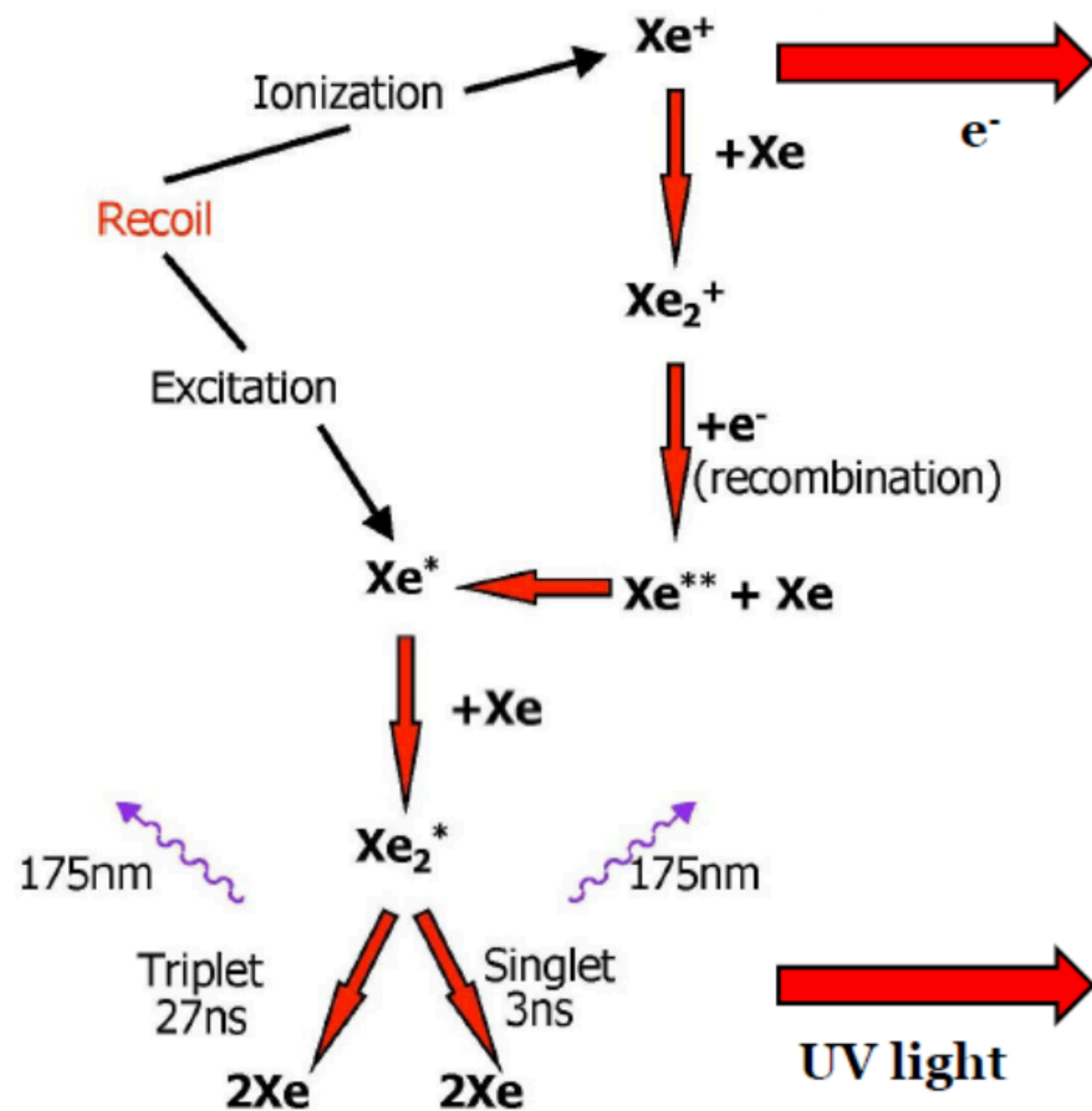
Liquid Noble Properties

| Property (unit) | Xe | Ar | Ne |
|---|-------|------|-------|
| Atomic Number | 54 | 18 | 10 |
| Mean relative atomic mass | 131.3 | 40.0 | 20.2 |
| Boiling Point T_b (K) | 165.0 | 87.3 | 27.1 |
| Melting Point T_m (K) | 161.4 | 83.8 | 24.6 |
| Liquid density at T_b (g cm^{-3}) | 2.94 | 1.40 | 1.21 |
| Volume fraction in Earth's atmosphere (ppm) | 0.09 | 9340 | 18.2 |
| Scintillation light wavelength (nm) | 175 | 128 | 78 |
| Triplet lifetime (ns) | 27 | 1600 | 15000 |
| Singlet lifetime (ns) | 3 | 7 | <18 |
| Electron mobility ($\text{cm}^2 \text{V}^{-1} \text{s}^{-1}$) | 2200 | 400 | low |
| Scintillation yield (photons/keV) | 42 | 40 | 30 |

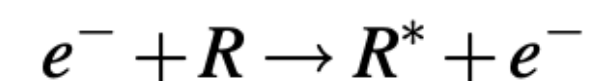
| Material | Ar | Kr | Xe |
|-------------------------------|-----------------------------|-----------------------------|-----------------------------|
| Gas | | | |
| Ionization potential I (eV) | 15.75 | 14.00 | 12.13 |
| W values (eV) | 26.4 ^a | 24.2 ^a | 22.0 ^a |
| Liquid | | | |
| Gap energy (eV) | 14.3 | 11.7 | 9.28 |
| W value (eV) | 23.6 \pm 0.3 ^b | 18.4 \pm 0.3 ^c | 15.6 \pm 0.3 ^d |

- Three different noble liquids have been considered for dark matter detection over the past few decades.
- Properties of the noble liquids determine many practical aspects of the detectors. For example, Xe has a high density and a large target mass (favorable) but it is not very abundant in the atmosphere (more expensive).
- The energy loss of an incident particle in noble liquids is shared between excitation, ionization and sub-excitation electrons liberated in the ionization process
- The average energy loss in ionization is slightly larger than the ionization potential or the gap energy, because it includes multiple ionization processes
- As a result, the ratio of the W -value (average energy required to produce an electron-ion pair) to the ionization potential or gap energy equals 1.6 - 1.7

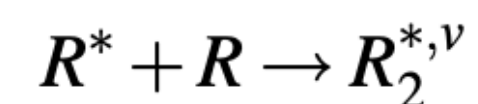
Liquid Noble Signal Production



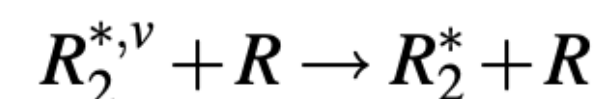
➤ Energy is transferred to a particle by excitation, ionization or heat (atomic motion).



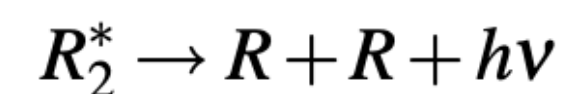
impact excitation



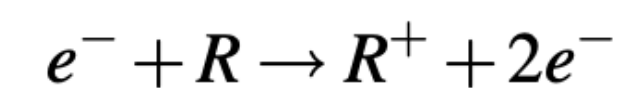
excimer formation



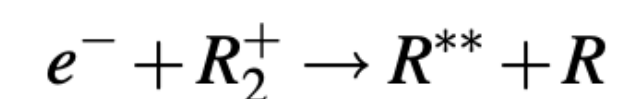
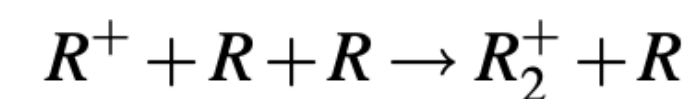
relaxation



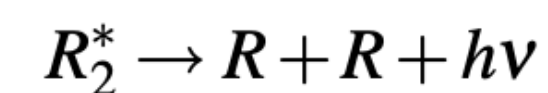
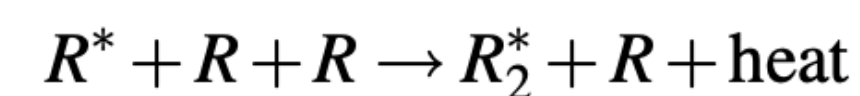
VUV emission



ionization

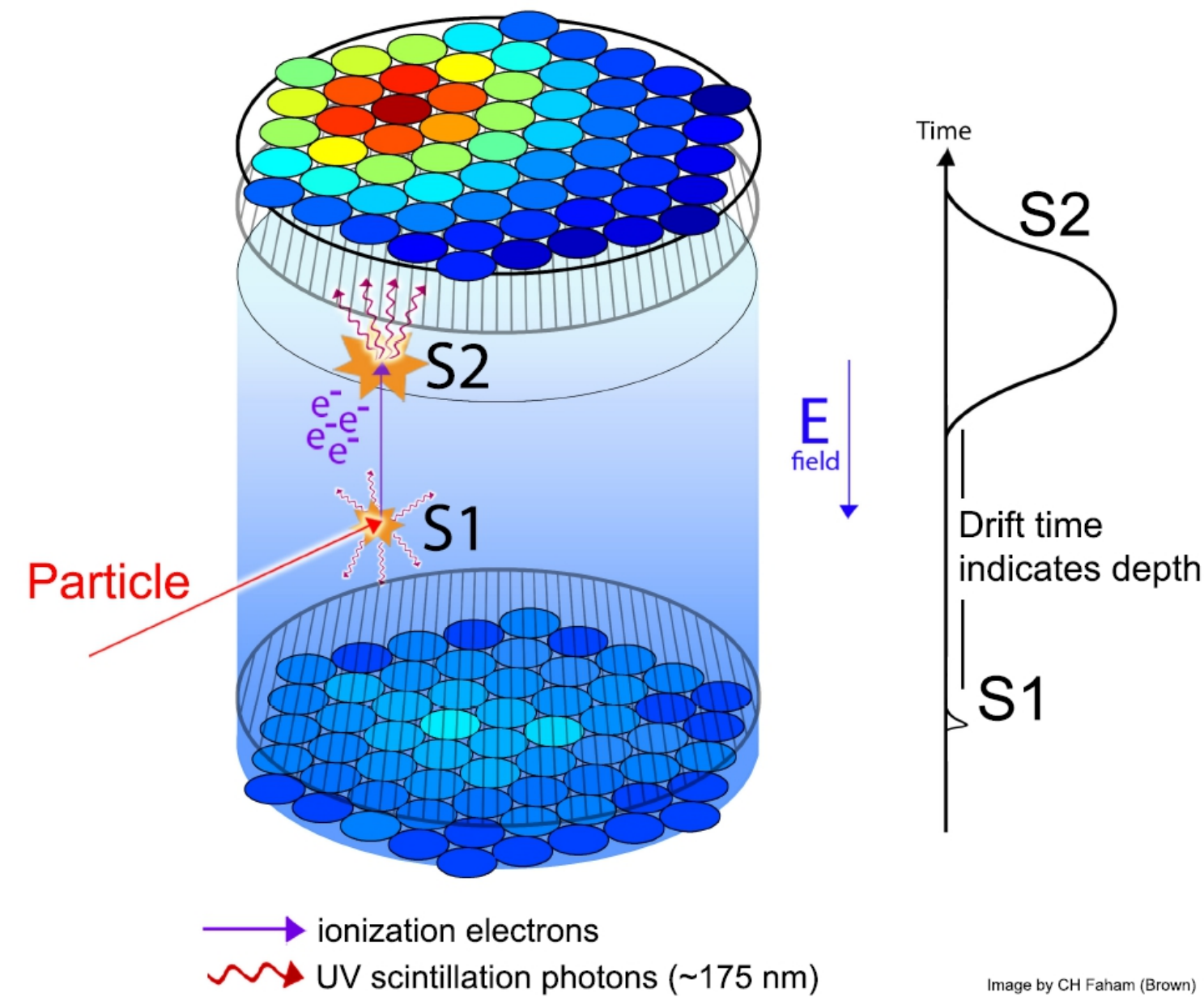


recombination



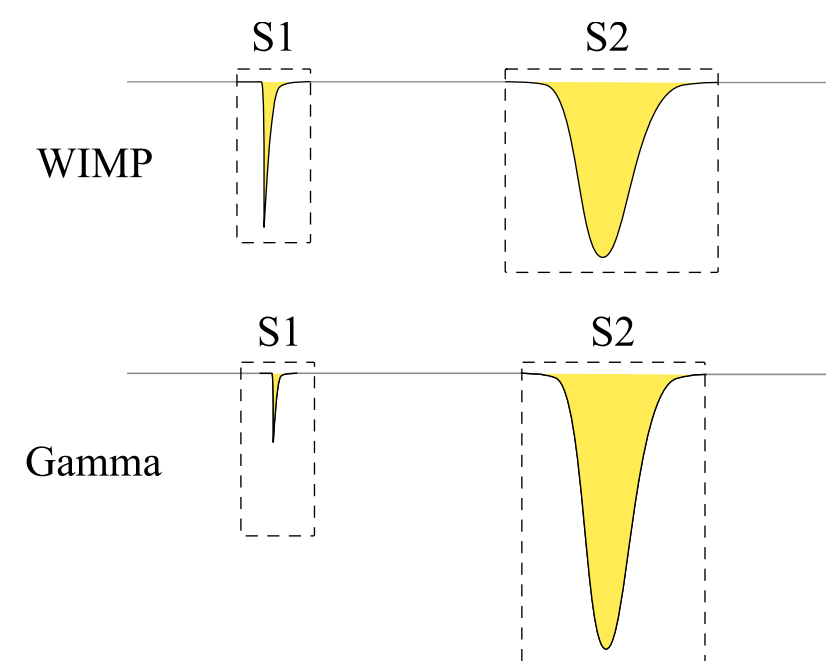
VUV emission

Liquid Noble Detectors

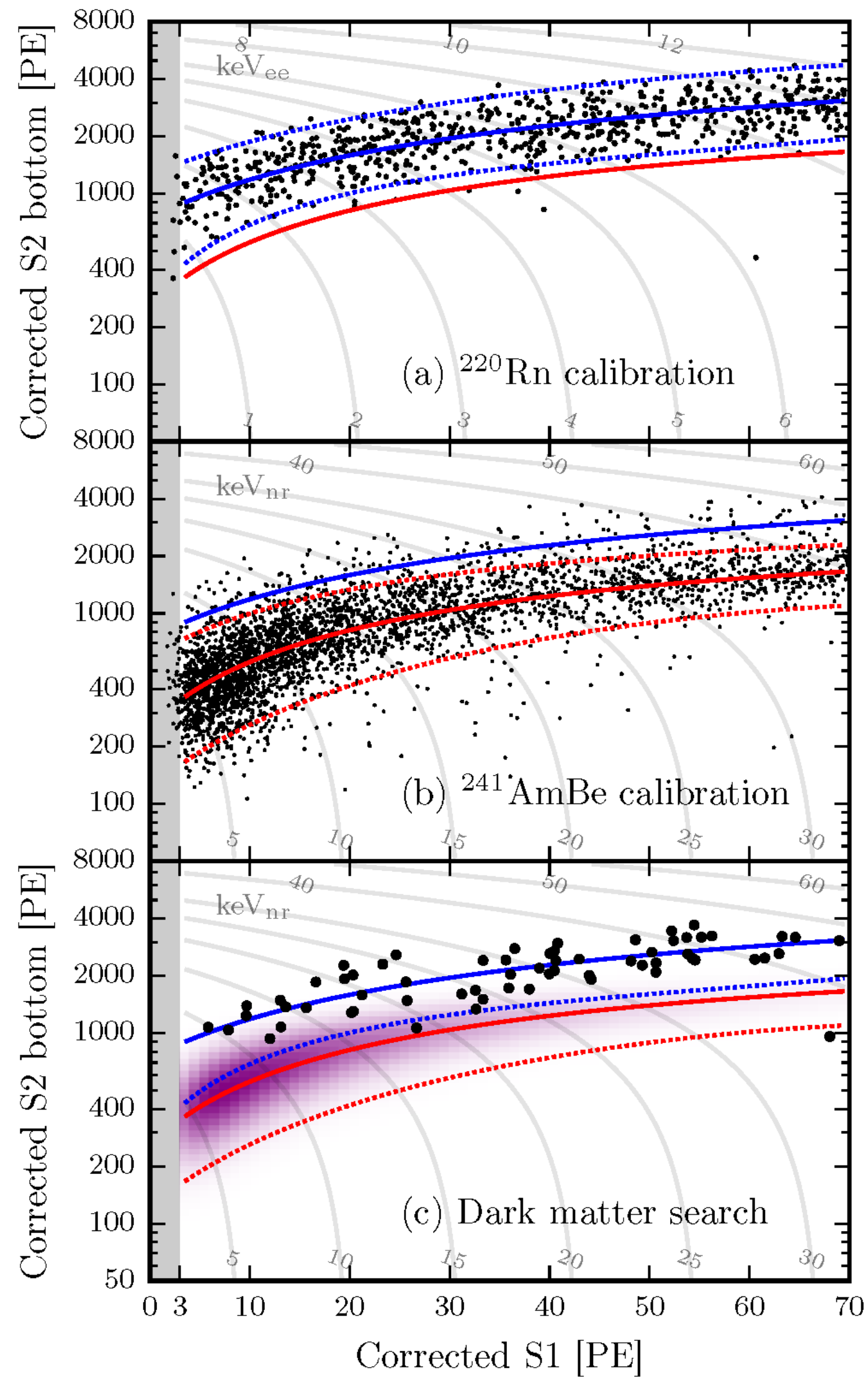


Dual Phase TPCs (XENON, LUX/LZ, Darkside PandaX, etc)

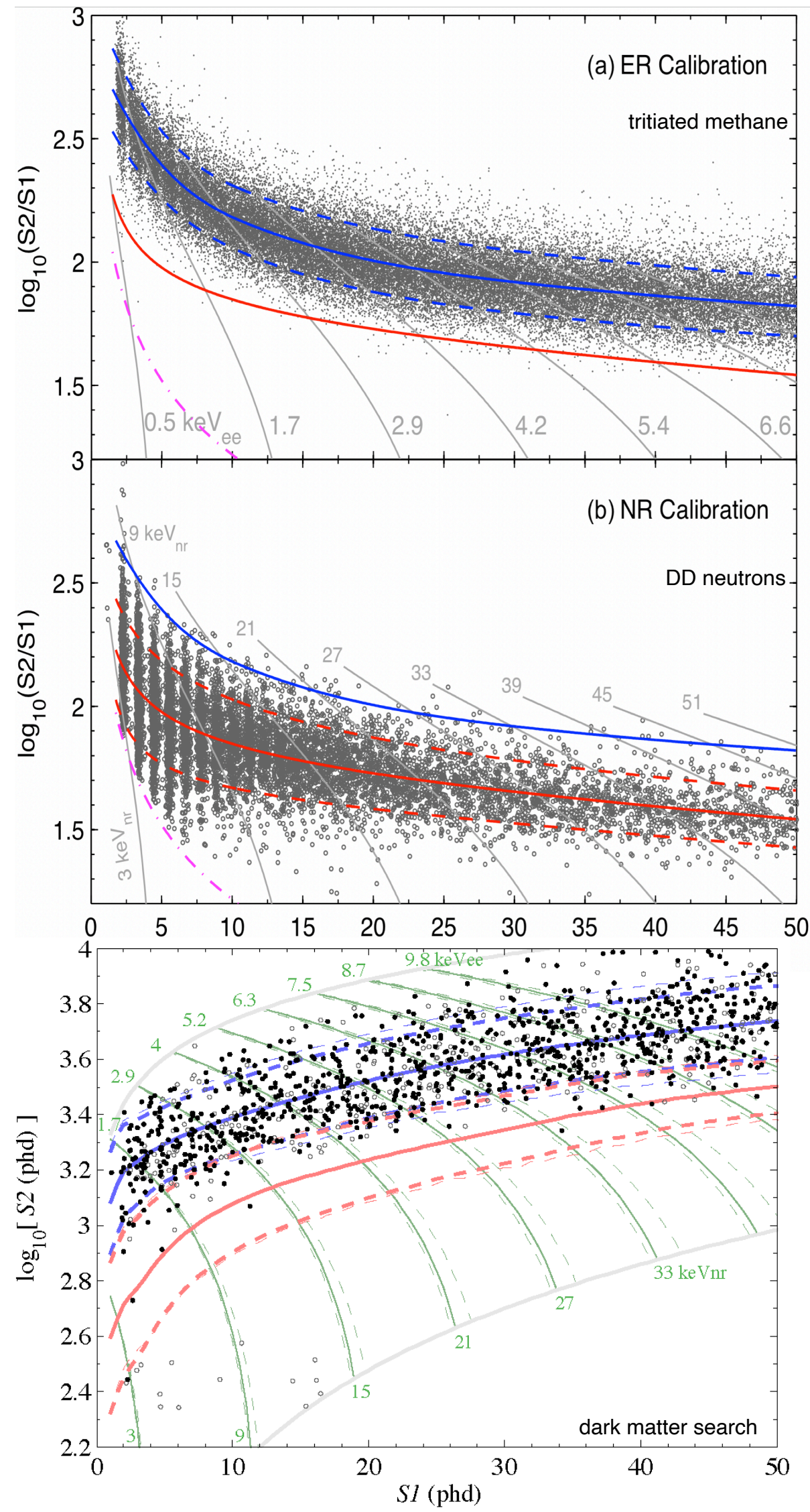
- Interactions in the liquid produce excitation and ionization.
- Excitation leads to scintillation light emission
- Ionization electrons are drifted with an applied electric field into the gas phase (S1).
- In the gas phase, electrons are further accelerated producing proportional scintillation (S2).
- PMTs on the bottom and top of the chamber record scintillation signals.
- Distribution of S2 give xy coordinates, drift time gives z coordinates
- Ratio of S2/S1 discriminates electron and nuclear recoils



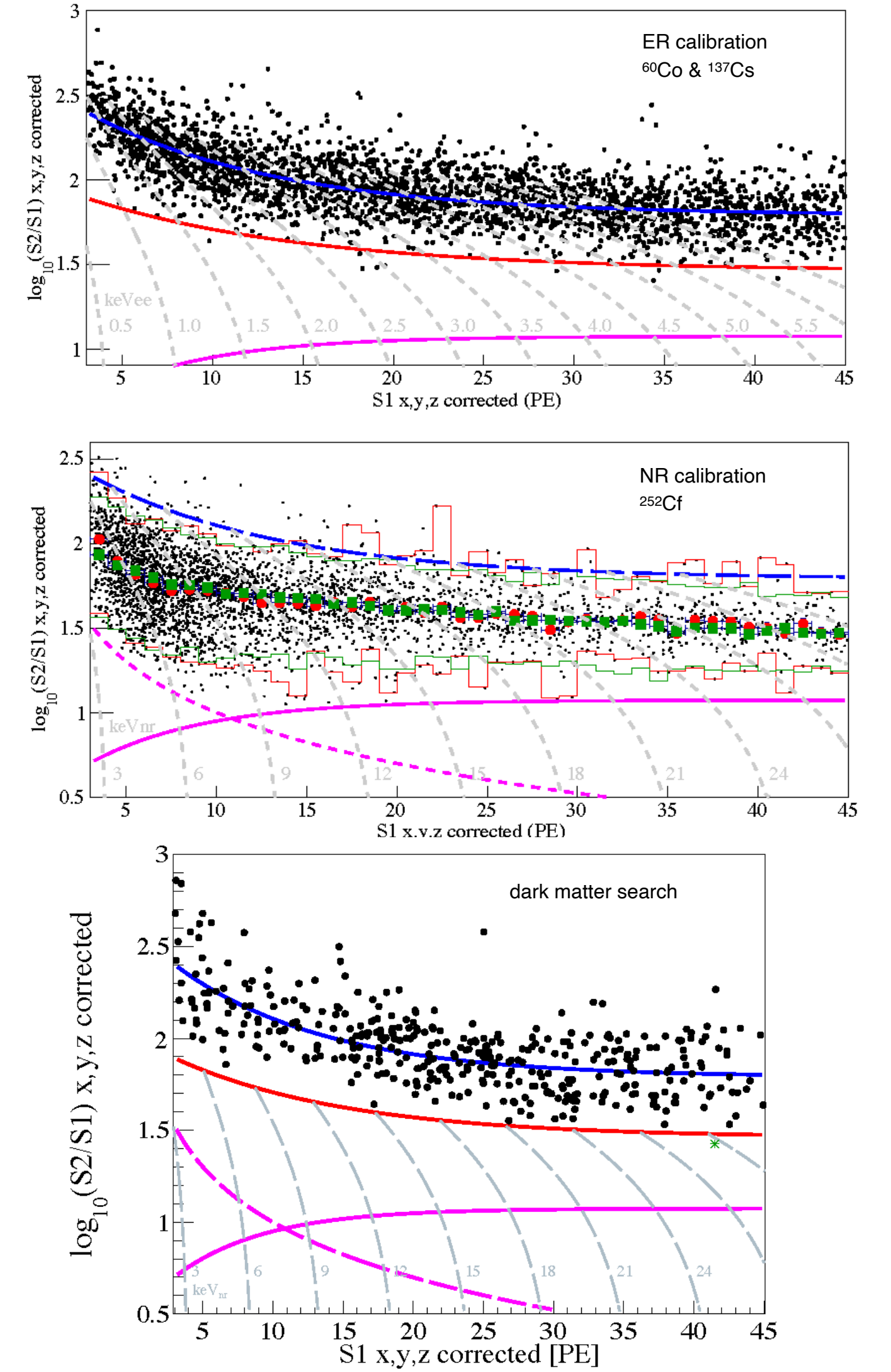
Xenon1T



LUX



PandaX-II



Nuclear recoils are measured through a combination of scintillation light and ionization. The nuclear recoil energy is related to S1 by

$$E_{nr} = \frac{S1}{L_y L_{eff}} \times \frac{S_e}{S_r}$$

[keV_{nr}] → E_{nr}
 observed scintillation [PE] → S1
 light yield [PE/keV_{ee}] → L_y
 scintillation efficiency of NR in LXe → L_{eff}
 suppression of scintillation signal from electric field for ER and NR events → $\frac{S_e}{S_r}$

L_{eff} accounts for the quenching of the scintillation signal for a nuclear recoil.

$$L_{eff} \equiv \frac{S1(E_{nr})/E_{nr}}{S1(122keV_{ee})/122keV_{ee}}$$

122 γ line from ⁵⁷Co source

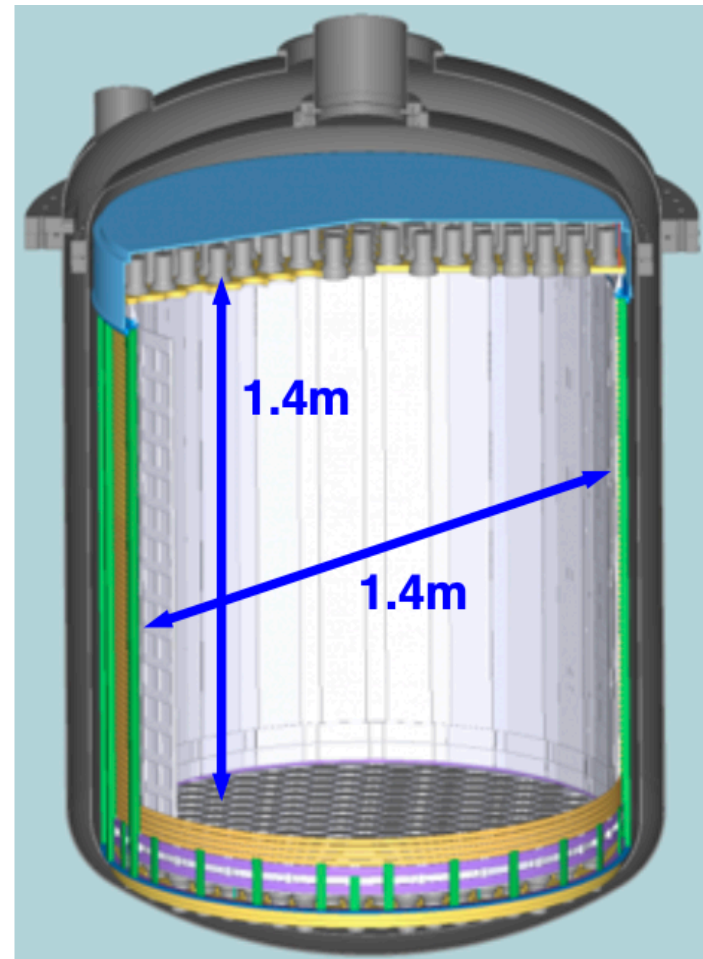
The nuclear recoil energy is related to S2 by

$$E = \frac{S2}{Y} \frac{1}{Q_y(E)}$$

[keV_{nr}] → E
 observed scintillation [PE] → S2
 secondary amplification factor [pe/e] → Y
 number of free electrons per unit energy → $Q_y(E)$

Status Of Current TPC Dark Matter Experiments

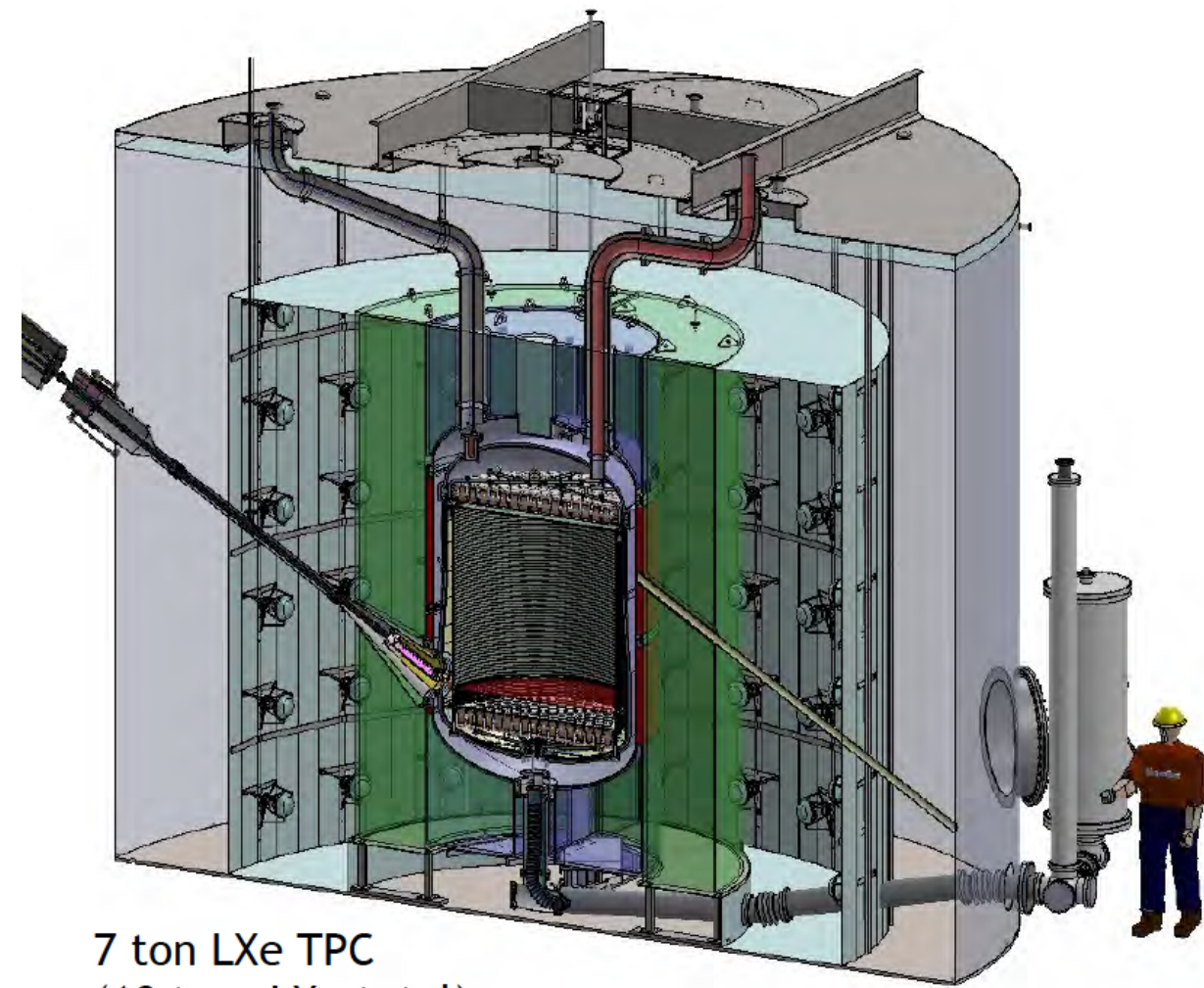
XENONnT



2019-2025

8T LXe

LZ



7 ton LXe TPC
(10 tons LXe total)

2021-2025

7t LXe

PandaX-4T

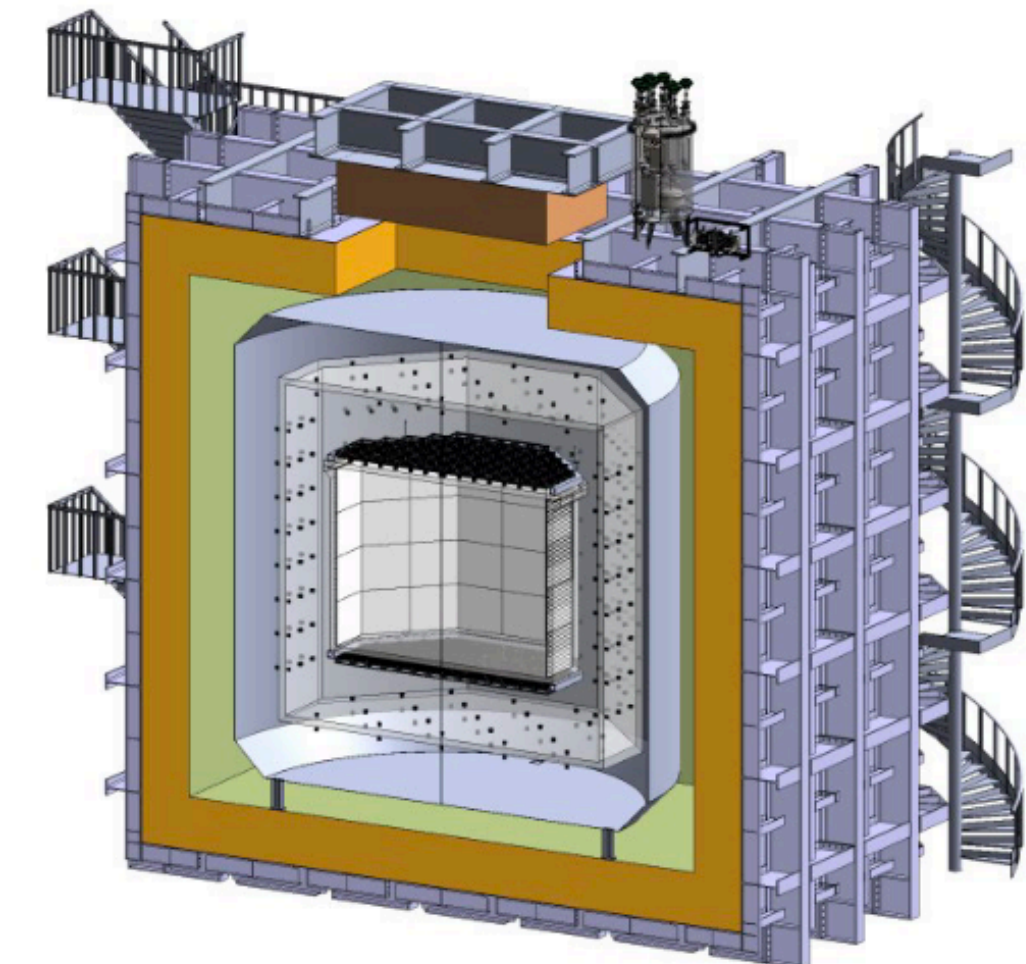


2020 - ?

4t LXe

Taking Data

DarkSide-20K



50t LAr

2026 - ?

Under Construction

Darwin

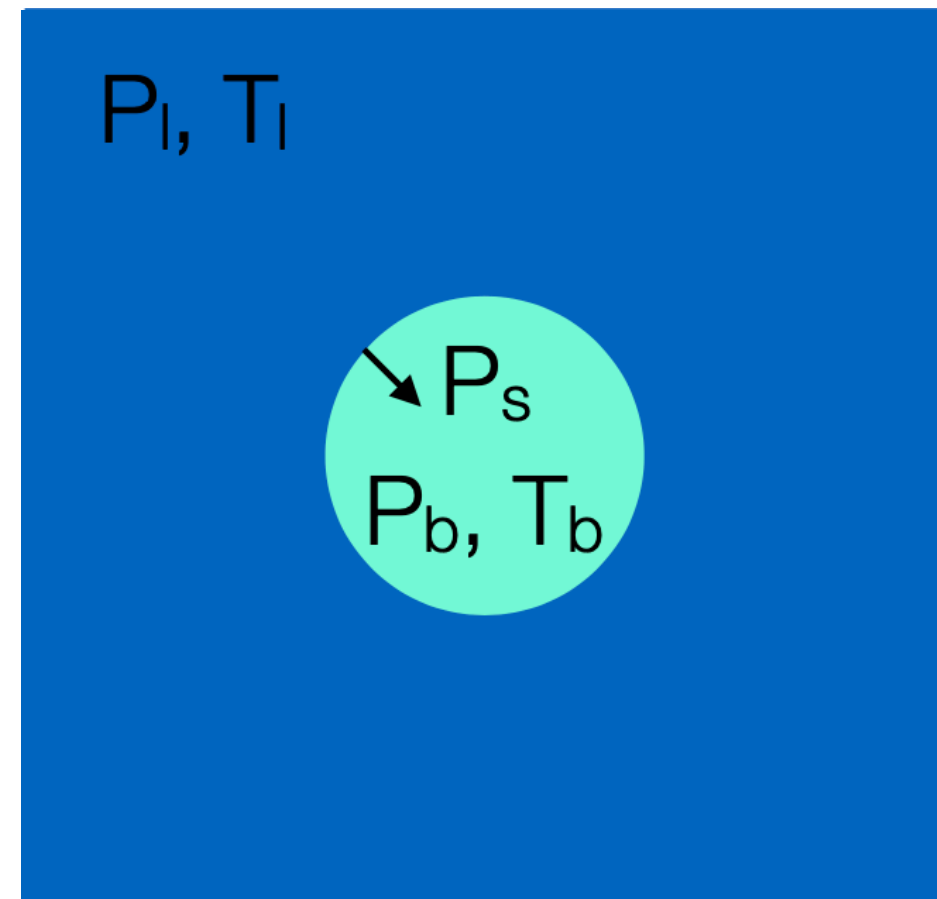
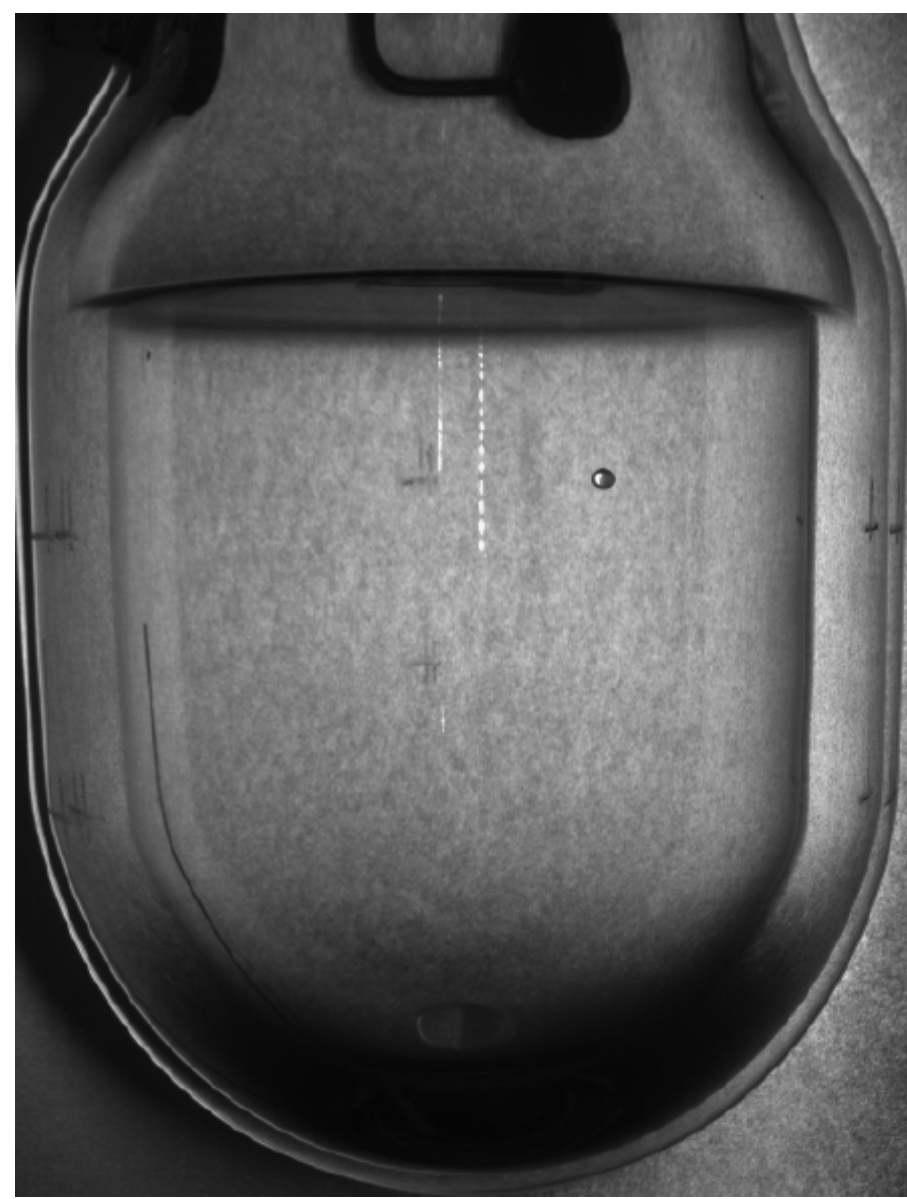
50T LXe

XLZD

50T LXe

Taking Data

Bubble Chambers



How Do Bubble Chambers Work?

- Start with a bubble in a liquid in thermal and chemical equilibrium

$$T_l = T_b$$

- If $P_b > P_l$ the bubble will expand (assuming no surface tension).

- Include surface tension, $P_s = 2\sigma/r$, bubble grows when

$$P_b > P_l + P_s$$

Leads to

$$r > r_c = \frac{2\sigma}{P_b - P_l}$$

- Bubbles that do not meet this criteria collapse

- The threshold for bubble nucleation is given by

$$E_T = r\pi r_c^2 \left(\sigma - T \left[\frac{d\sigma}{dT} \right]_{\mu} \right) + \frac{4\pi}{3} r_c^3 \rho_b (h_b - h_l) - \frac{4\pi}{3} r_c^3 (P_b - P_l)$$

surface energy

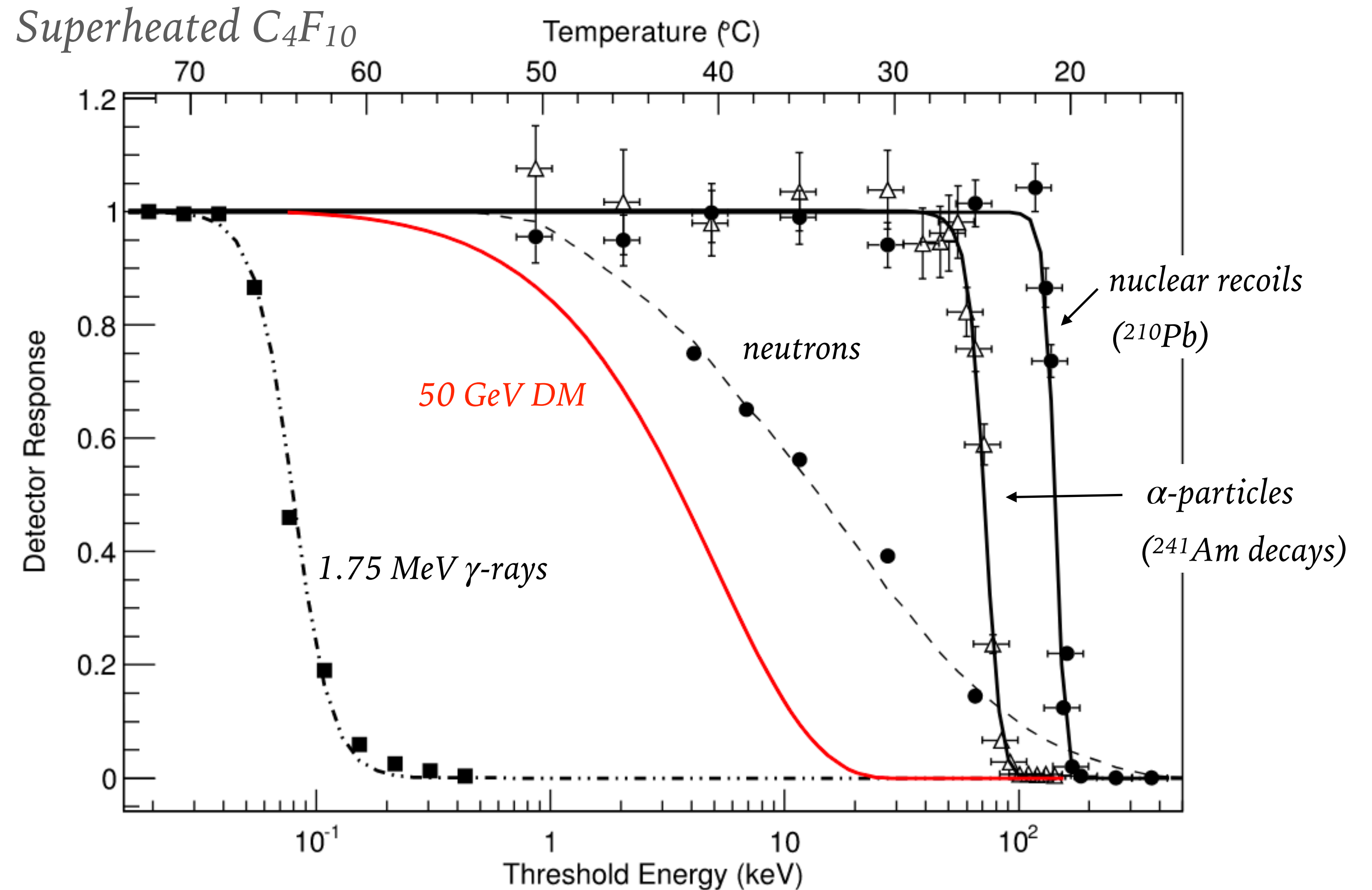
bulk energy

reversible work

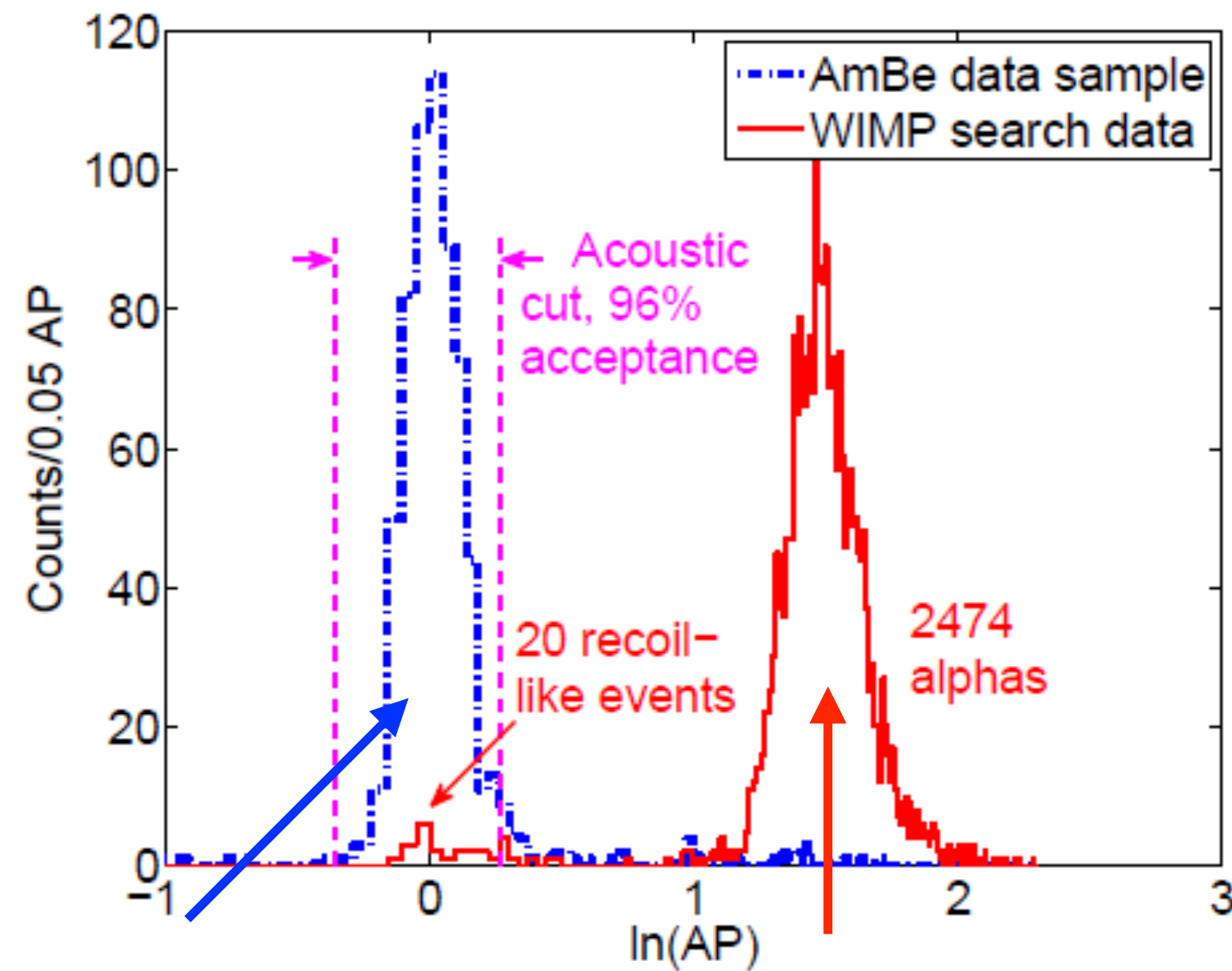
$\rho = \text{density and } h = \text{specific heat}$

Detector Response

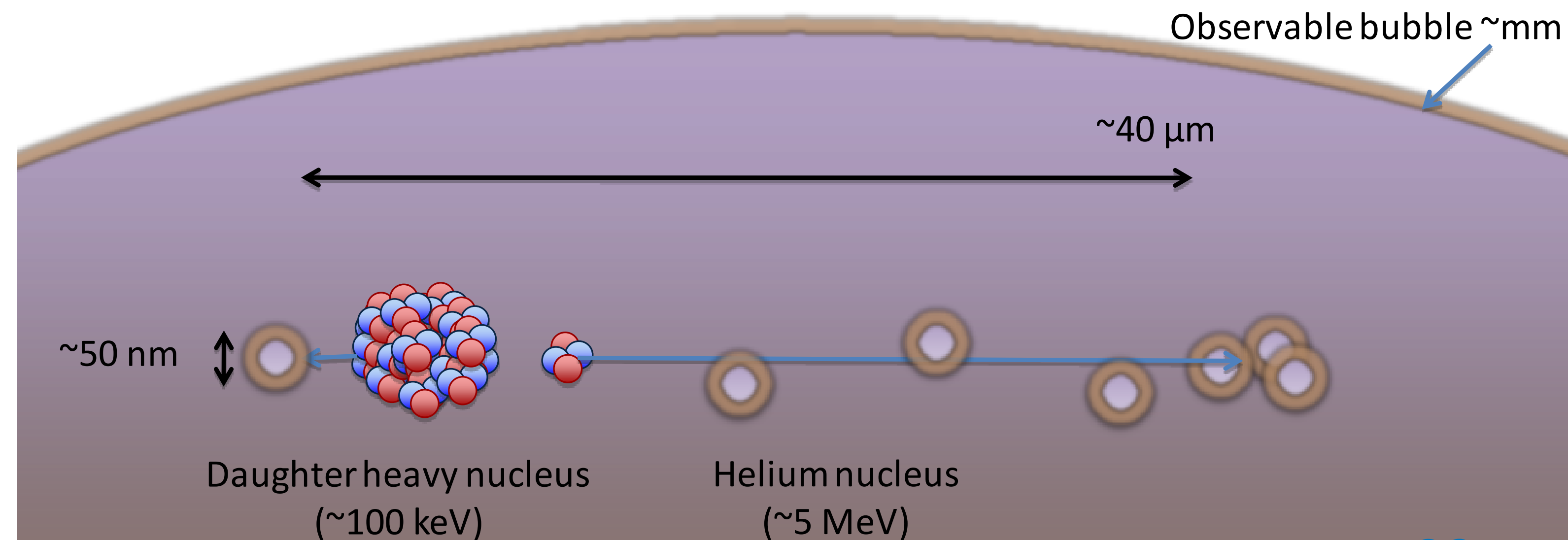
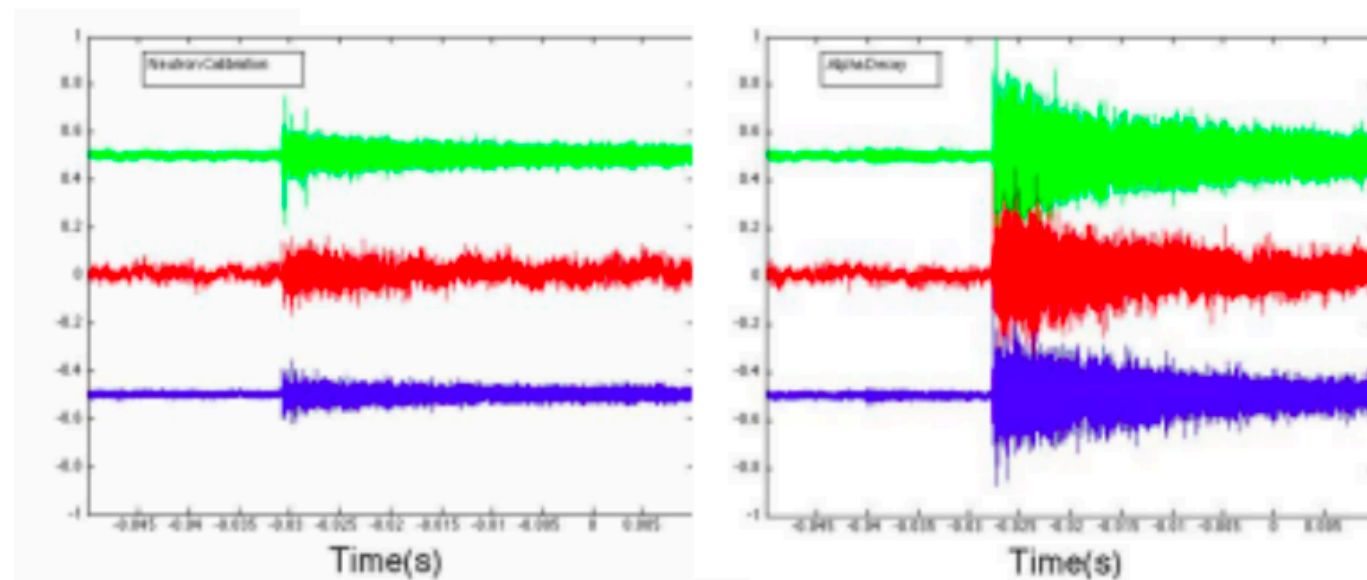
- Heavier particles have higher thresholds
- Tune the chamber to be unresponsive to most backgrounds (ER).
- Underground location and shielding to mitigate neutrons.
- But what about alphas?



Liquid Noble Properties

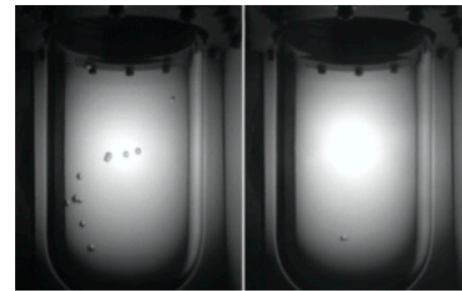
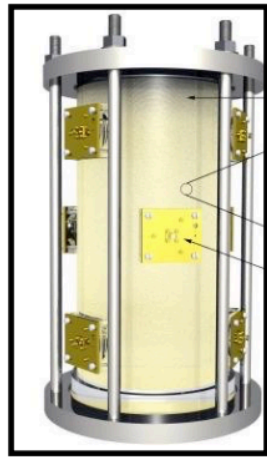


- ▶ Alphas deposit their energy over 10s of microns
- ▶ Nuclear recoils deposit their energy over 10s of nanometers
- ▶ Alpha particles are ~ 4 times louder than NR. This can be measured by piezoelectric sensors



PICO Program

PICASSO

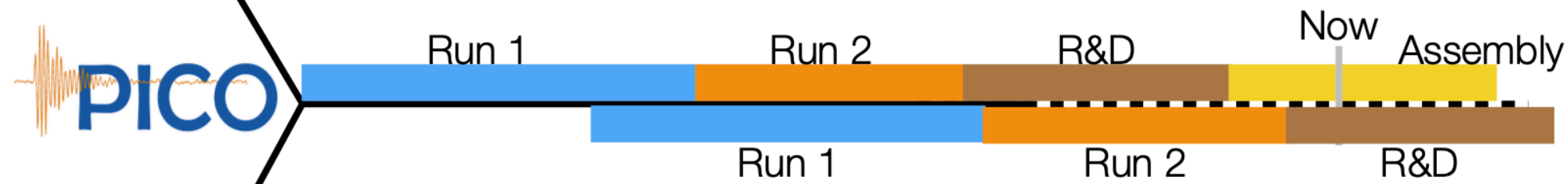


COUPP

PICO-2L



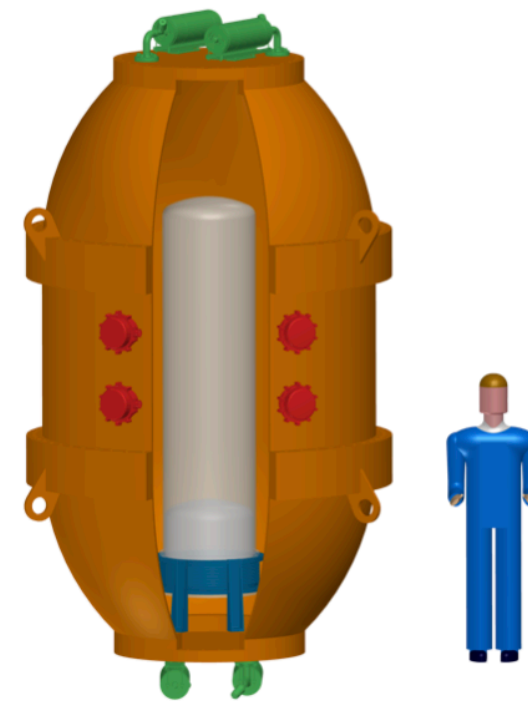
PICO-40L



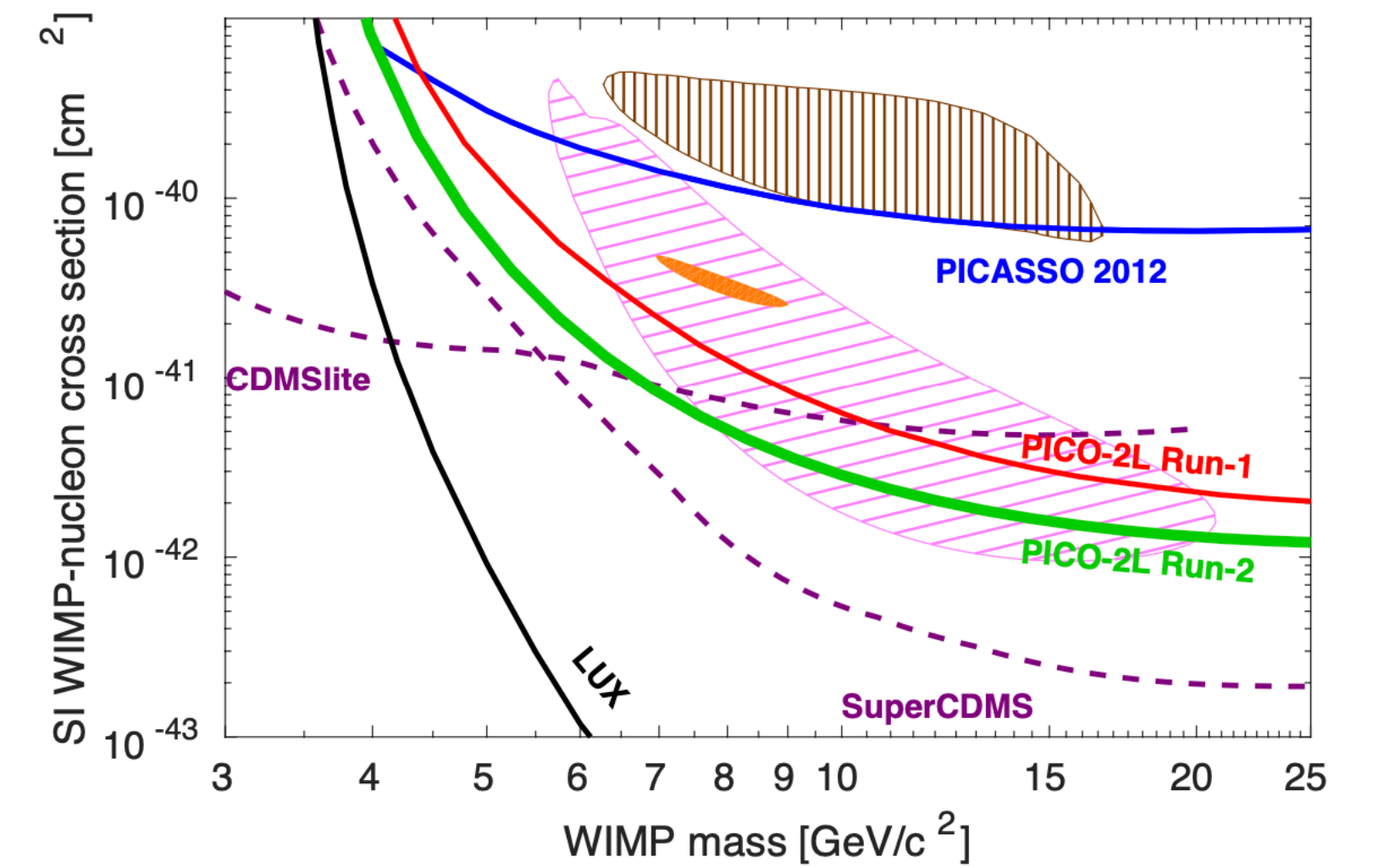
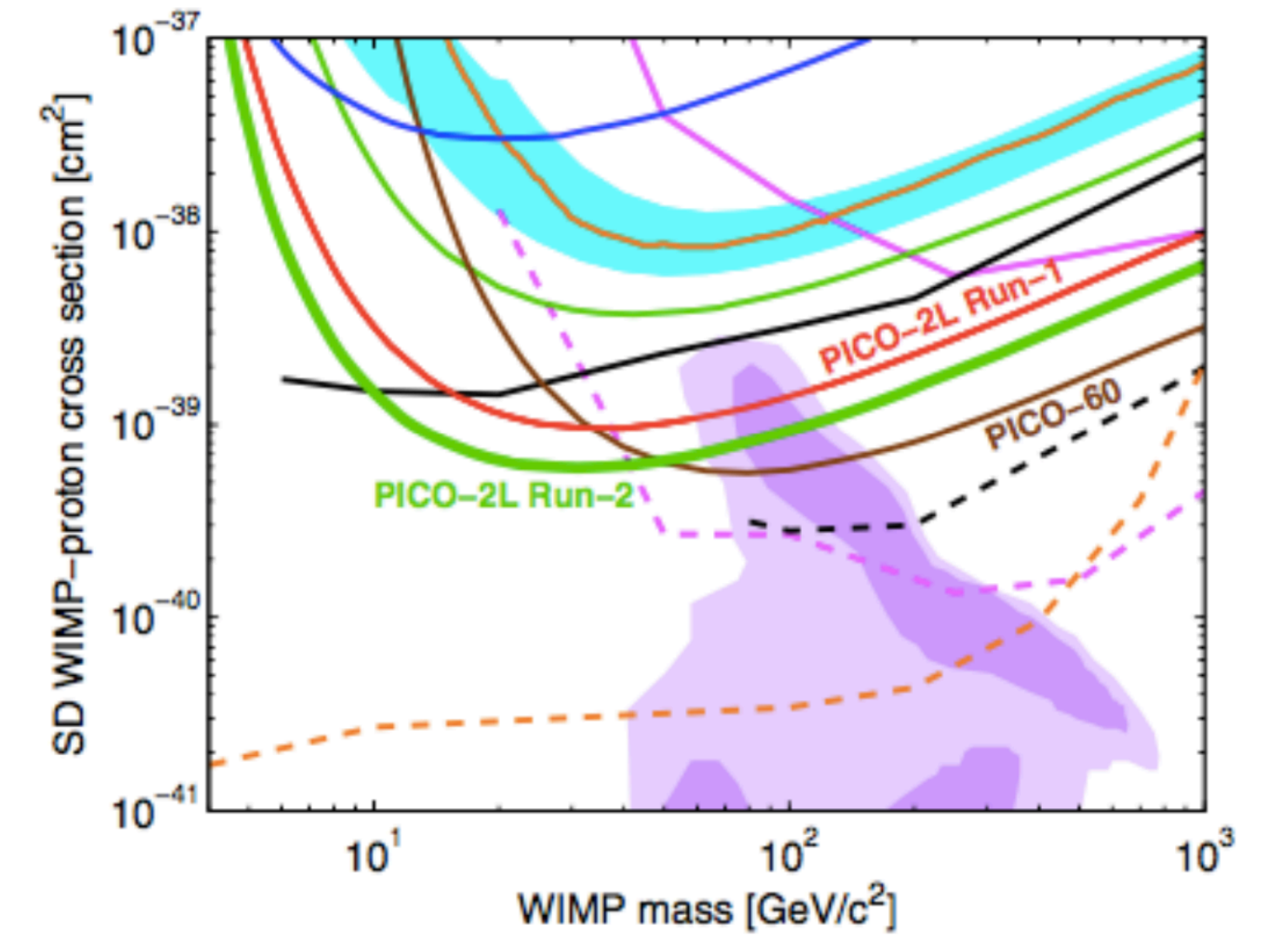
PICO-60



PICO-500

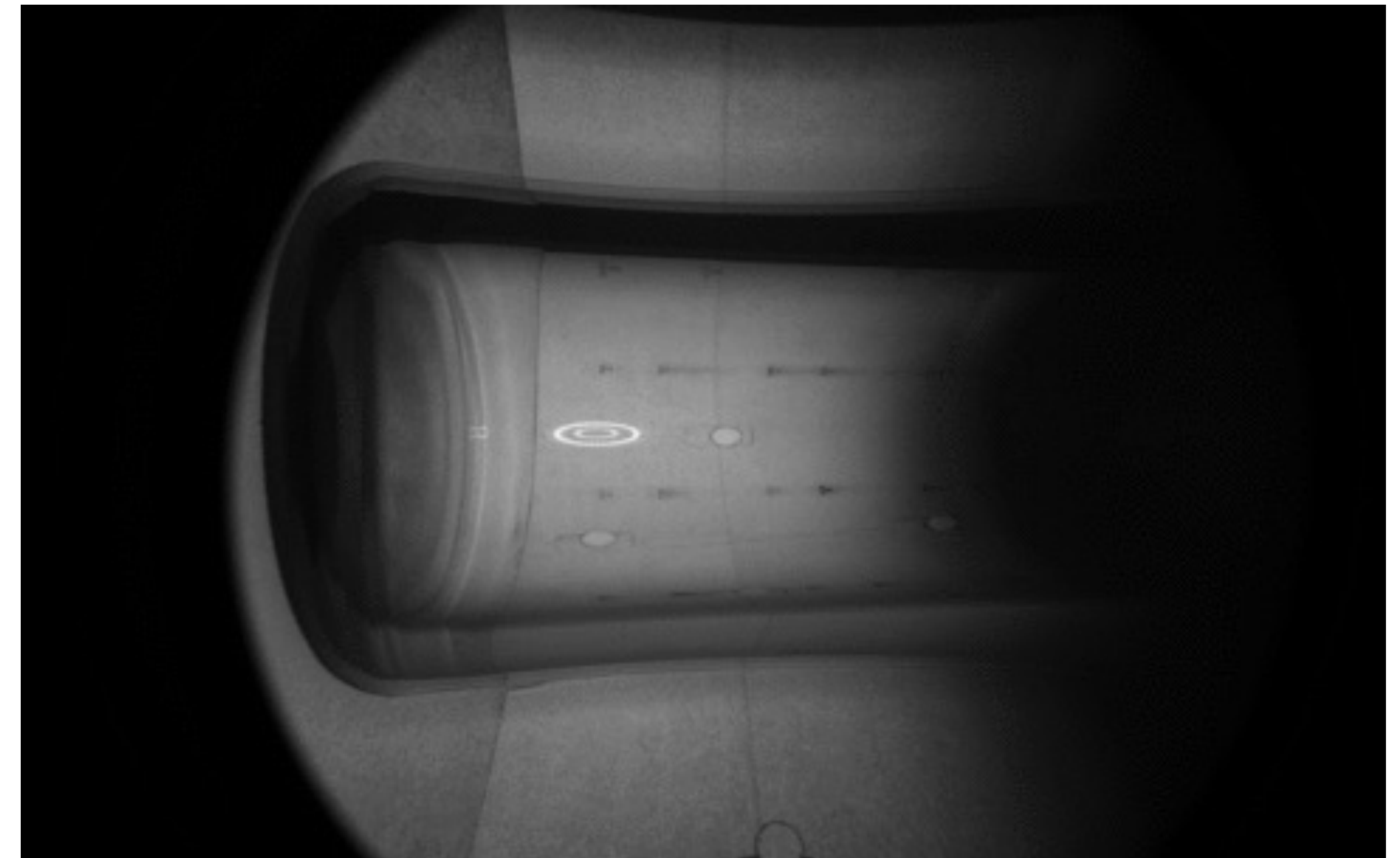
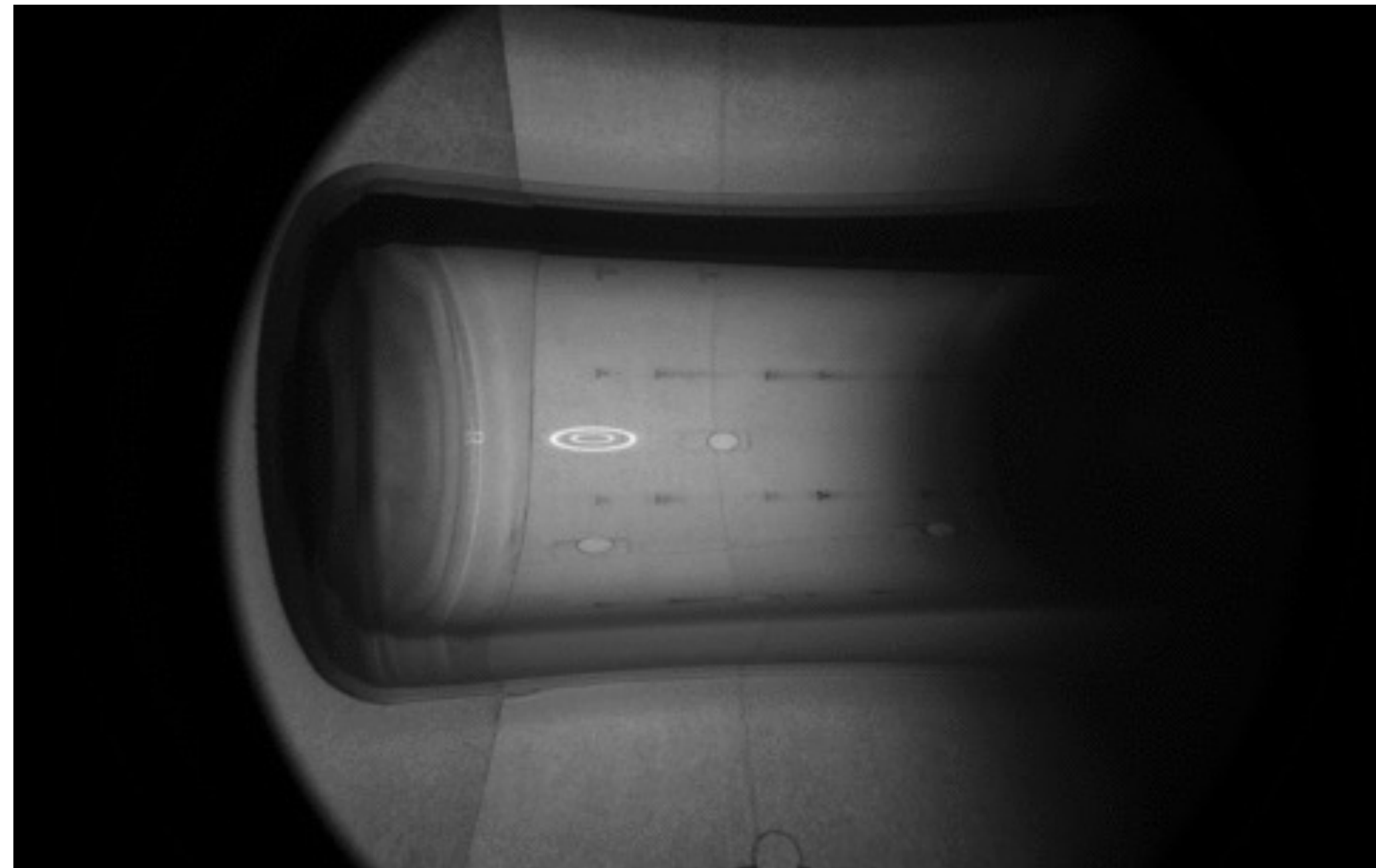


PICO-2L Results



Ken Clark

PICO-40L Begins Operations!



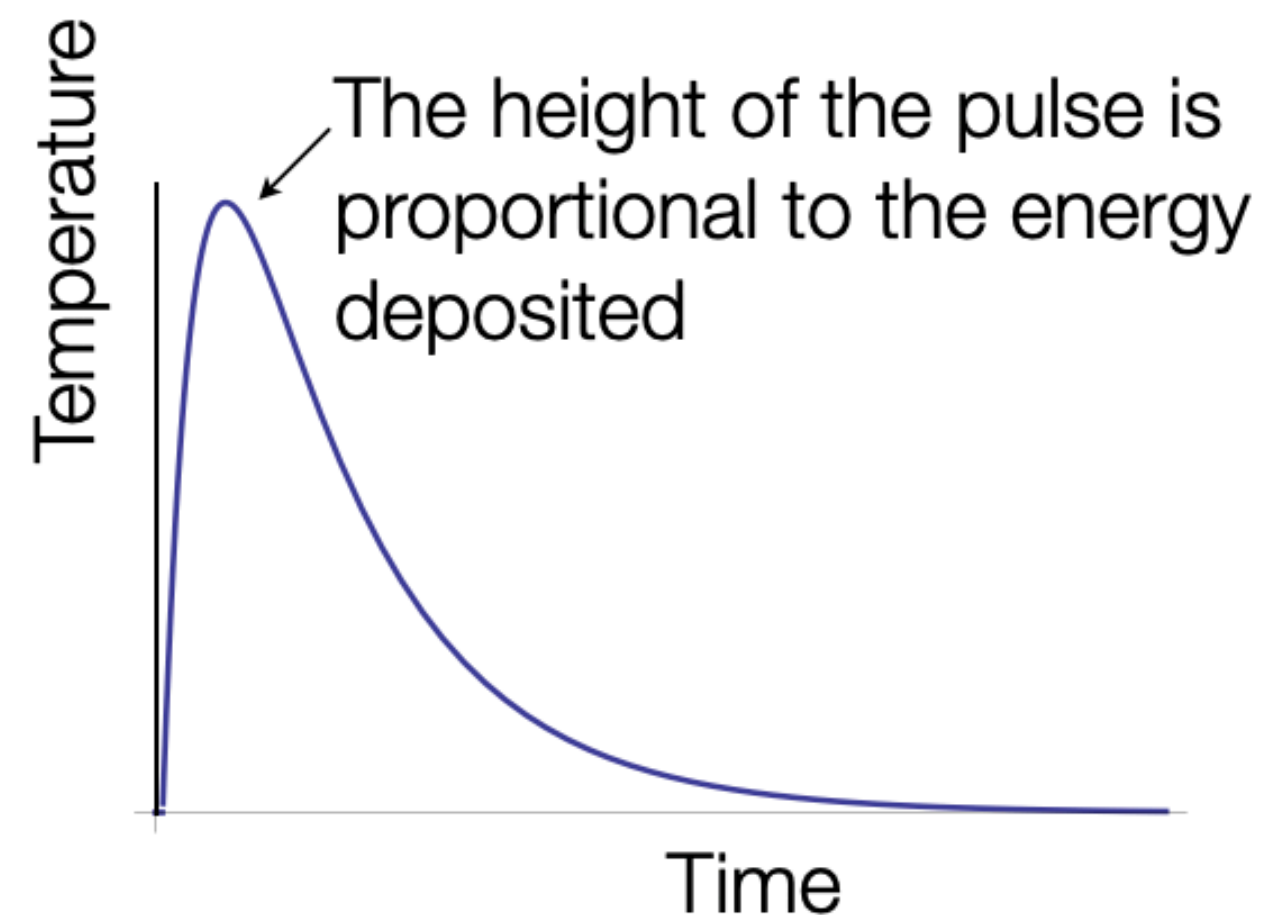
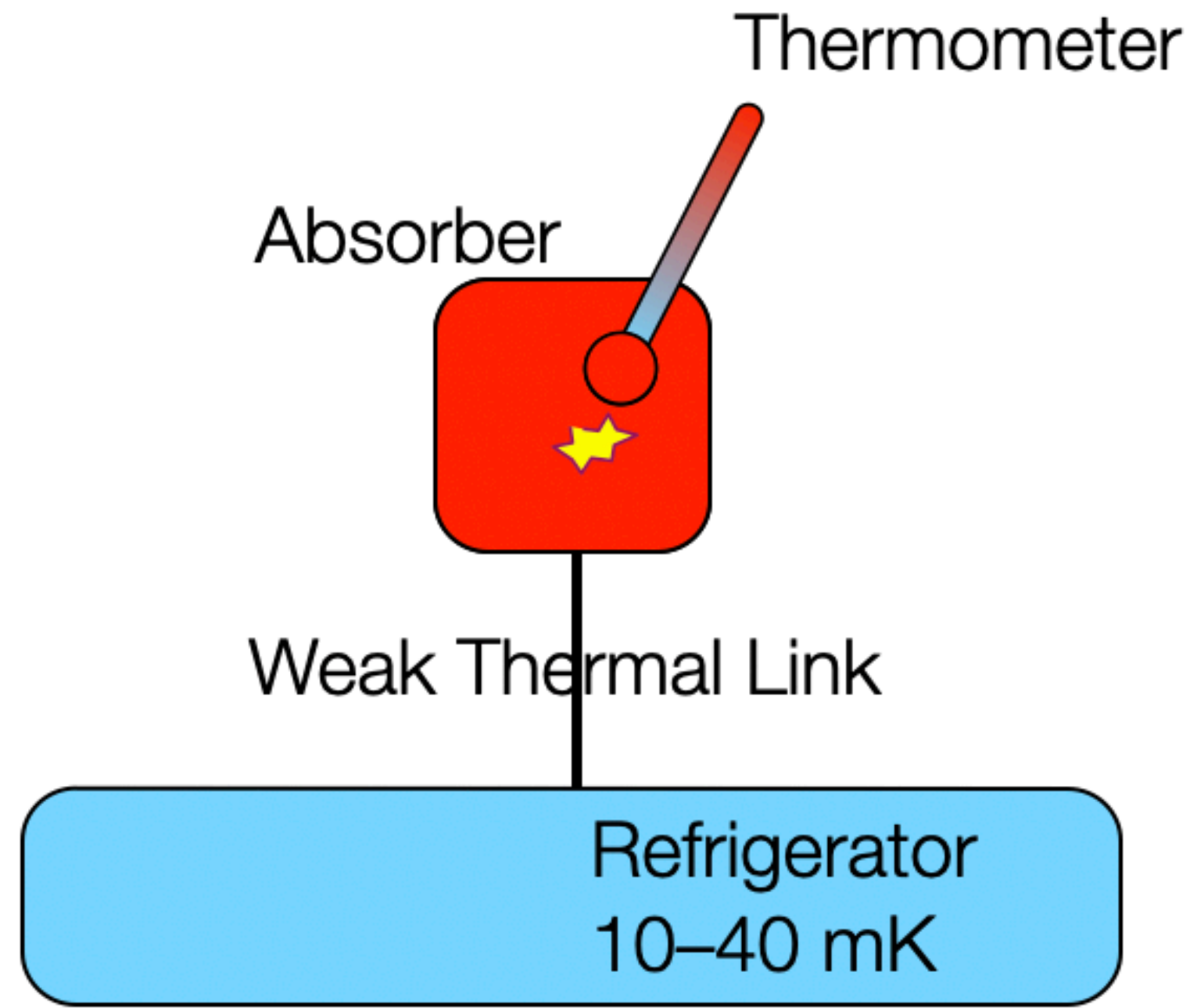
Courtesy of the PICO Collaboration.

PICO-40L bubbles! Regular operations began in February.



Cryogenic Solid State Detectors

Cryogenic Detectors: Phonon and Heat Signals



$$\Delta T = \frac{E}{C(T)} e^{-\frac{t}{\tau}}$$

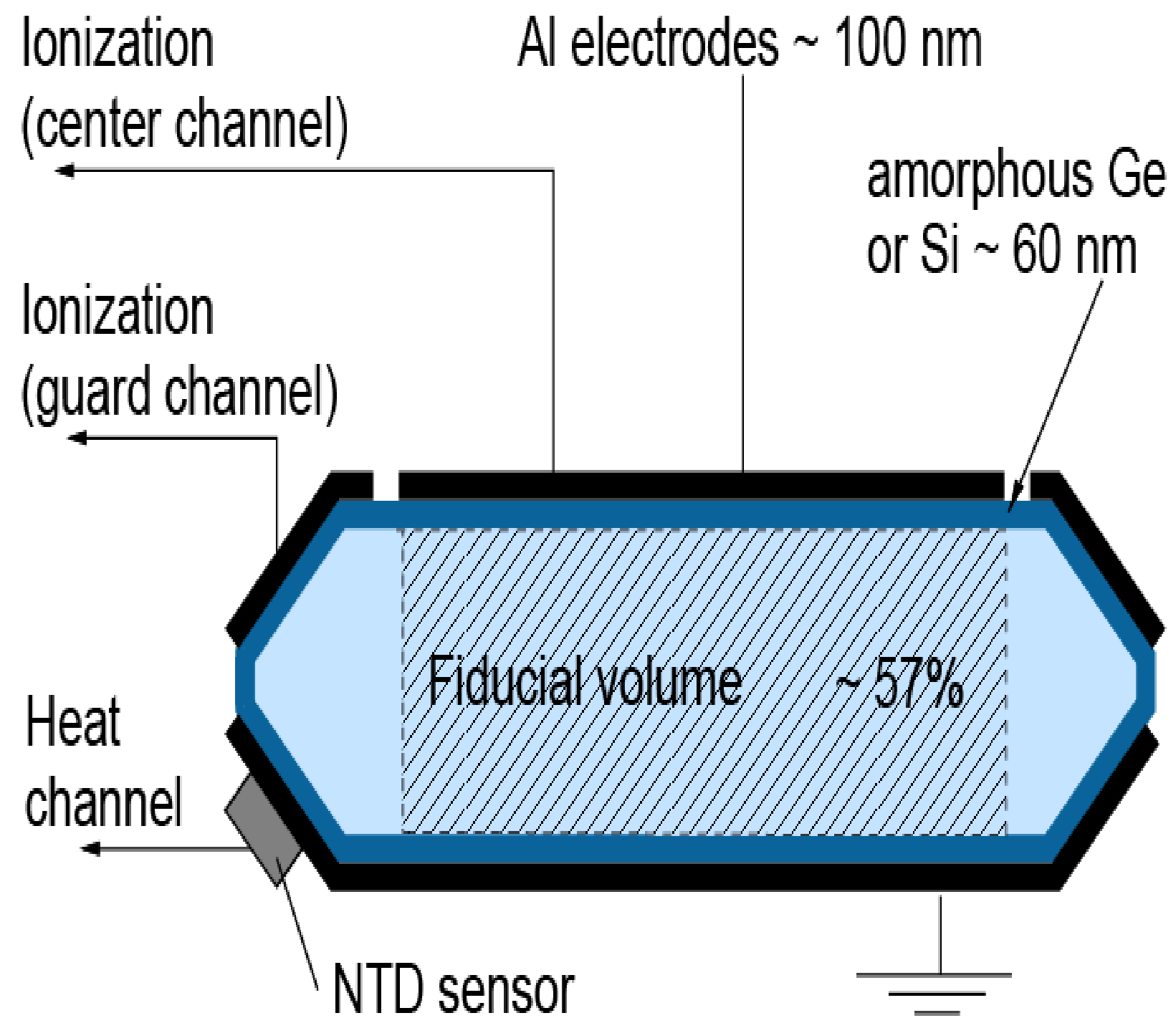
$$\tau = \frac{C(T)}{G(T)}$$

$C(T)$ = heat capacity
of absorber

$G(T)$ = thermal
conductance of the
link between absorber
and reservoir at T_0

- Two families of sensors for phonon signal: thermal and athermal
- Thermal sensors - wait for the full thermalization of the phonons within the bulk of the detector and the sensor itself
- Athermal sensors detect fast, non-equilibrium phonons
- Temperature increase is equal to the deposited energy over the heat capacity of the system.
- Two most widely used technologies to measure these signals are neutron doped germanium sensors (NTD) and transition edge sensors (TES)

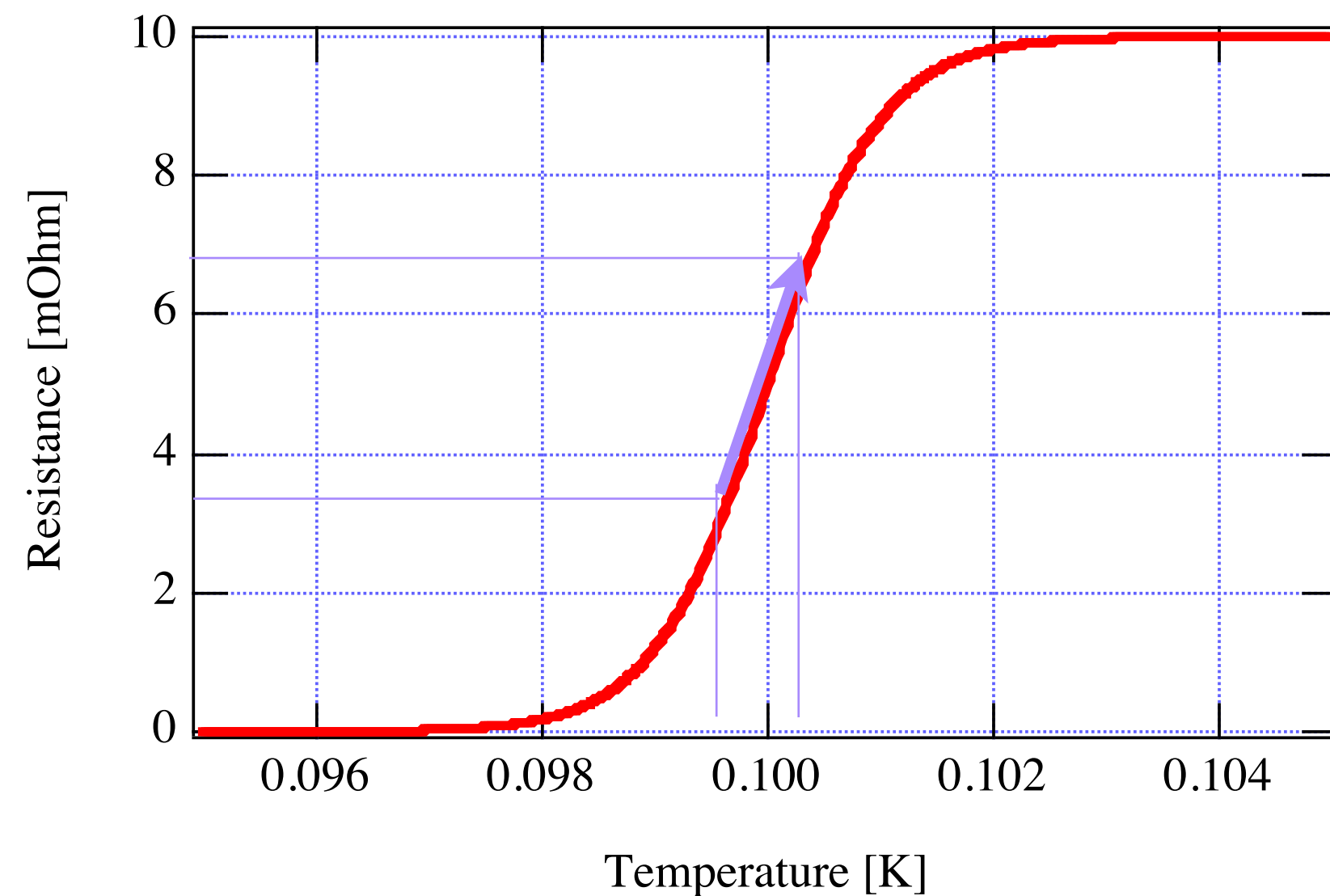
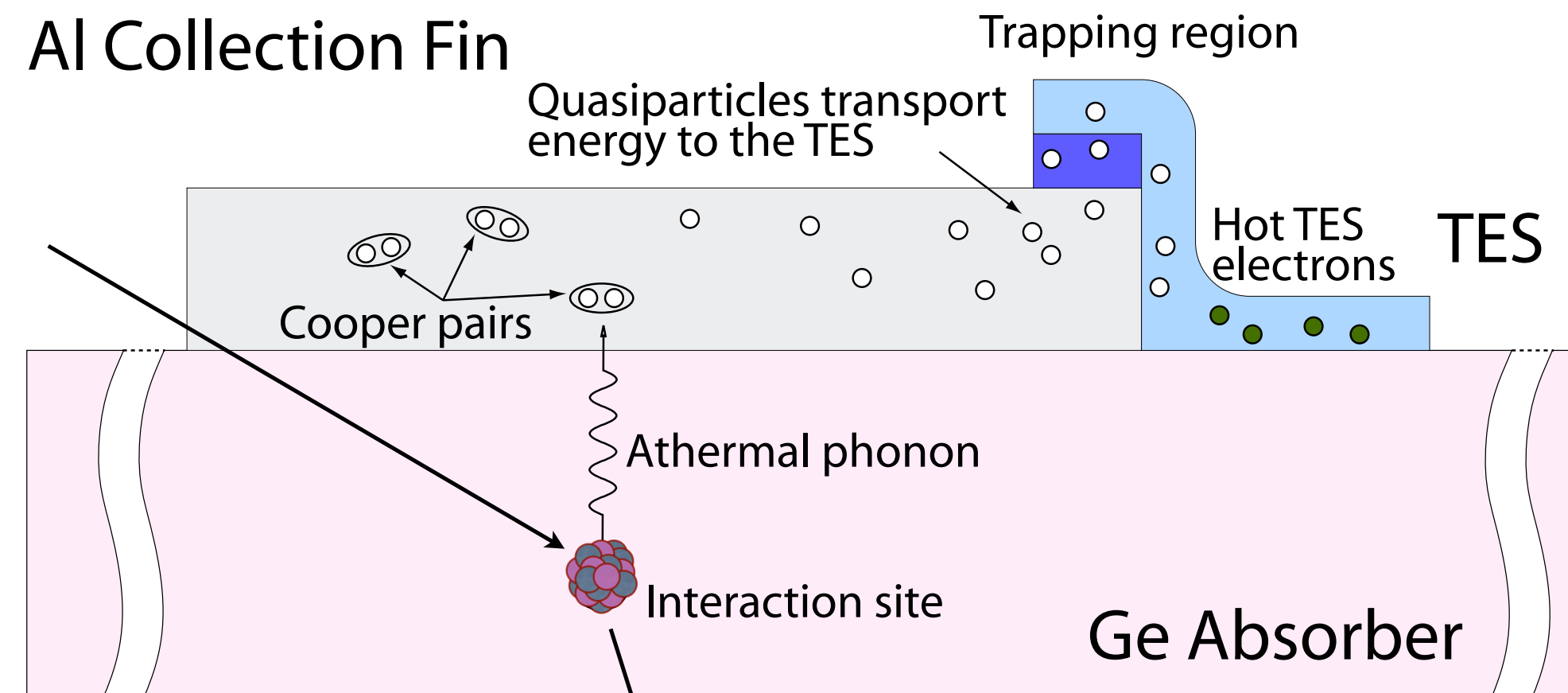
NTDs



Schematic "Ge-NTD"
EDELWEISS detector

- NTDs are small Ge semiconductor crystals that have been exposed to a neutron flux to make a large, controlled density of impurity.
- NTD measures small temperature variations relative to T_0 , which is set to be on the transition from superconducting and resistance regime with dependence of the resistance with temperature T
- Resistance is continuously measured by flowing current through it and measuring the resulting voltage.
- Sensors are glued onto detector.

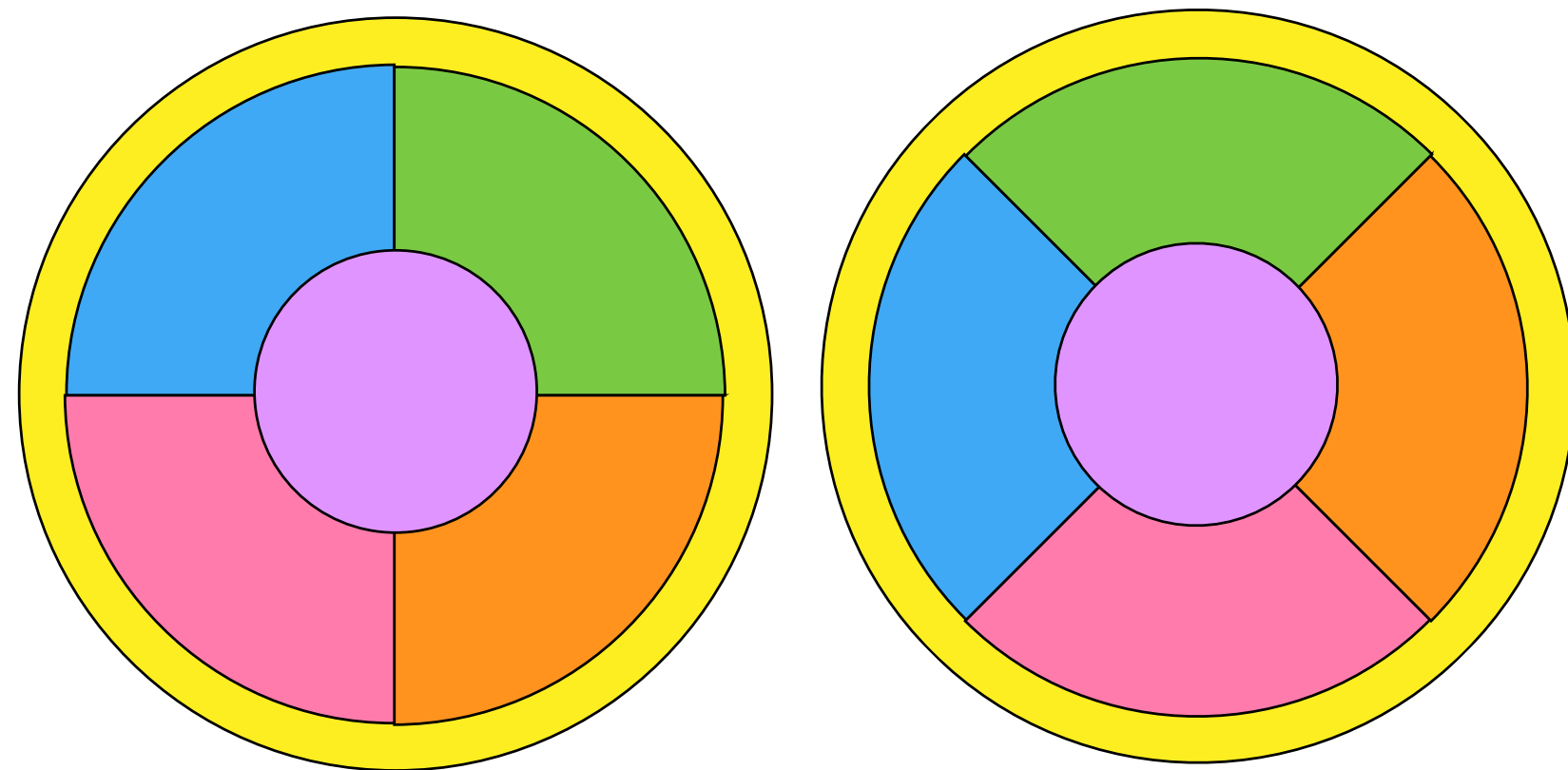
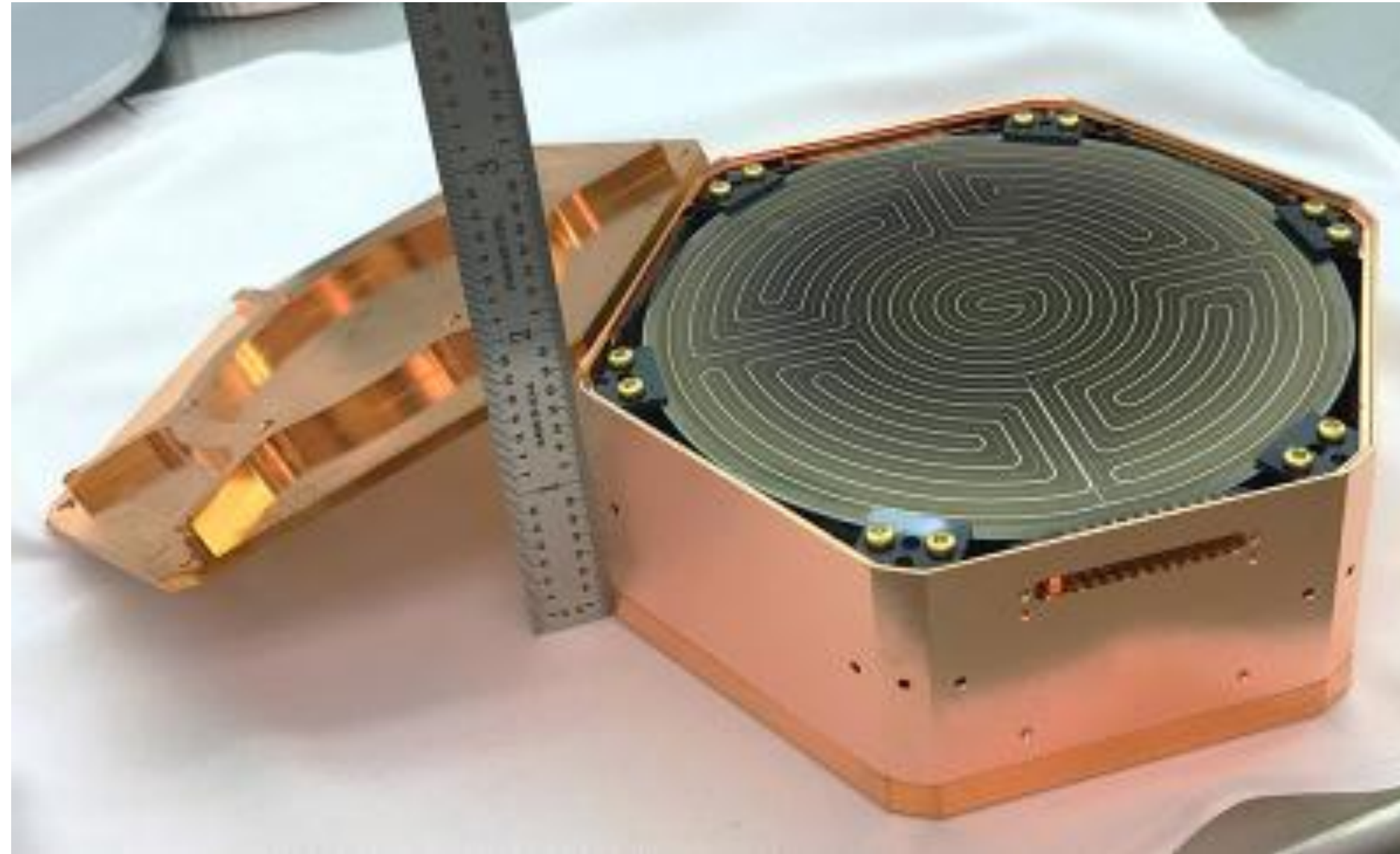
Transition Edge Sensors



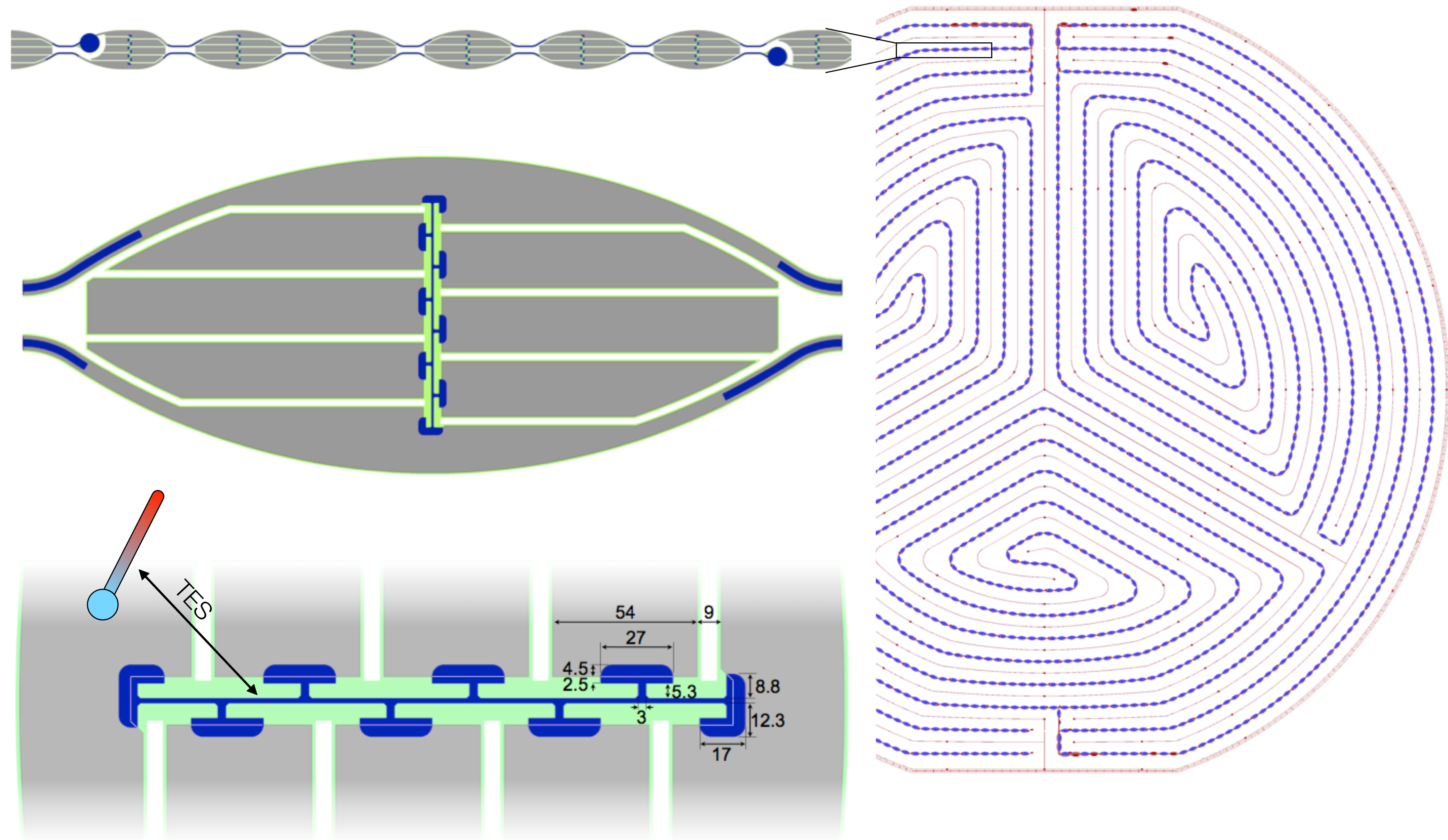
- TES is a thin superconducting film operated near its T_c .
- Refrigerator temperature needs to be close to absolute zero.
- A heater with an electrothermal feedback system maintains temperature at superconducting edge.
- Temperature changes are detected by a change in the feedback current, collected by a SQUID.

SuperCDMS SNOLAB Detectors

- Initial payload 4 towers, each w/6 detectors (1.39 kg Ge crystals, 0.61 kg Is crystals) each 100 mm diameter, 33.3 mm thick:
 - 2 HV (4 Ge + 2 Si)
 - 2 iZIP (6 Ge & 4 Ge + 2 Si)
- iZIP detectors
 - 8 phonon channels + 2 charge sensors each side
- HV detectors
 - 6 phonon channels on each side

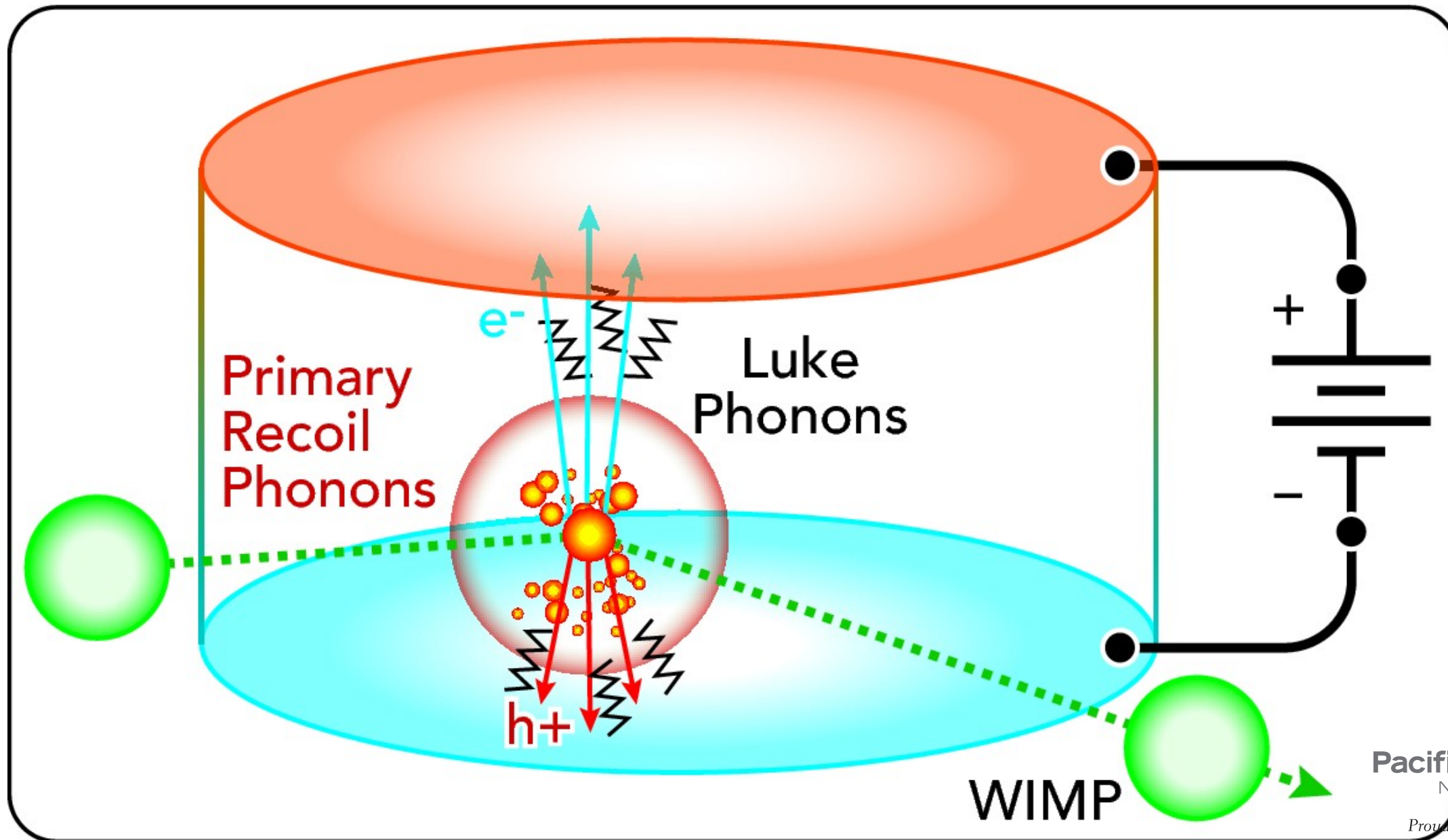


iZIP Detector

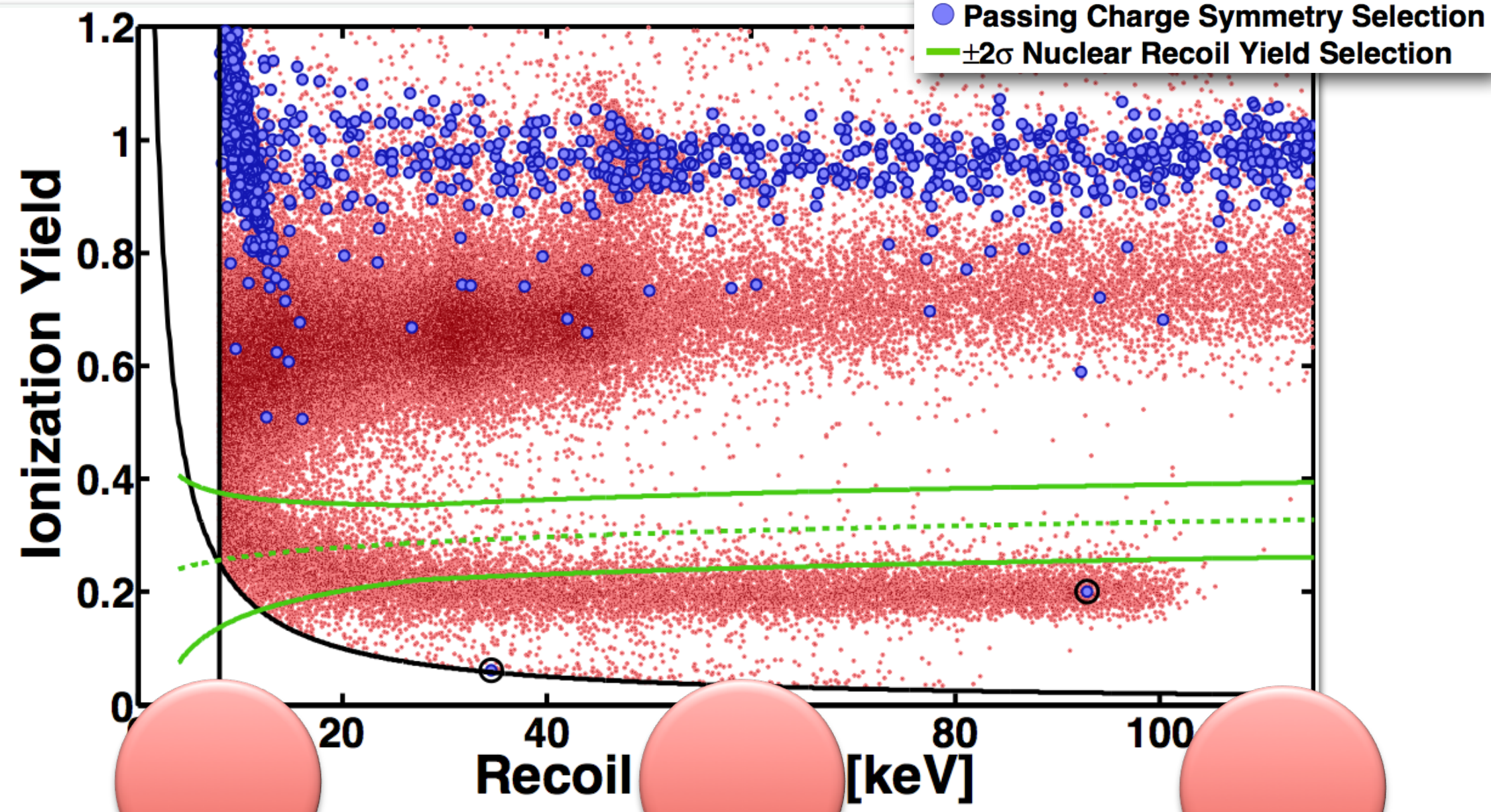


SuperCDMS - iZIP Mode

- Primary (prompt) phonon and ionization signals allow for discrimination between NR and ER events
- High resolution phonon and charge readout
- All surface and ER backgrounds above a few keV can be easily removed with selection criteria.

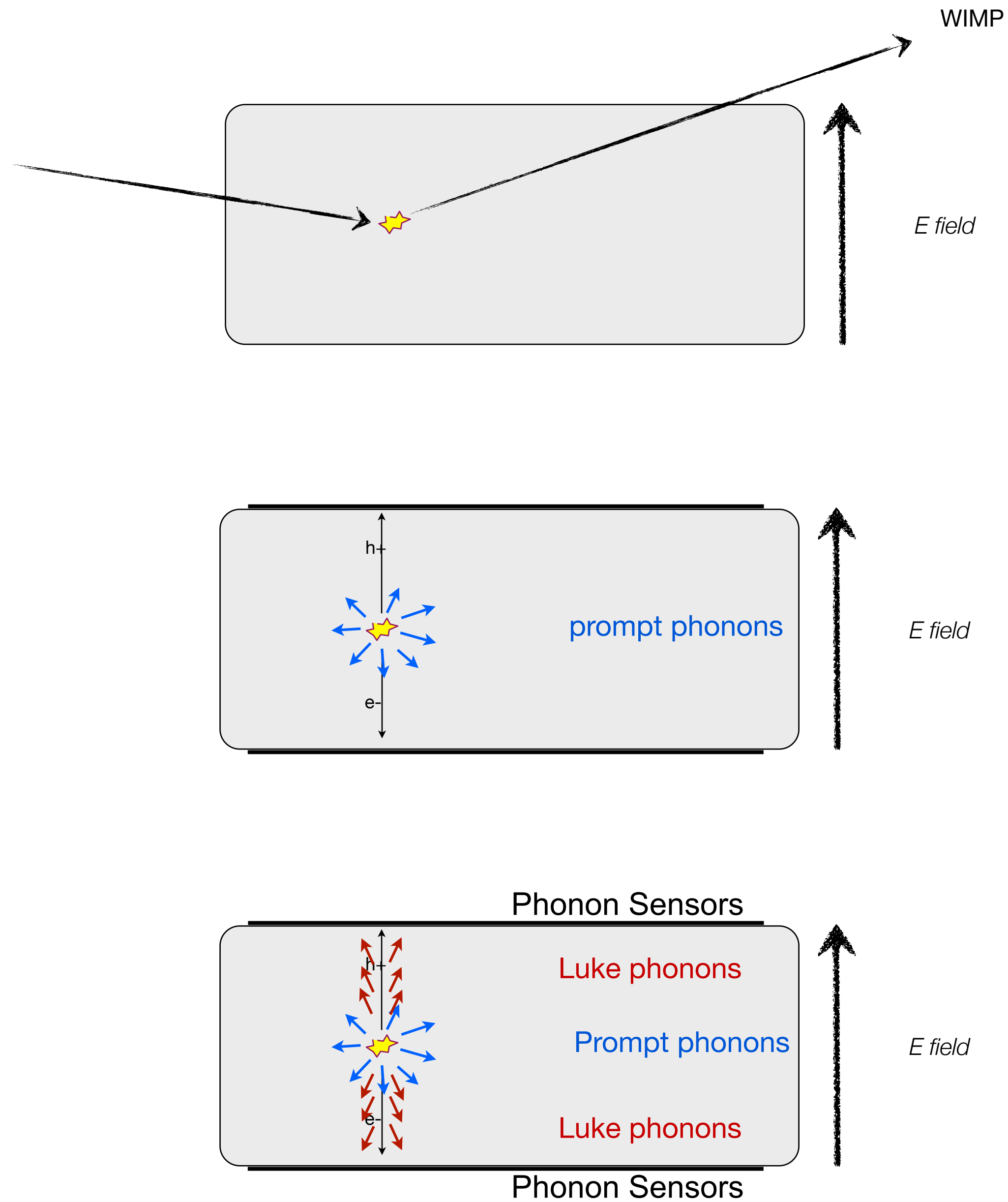


APL 103, 164105 (2013)



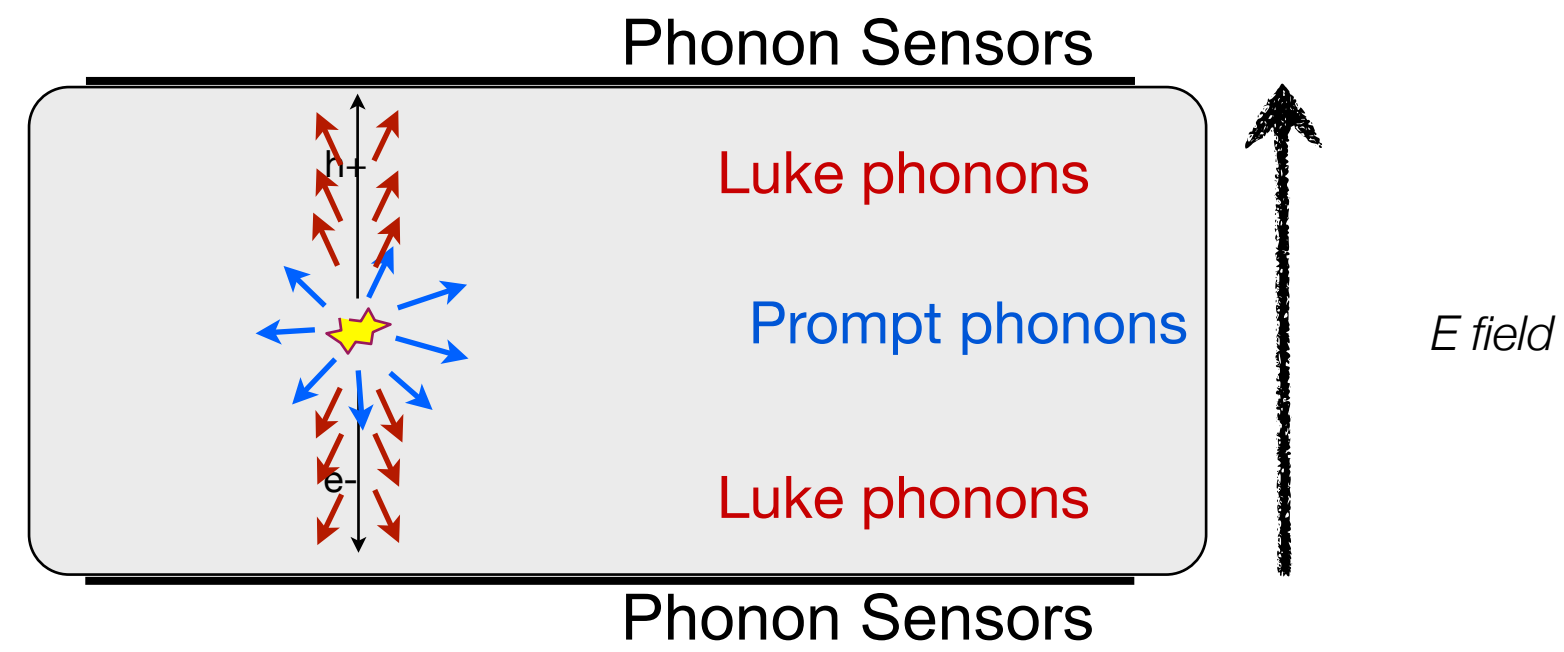
SuperCDMS - HV Mode

- Drifting electrons across a potential (V) generates a large number of phonons (NLT phonons)

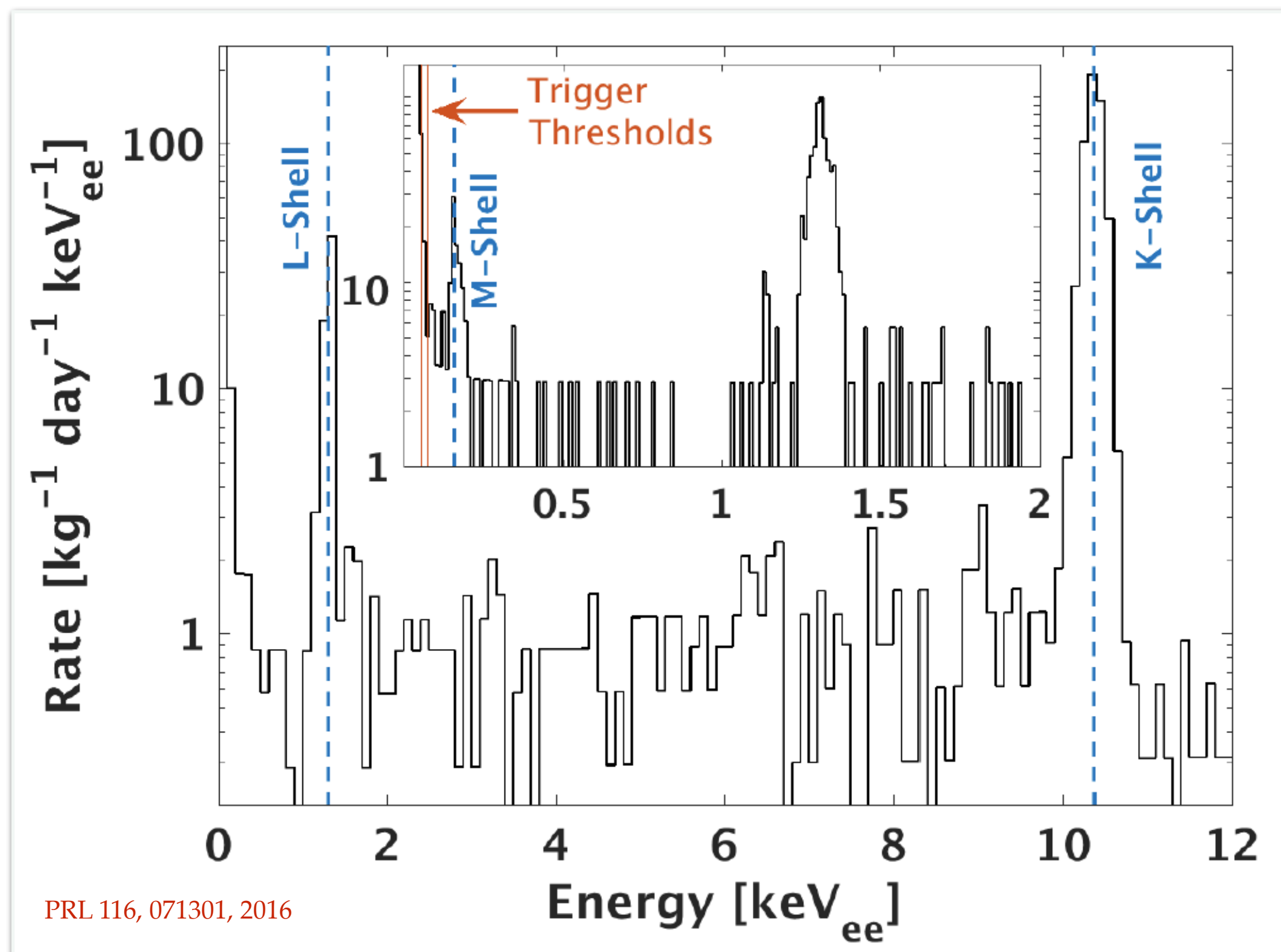


$$E_t = E_r + N_{eh}eV_b$$

↑ total phonon energy ↑ primary recoil energy ↑ Luke phonon energy



- Drifting electrons across a potential (V) generates a large number of phonons (N phonons)



PRL 116, 071301, 2016

$$E_t = E_r + N_{eh}eV_b$$

\uparrow total phonon energy \uparrow primary recoil energy \uparrow Luke phonon energy

- Ultra high resolution indirect charge measurement
- Thresholds 75 eV_{ee} and 56 eV_{ee}
- No yield or detector face discrimination

On Units

We know that NTL phonon energy is given by

$$E_{NTL} = N_{eh} V_b$$

The number of electron hole pairs generated in an interaction is given by

$$N_{eh} = \frac{E_r}{\epsilon} \quad \epsilon G_e = 3.0 \text{ eV}$$

The total energy (phonon) is given by

$$E_t = E_r + eV_b N_{eh}$$

NR produce eh-pairs less efficiently than ER. Take this into account, define $Y \equiv 1$ for ER.

$$N_{eh} = Y(E_r) \frac{E_r}{\epsilon}$$

The total energy can then be written

$$E_{tot} = E_r \left(1 + Y(E_r) \frac{eV_b}{\epsilon} \right)$$

If we calibrate detectors using ER, the resulting energy scale is keV_{ee} to convert to keV_{nr} equate for NR and ER.

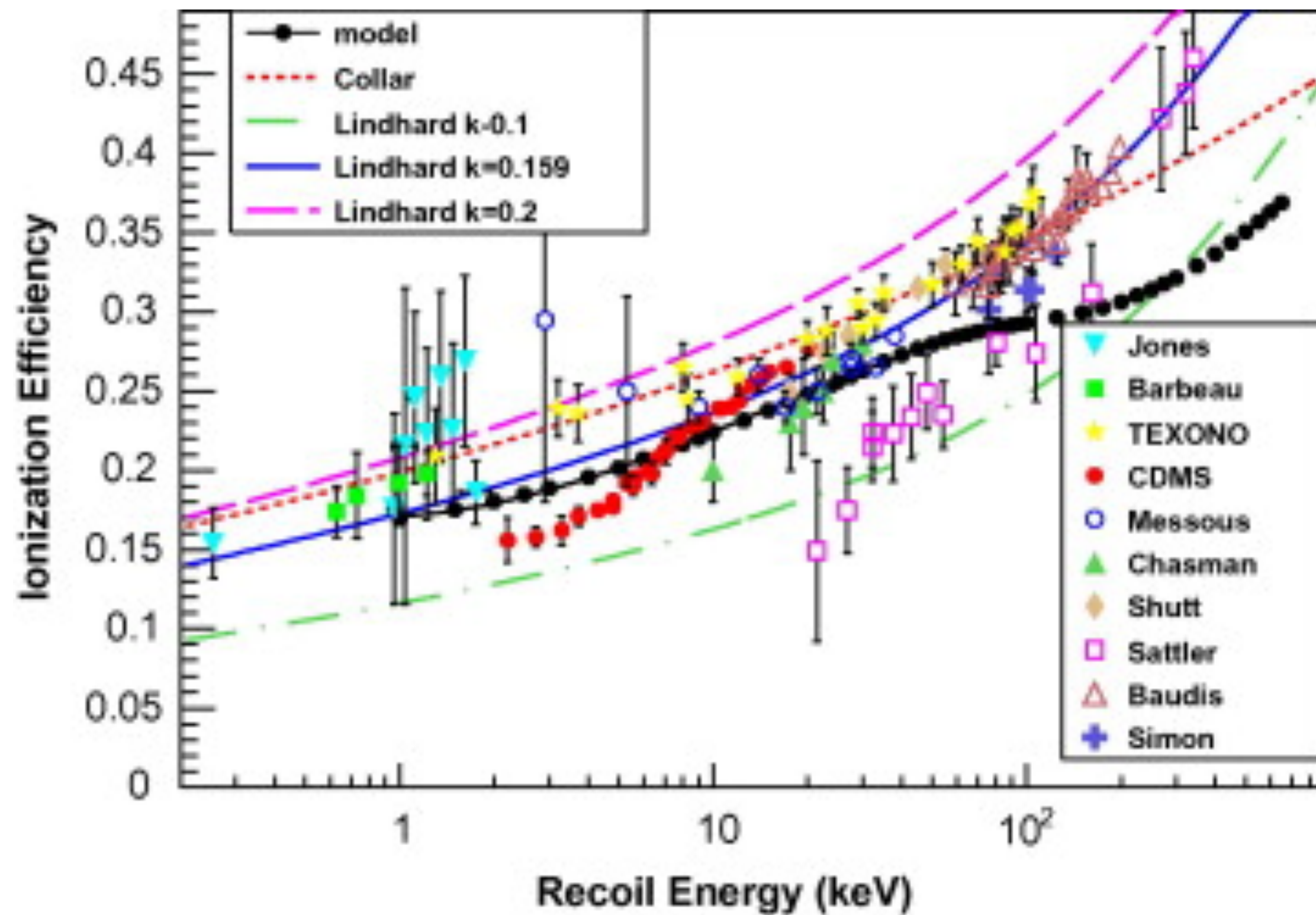
$$E_{nr} \left(1 + Y(E_{nr}) \frac{eV_b}{\epsilon} \right) = E_{ee} \left(1 + \underbrace{Y(E_{ee})}_{\text{recall } Y = 1 \text{ for ER}} \frac{eV_b}{\epsilon} \right)$$

recall $Y = 1$ for ER

$$E_{nr} = E_{ee} \left(\frac{1 + eV_b/\epsilon}{1 + Y(E_{nr})eV_b/\epsilon} \right)$$

How to Determine Y?

- Either you need to measure it directly or model it.
- The most utilized model is from Lindhard.



$$Y(E_{nr}) = \frac{k \cdot g(\epsilon)}{1 + k \cdot g(\epsilon)}$$

where

$$g(\epsilon) = 3\epsilon^{0.15+0.7\epsilon^{0.6}+\epsilon}$$

$$\epsilon = 11.5E_{nr}(\text{keV})Z^{-7/3}$$

$Z = \text{atomic number}$

Aside: Energy

The total energy (phonon) is given by

$$E_{tot} = E_r + eV_b N_Q$$

[keV_{nr}]
total phonon energy Neganov-Luke Phonons

- Assuming that an event is an ER and that the detector bias voltage is 3V, the recoil energy in [keV_{ee}] can be expressed as

$$\begin{aligned}
 E_r &= E_{tot} - eV_b N_Q \\
 &= E_{tot} - eV_b \frac{E_Q}{\epsilon} \\
 &= E_{tot} - E_Q
 \end{aligned}$$

ϵ_{Ge} = 3.0 eV

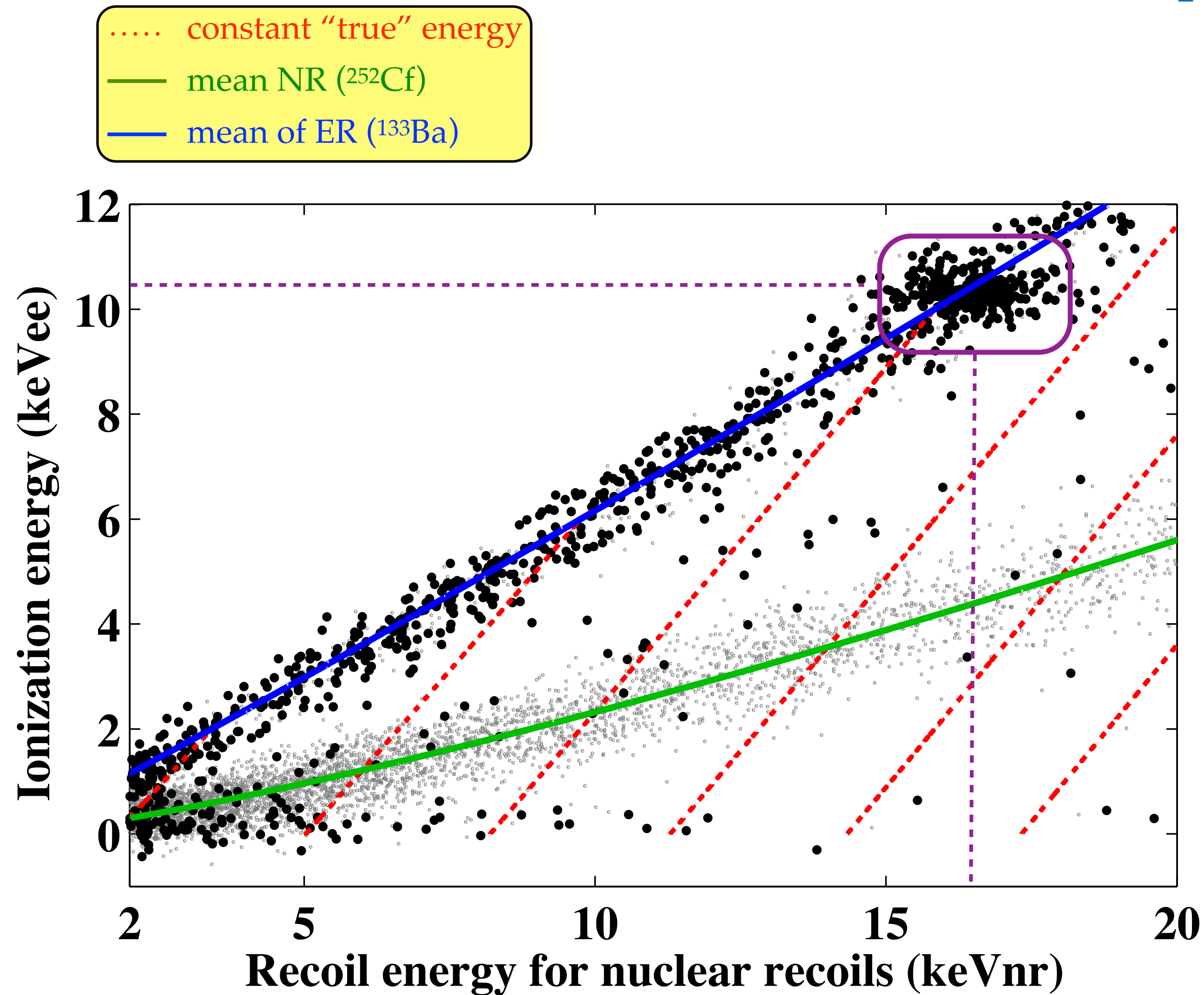
- Assuming that an event is a NR, a smaller correction for the Luke phonons is applied. The mean ionization energy for nuclear recoils ($\mu_{Q,nr}(p_t)$) is determined using calibration data from a 252Cf source.

$$E_r(p_t) = p_t - \mu_{Q,NR}(p_t)$$

[keV_{nr}] total phonon energy - Luke energy

where $\mu_{Q,NR} = AE_r^B$

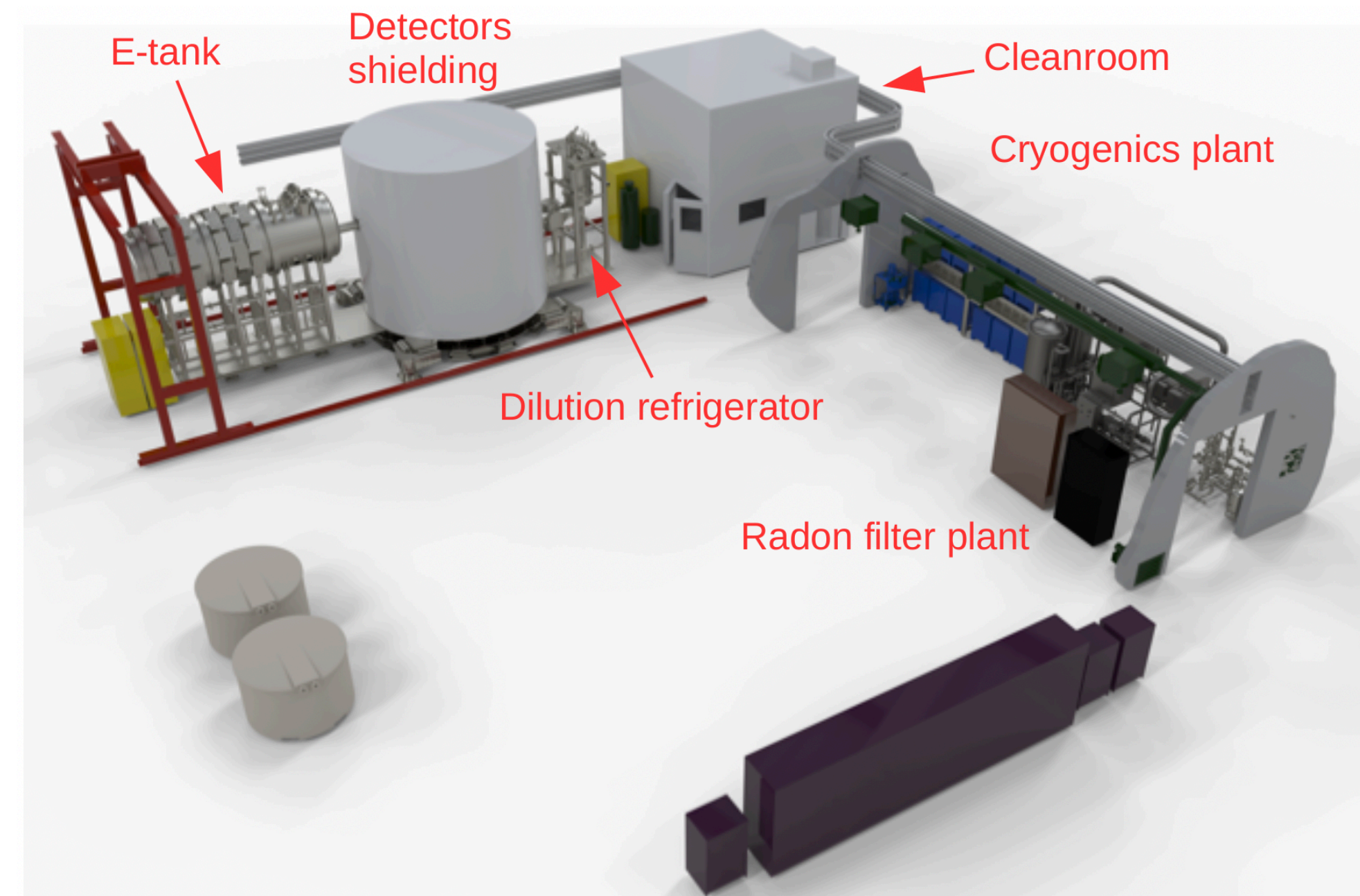
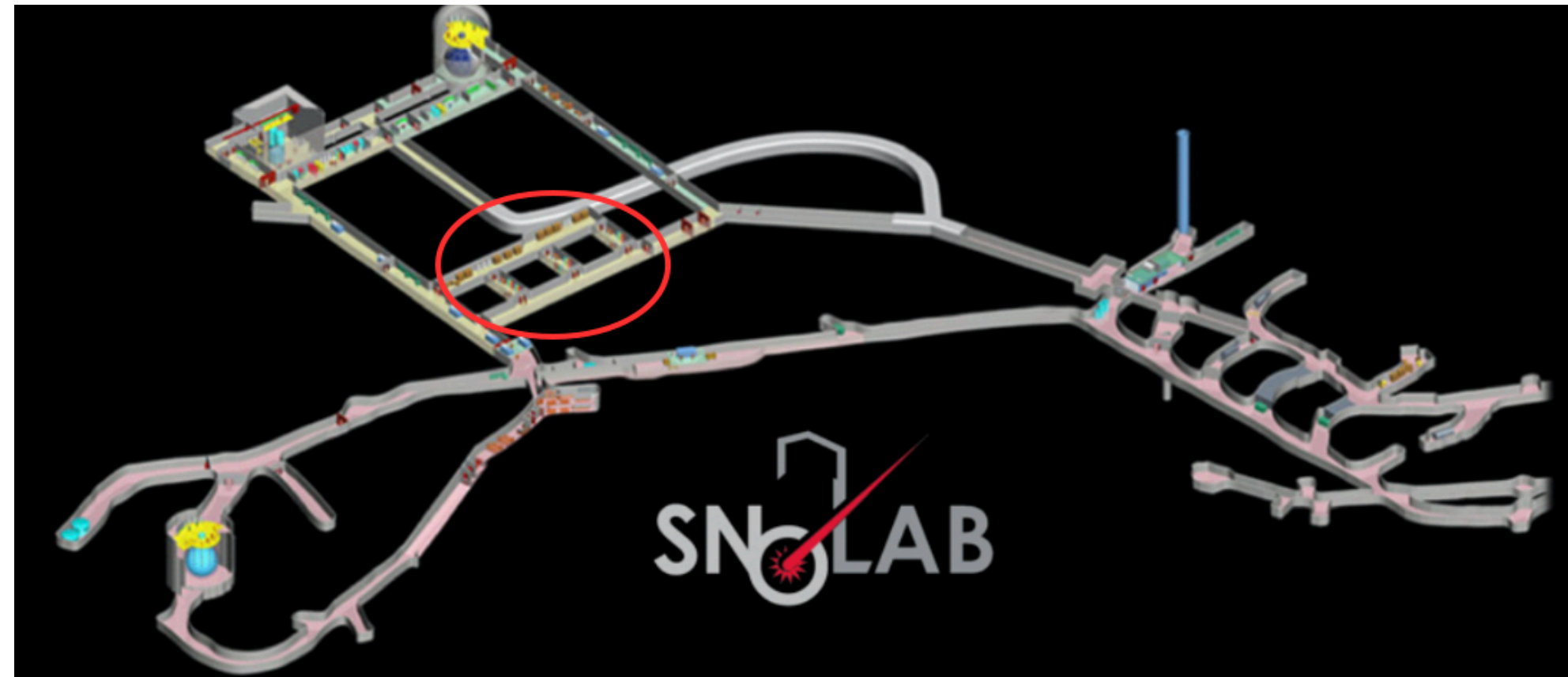
KeV_{ee} vs KeV_{nr}



- ▶ Ionization energy vs recoil energy assuming NR scale consistent with Luke phonon contributions for NR.
- ▶ ER recoils are pushed to higher energies using the NR scale.
- ▶ Example - 10.4 keV_{ee} ER line appears at ~16 keV_{nr}

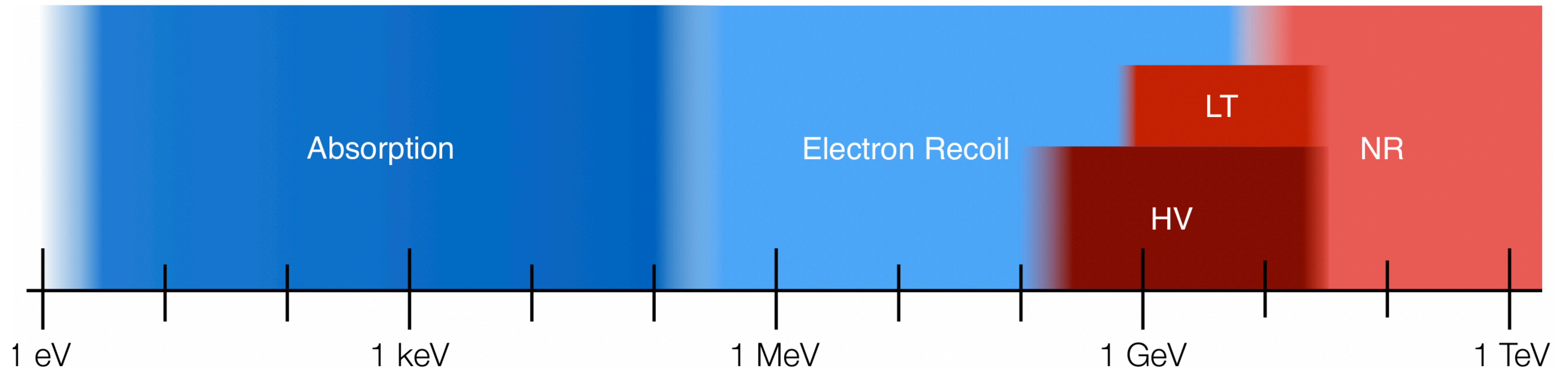
*A good reference is David Moore's thesis, Chapters 3 and 4
<http://thesis.library.caltech.edu/7043/>

SuperCDMS SNOLAB



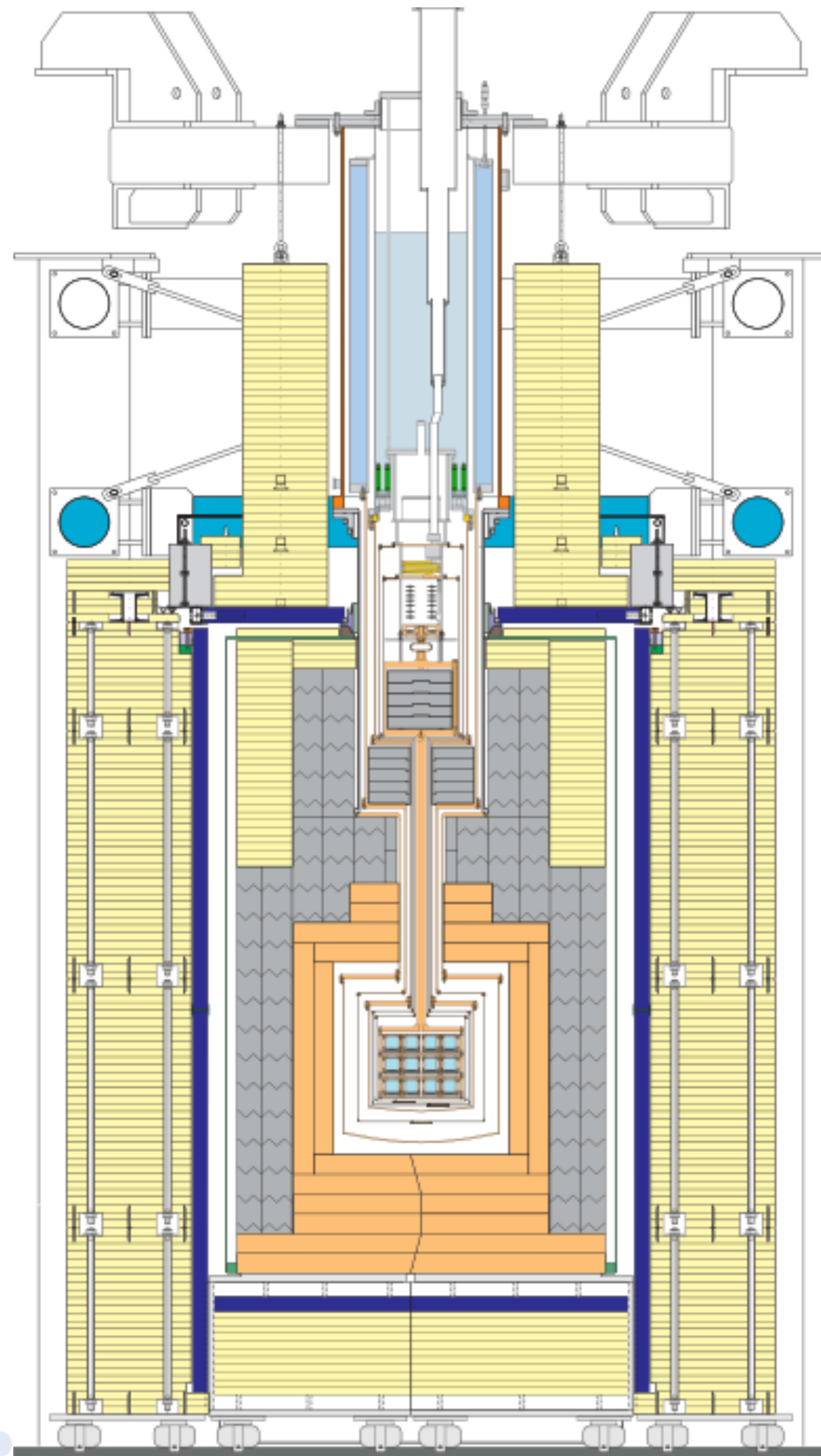
- Generation-2 dark matter experiment under construction at SNOLAB
- Infrastructure:
 - depth ~ 6900 mwe (results in a factor 100 reduction in muon flux from cosmic rays as compared to Soudan)
 - class 2000 or better cleanroom
 - Cryostat will be able to accommodate up to 7 towers
 - (0.1) dru gamma background
 - 15 mK base temperature
 - vibration isolation
- Initial payload: ~ 30 kg total, 4 towers with 6 detectors per tower (12 iZIP, 12 HV)

SuperCDMS Dark Matter Sensitivity

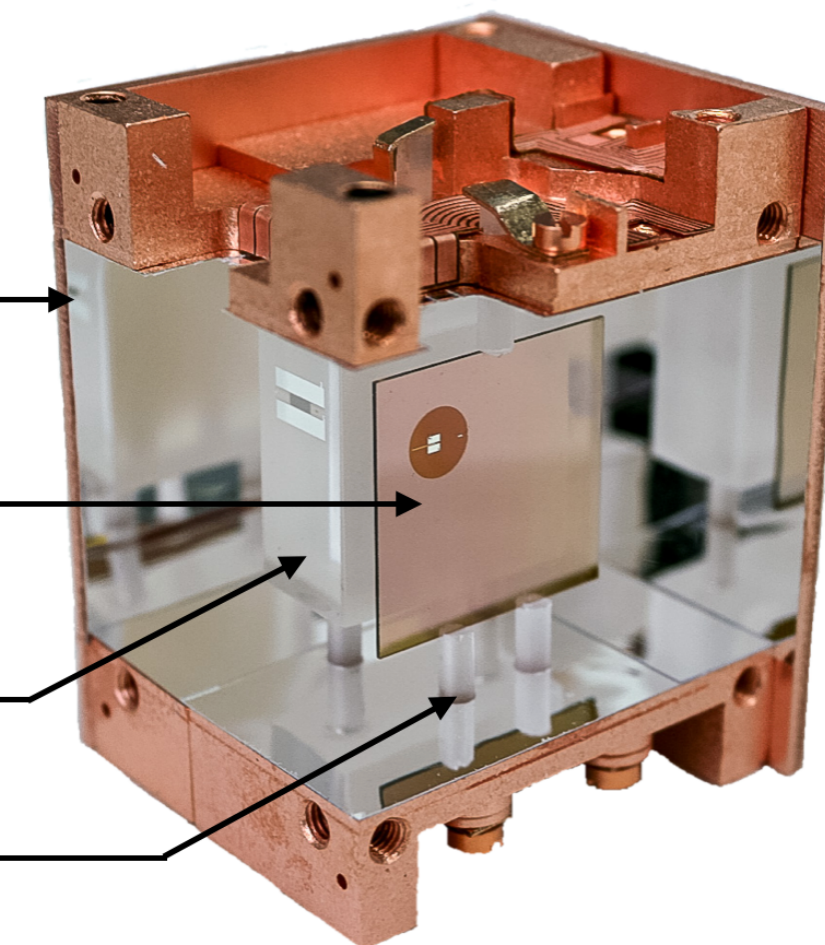
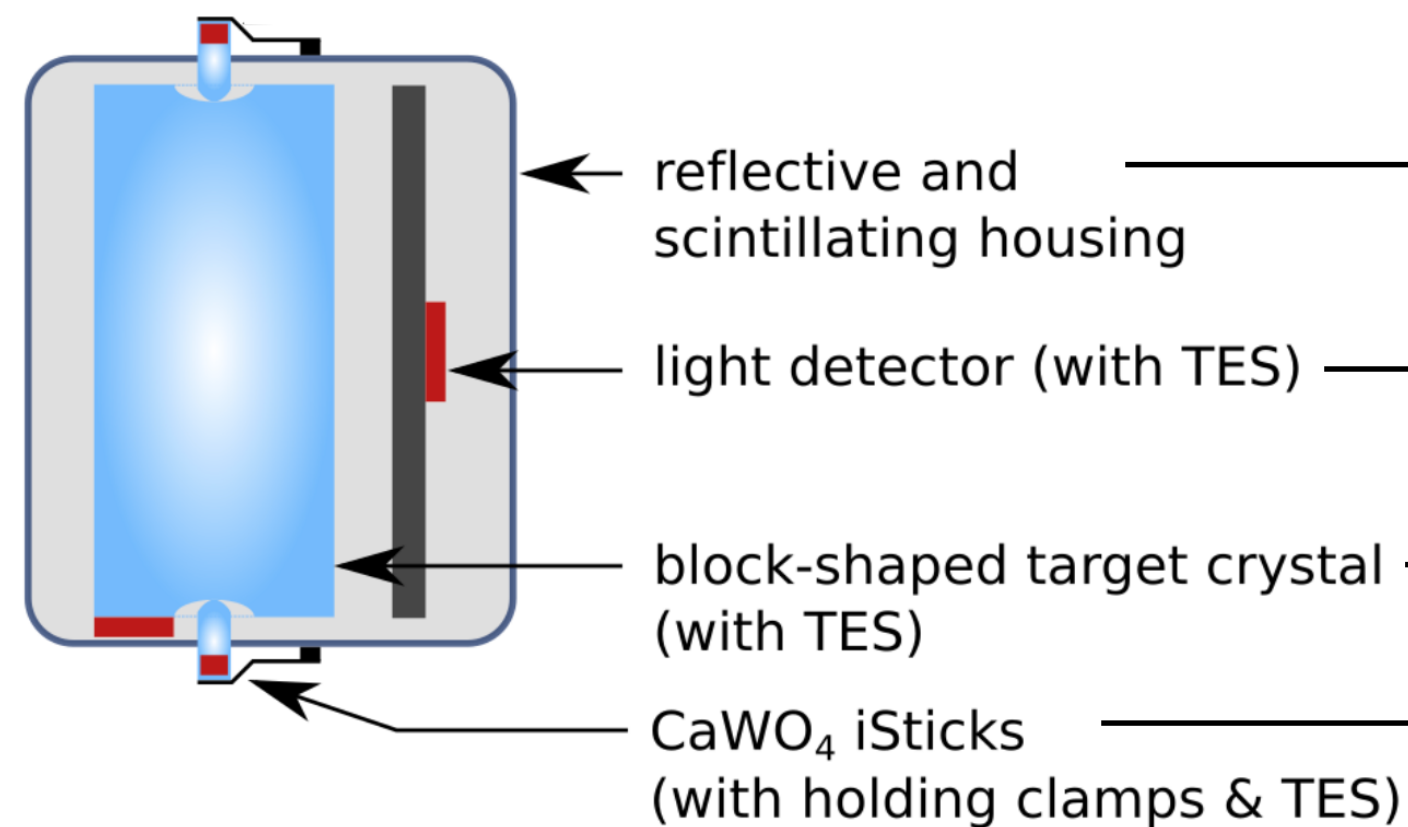
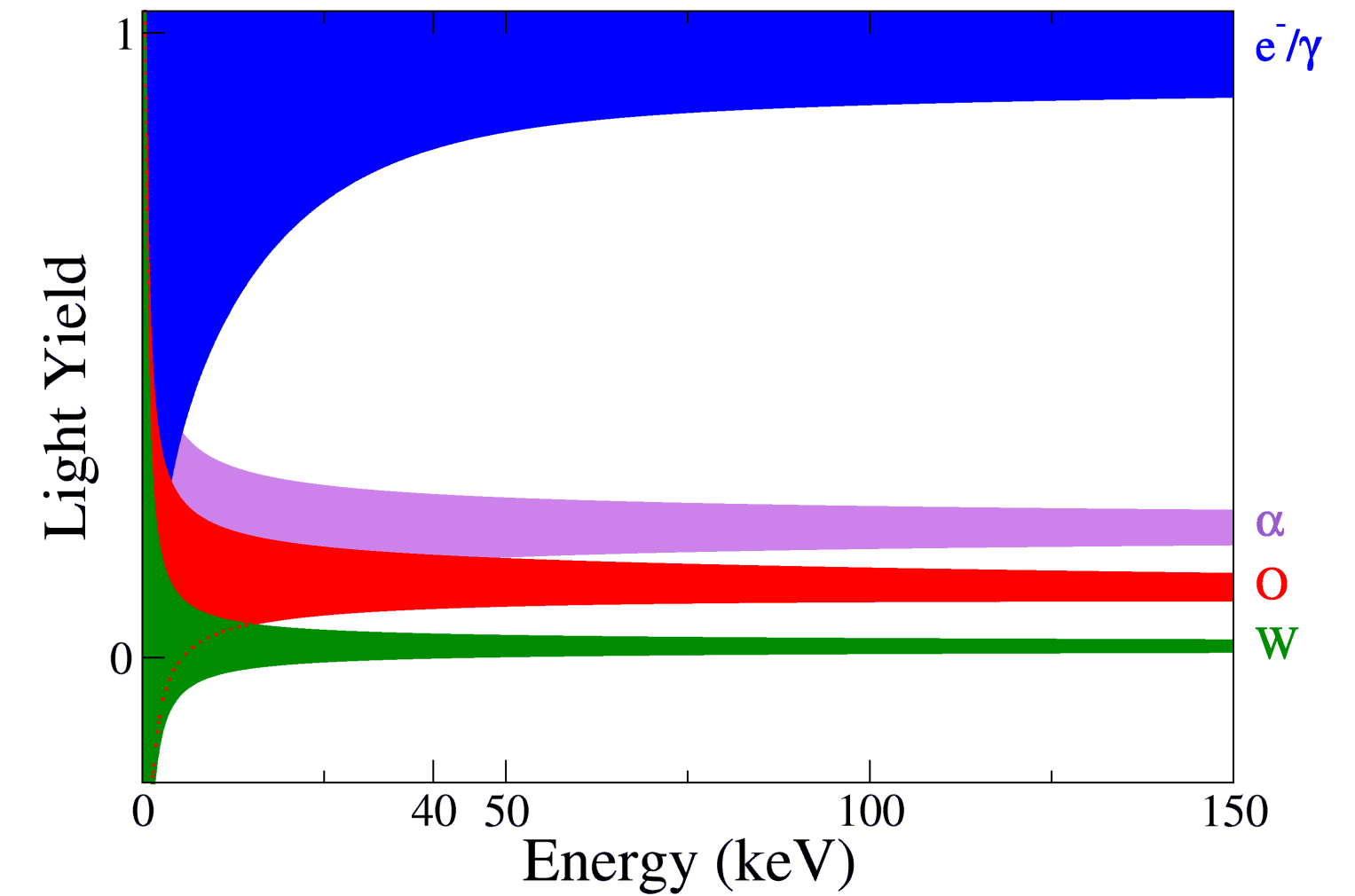


| | | |
|--|------------------------------|-------------------------------|
| Traditional NR: | iZIP, Background free | >5 GeV |
| Low Threshold NR: | iZIP, limited discrimination | >1 GeV |
| HV Mode: | HV, no discrimination | ~0.3 - 10 GeV |
| Electron Recoil: | HV, no discrimination | ~0.5 MeV - 10 GeV |
| Absorption (Dark Photons, ALPs) | HV, no discrimination | ~1 eV - 500 keV (peak search) |

CRESST Experiment Operation Principles

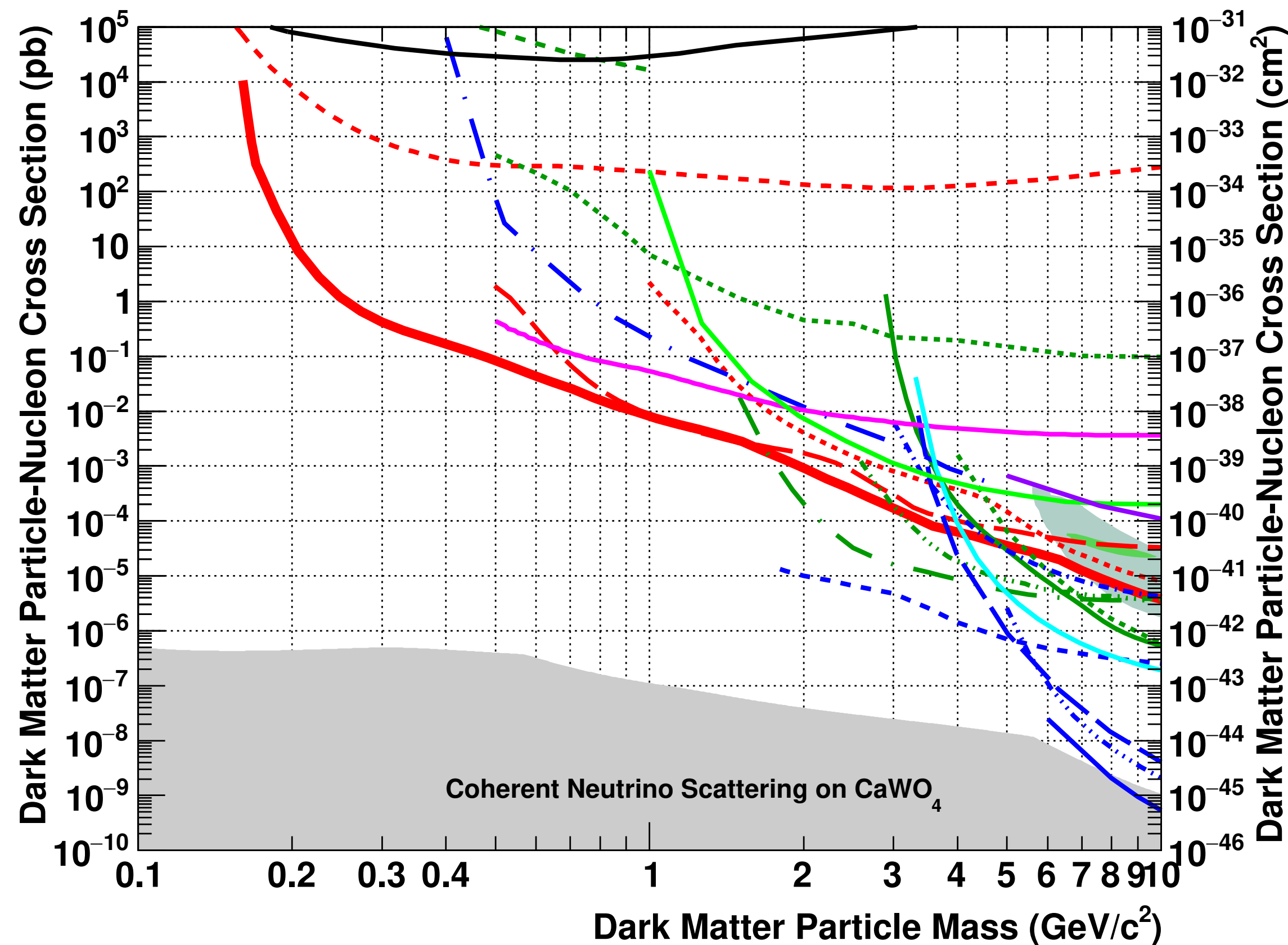
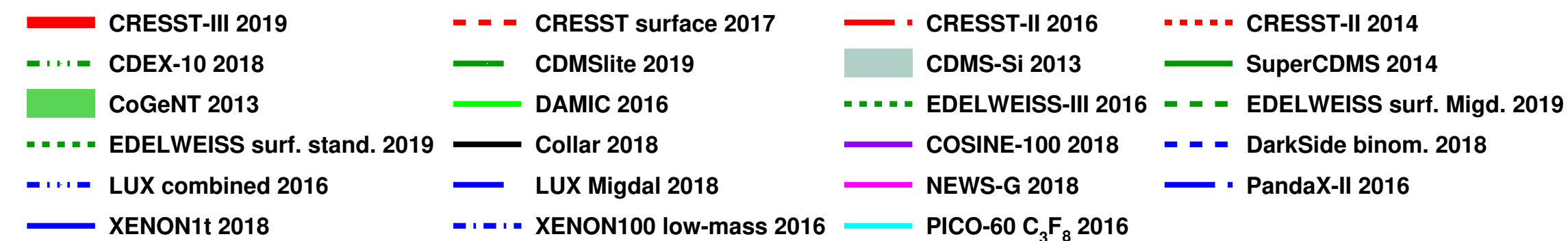


- Search of light DM direct interactions with CaWO_4 cryogenic detectors
- Operating temperature ~ 15 mK
- Second cryogenic detector to collect emitted scintillation light: particle identification
- Single detector mass ~ 24 g
- Energy Threshold: 30 eV

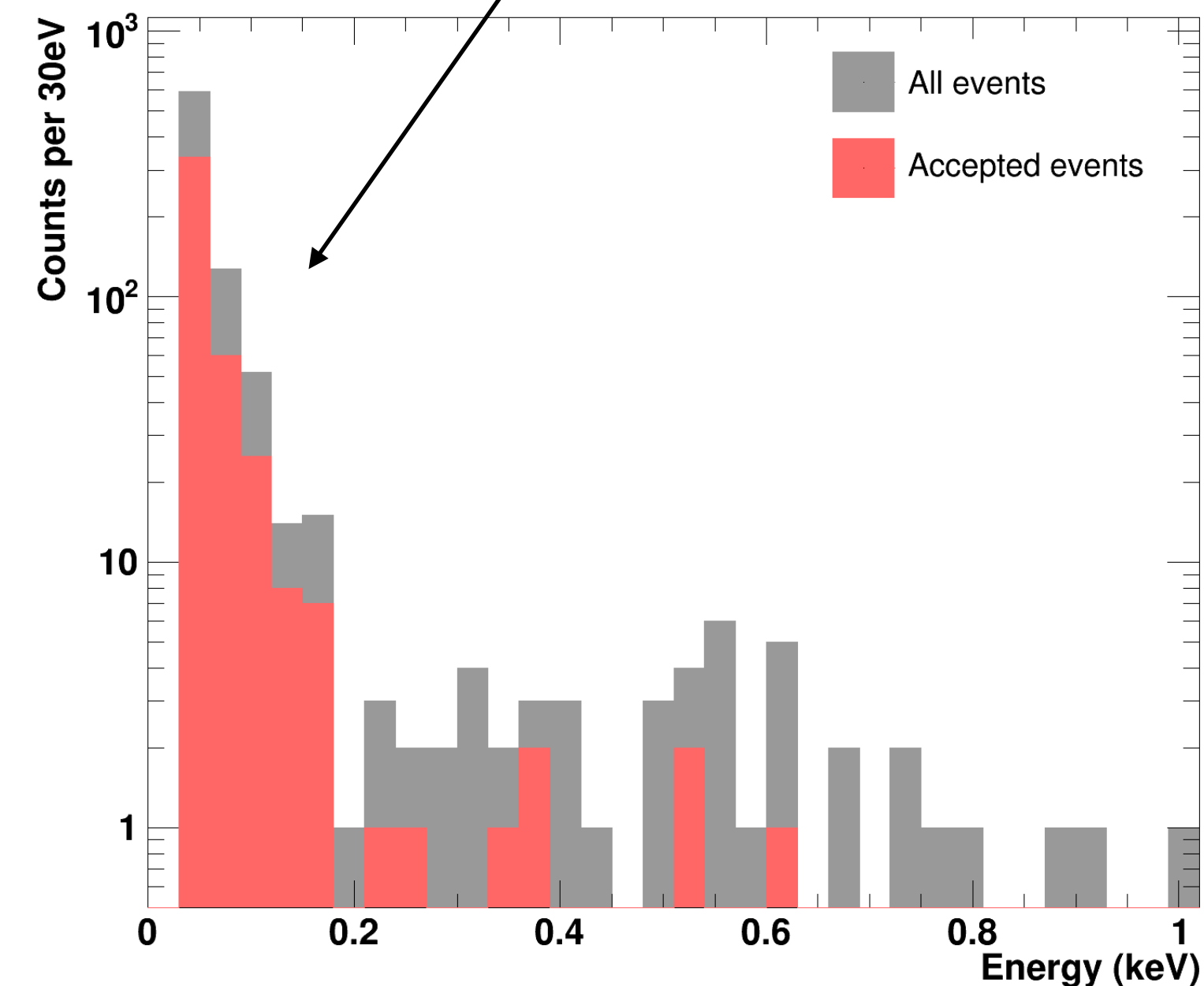




Limitations: CRESST-III Recent Results



- More than one order of magnitude improvement at $0.5 \text{ GeV}/c^2$
- Extended reach from $0.5 \text{ GeV}/c^2$ to $0.16 \text{ GeV}/c^2$
- Sensitivity limited by unknown background below 200 eV



CRESST Future Plans

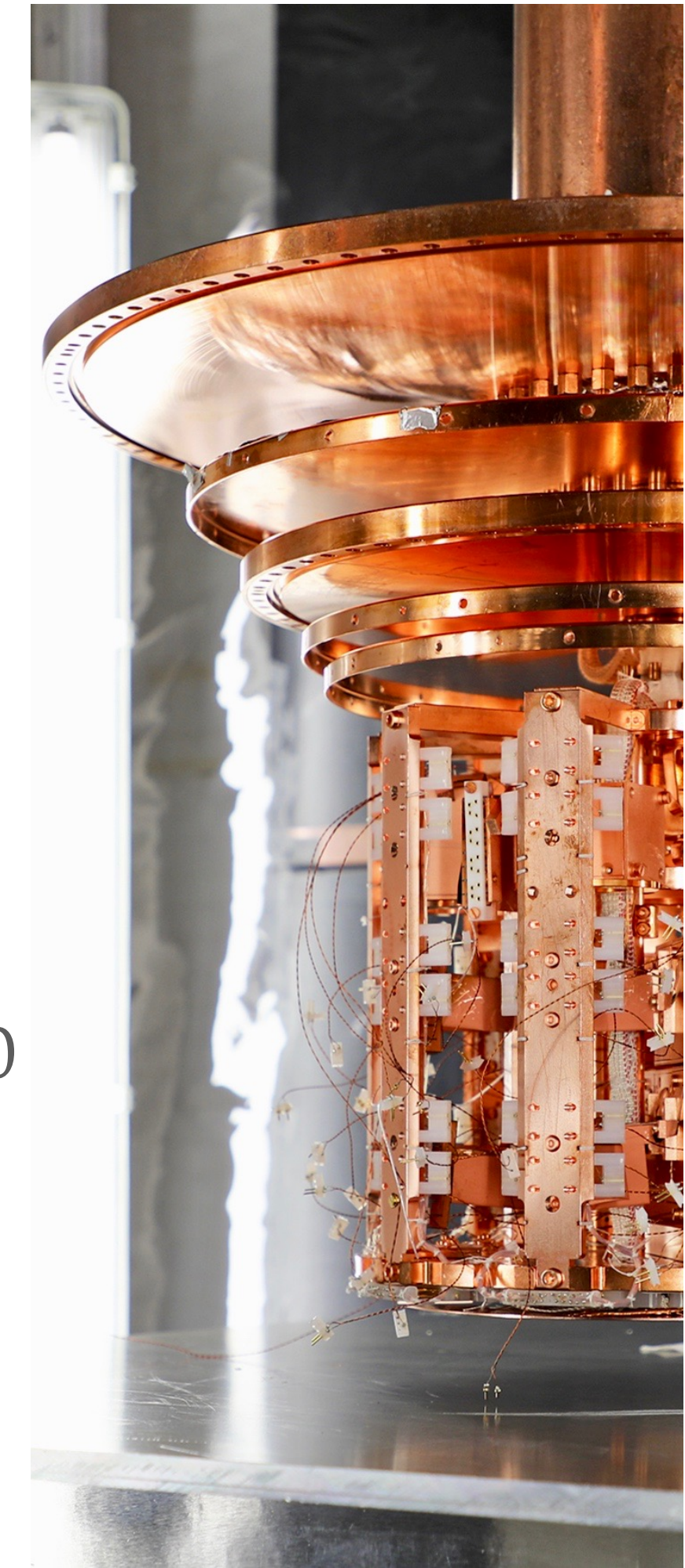


CRESST Upgrade

- Upgrade to 288 readout channels to accommodate 100 modules for O(2 kg) target mass
- Final planning, prototyping and testing of SQUID read-out electronics, biasing system and DAQ
- Sensor development to further push detector threshold (10 eV)
- Complementary detector materials (LiAlO₂,) which also yield sensitivity for spin-dependent interactions

Run3 2020 - 2021

- 2nd round with additional modifications.
- Successful cool-down in 03/2020, but stopped due to Corona virus pandemic
- Cool-down started July 20, 2020
- Detetor commissioning Aug - Oct 2020
- November 2020 - August 2021 science data!
- Following science run, dedicated neutron calibration runs to study low energy event excess.

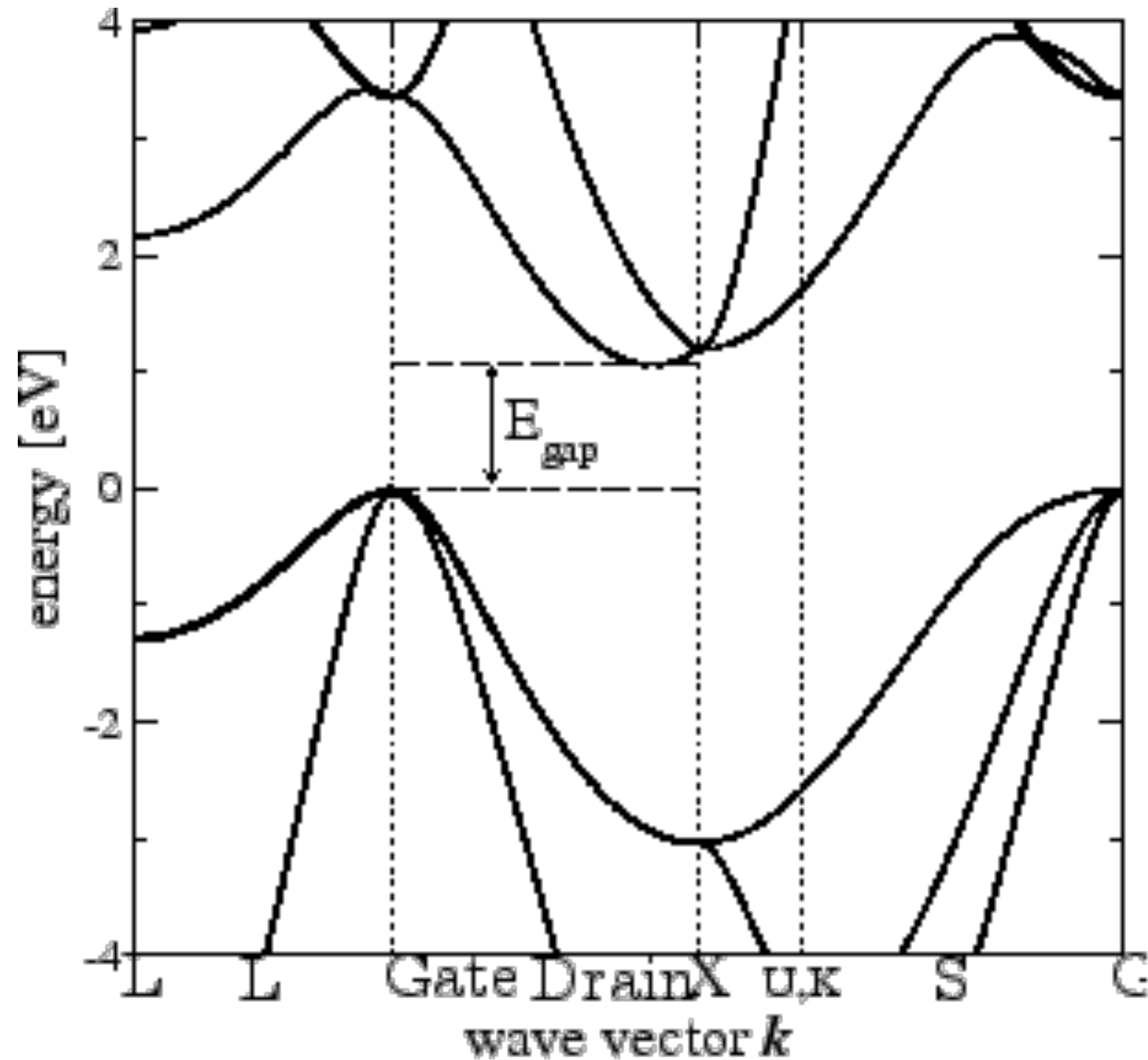


Single e^-/h^+ Pair Sensitivity



Energy Scale in Semiconductors

Band Diagram for Si



- ▶ e- excitation momentum and energy scales in semiconductors can be exploited to search for light mass dark matter
- ▶ Si $E_{\text{gap}} \sim 1.2$ eV
 - ▶ Indirect band gap requires phonon for transition to happen.
 - ▶ Temperature dependent
- ▶ $\epsilon_{\text{Si}} \sim 3.6$ eV
 - ▶ Average energy to produce e/h pair
 - ▶ Temperature dependent
- ▶ Sensitive to energy deposits of $\mathcal{O}(\text{eV})$ (electron scattering) to $\mathcal{O}(10 \text{ eV})$ (nuclear scattering)

Realm of Solid State Physics



Solid state physics

$E < 30 \text{ eV}$

Multi-body system

Allowed energies/momenta given
by dispersion relation

Particles may have effective
masses

Particle physics

$E > \text{keV}$

Free particles

$E = p^2/2m$

Particle masses well defined

Challenges

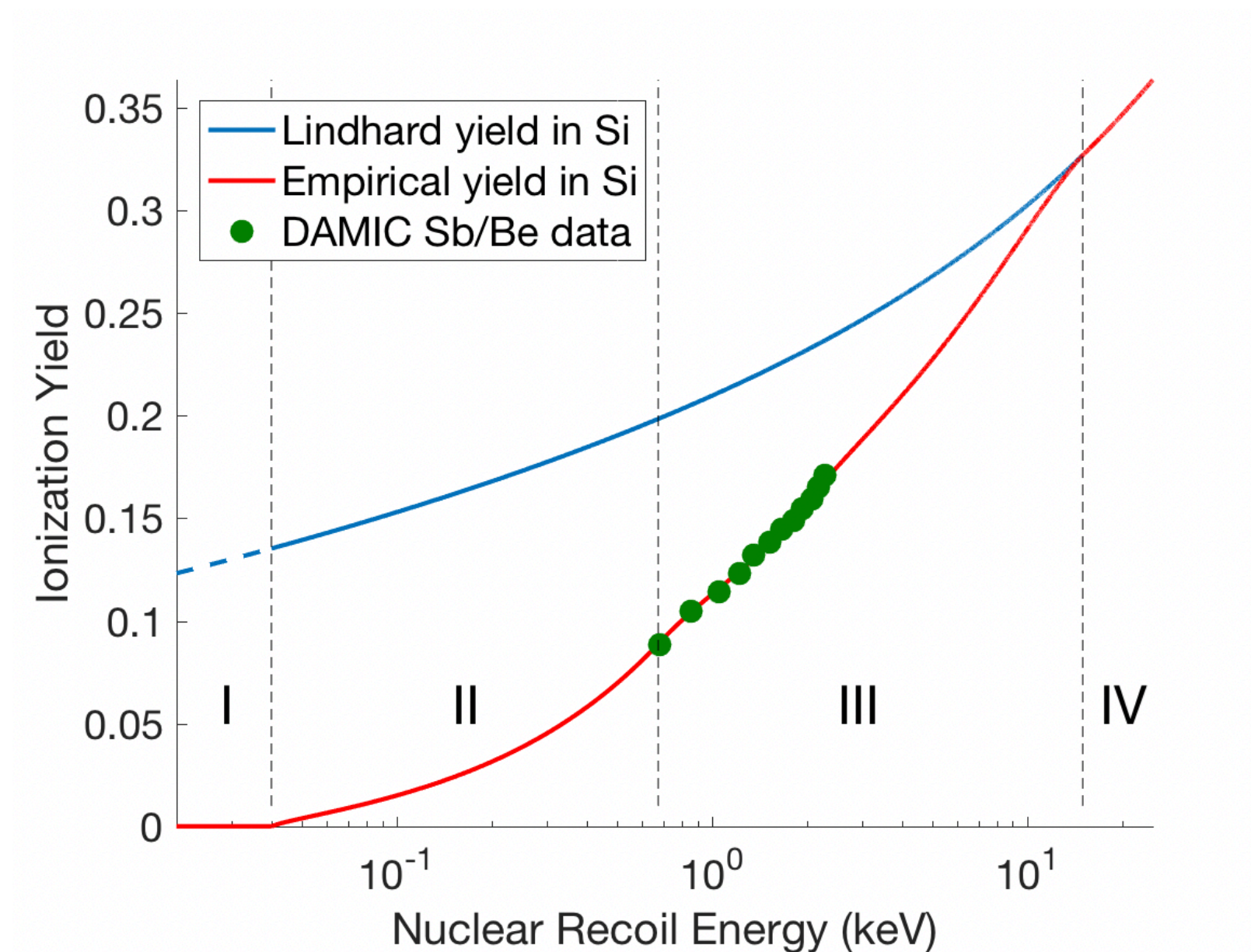


- **Detector Response**
 - Details of the band structure become increasingly important

Challenges

► Detector Response

- Details of the band structure become increasingly important
- PDF to get the numbers of e/h pairs given an energy deposition required, $P(n_{eh} | E_{dep})$
 - Fano statistics (dispersion probabilities)
 - For NR: quenching (ionization yield < 1)



Challenges

► Detector Response

- Details of the band structure become increasingly important
- PDF to get the numbers of e/h pairs given an energy deposition required, $P(n_{eh} | E_{dep})$
 - Fano statistics (dispersion probabilities)
 - For NR: quenching (ionization yield < 1)
- Crystal impurities can lead to partial energy deposits —> gives events between quantization peaks

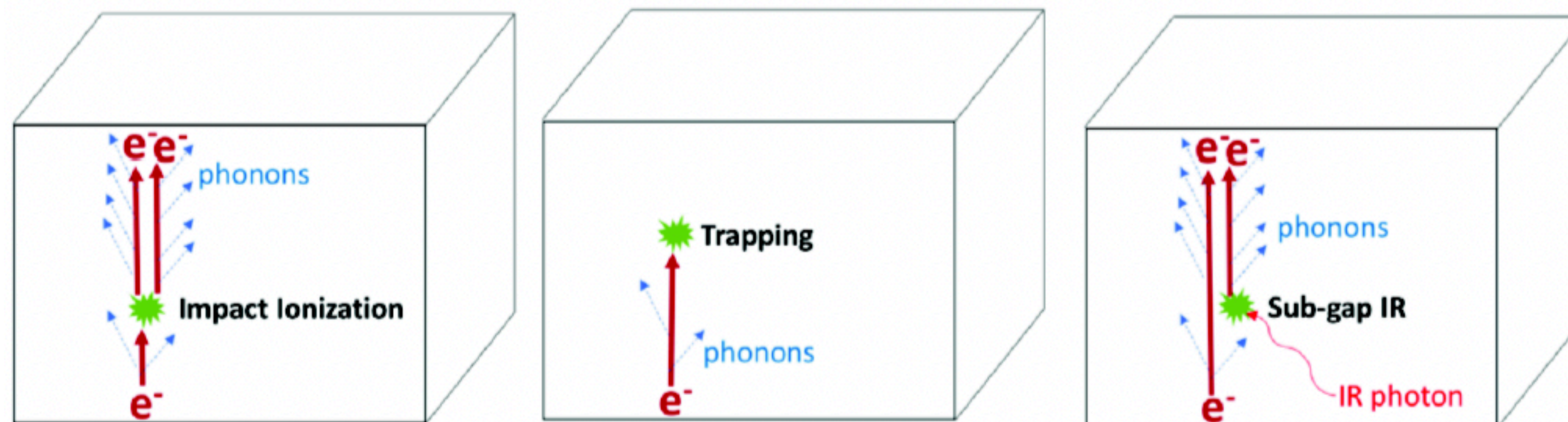


Figure: R.K. Romani

Challenges



➤ Detector Response

- Details of the band structure become increasingly important
- PDF to get the numbers of e/h pairs given an energy deposition required, $P(n_{eh} | E_{dep})$
 - Fano statistics (dispersion probabilities)
 - For NR: quenching (ionization yield < 1)
- Crystal impurities can lead to partial energy deposits —> gives events between quantization peaks

➤ Backgrounds

- Spectral information about radioactive decays at eV scale required.

Challenges



➤ Detector Response

- Details of the band structure become increasingly important
- PDF to get the numbers of e/h pairs given an energy deposition required, $P(n_{eh} | E_{dep})$
 - Fano statistics (dispersion probabilities)
 - For NR: quenching (ionization yield < 1)
- Crystal impurities can lead to partial energy deposits —> gives events between quantization peaks

➤ Backgrounds

- Spectral information about radioactive decays at eV scale required.
 - Relevance is exposure dependent
- IR and optical photons become significant backgrounds at lowest energies.

Challenges



➤ Detector Response

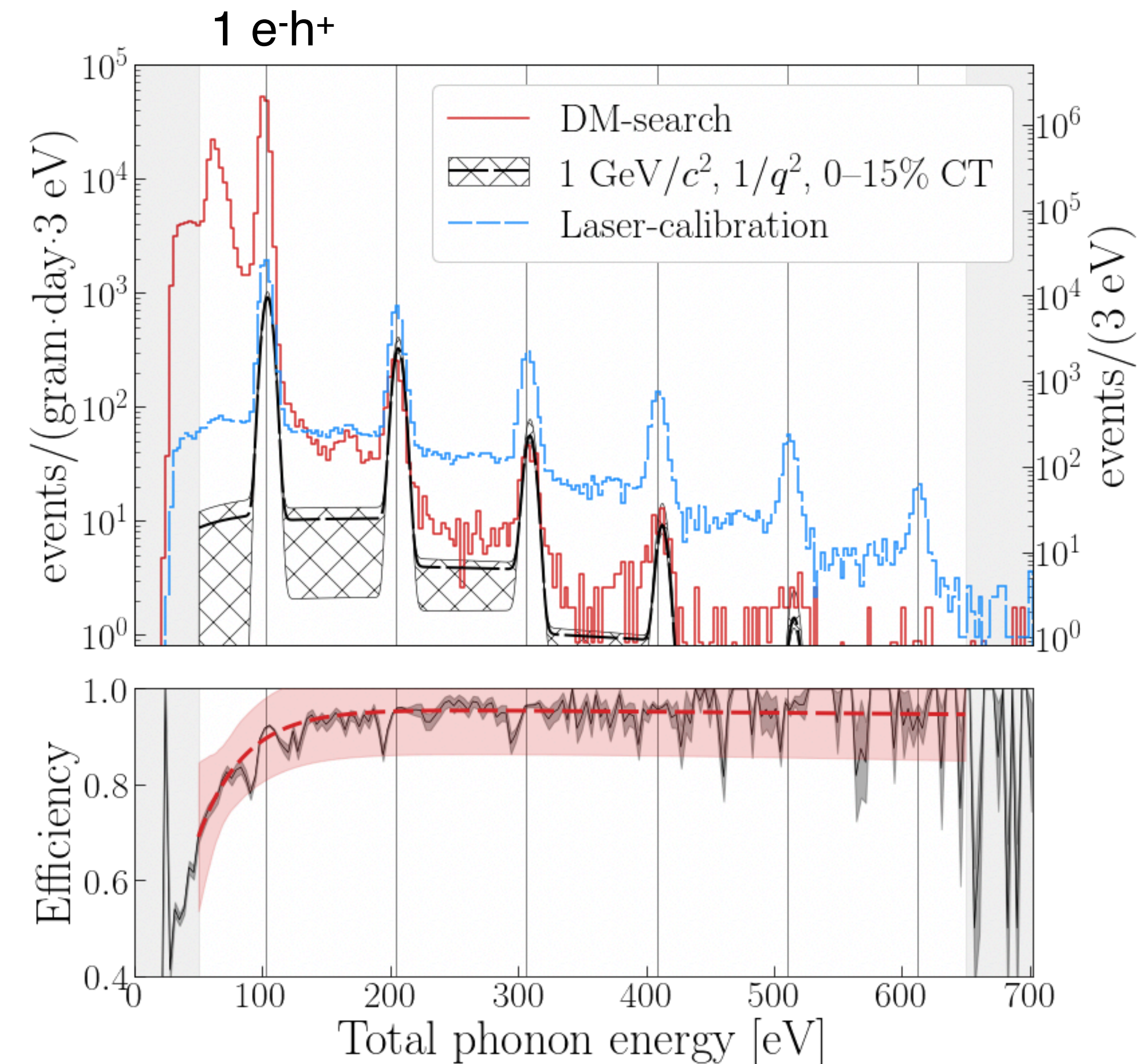
- Details of the band structure become increasingly important
- PDF to get the numbers of e/h pairs given an energy deposition required, $P(n_{eh} | E_{dep})$
 - Fano statistics (dispersion probabilities)
 - For NR: quenching (ionization yield < 1)
- Crystal impurities can lead to partial energy deposits —> gives events between quantization peaks

➤ Backgrounds

- Spectral information about radioactive decays at eV scale required.
 - Relevance is exposure dependent
- IR and optical photons become significant backgrounds at lowest energies.
- Dark/leakage current can be significant, dominant background at lowest energies.

HVeV Detectors

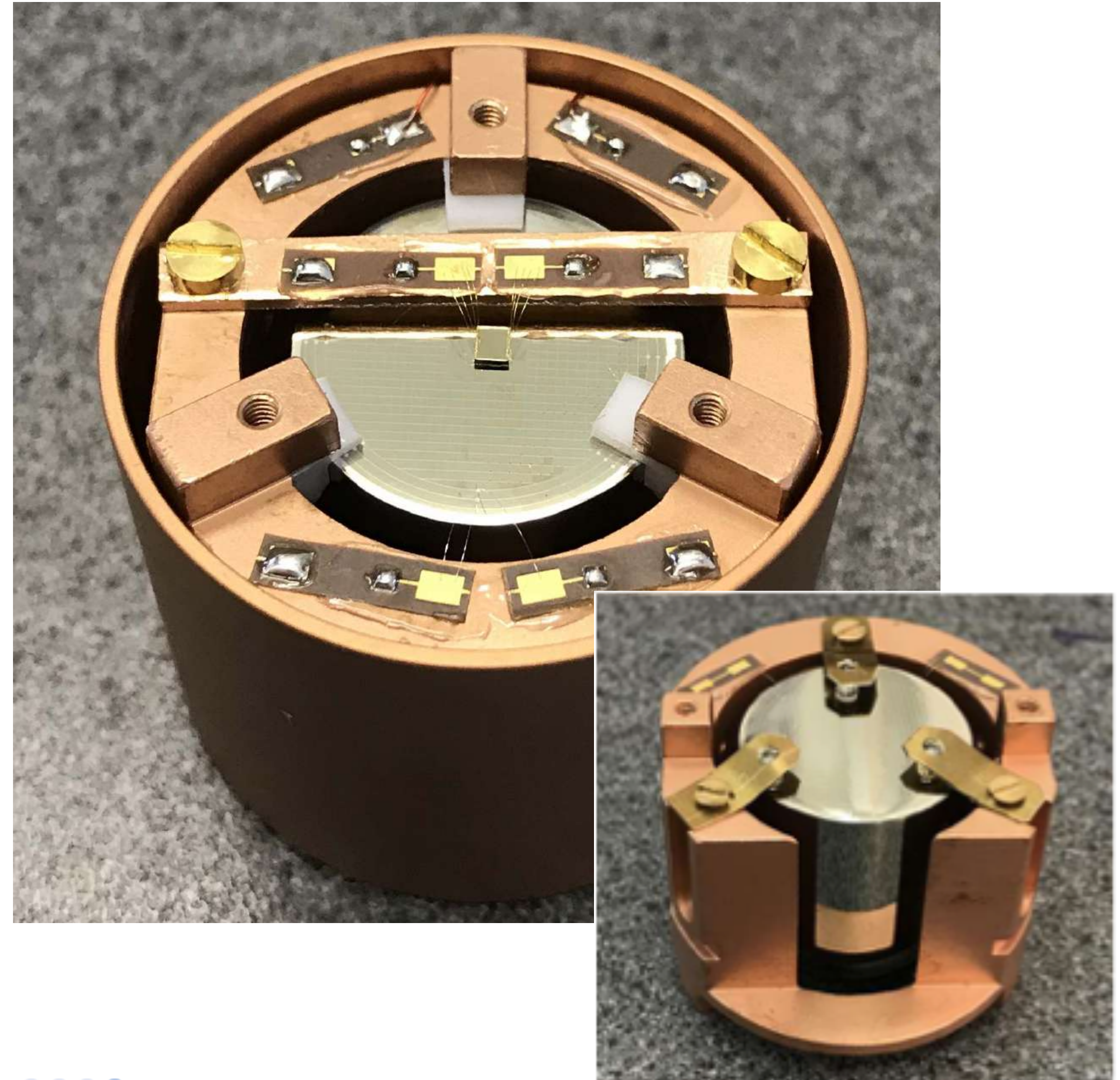
- Single-hole e/h-pair resolution devices will have sensitivity to a variety of sub-GeV DM models with $g \cdot d$ exposures
- 0.93 g Si crystal ($1 \times 1 \times 0.4 \text{ cm}^3$) operated at 50-52 mK at a surface test facility.
- Exposure: 3.0 gram-days (collected over 3 days)
 - operation voltage: 100 V
 - energy resolution: $\sigma_{\text{ph}} = 3 \text{ eV}$
 - charge resolution: $\sigma_{\text{eh}} = 0.03 \text{ e-h}^+$
- Calibrations with in-run monochromatic 635 nm laser fiber-coupled to room temperature.
- Data selection criteria were applied to remove leakage and surface events.



Edelweiss RED 30 Detector: HV Operation



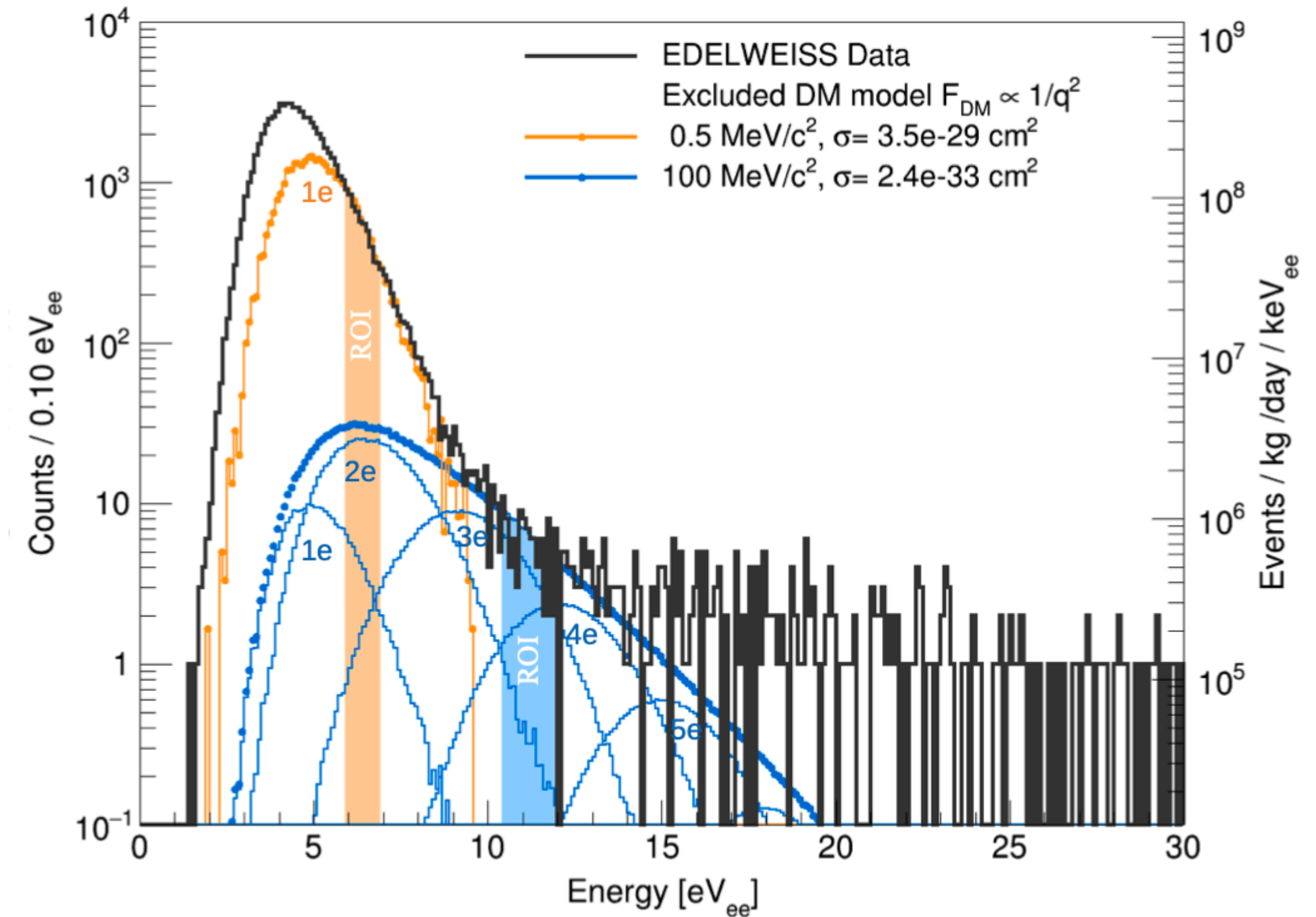
- 33.4 g (20 x 20 mm) Ge bolometer with NTD sensor and electrodes operated in LSM ($5 \mu\text{m}^2/\text{d}$)
- Exposure: 2.44 days
 - operation voltage: 78 V
 - energy resolution: $\sigma_{\text{ph}} = 44 \text{ eV}$ (1.6 eVee)
 - charge resolution: $\sigma_{\text{eh}} = 0.53 \text{ e-h}^+$
- Calibrations using ^{71}Ge KLM (0.16, 1,30 and 10.37 keV) activation lines from AmBe neutron source.
- Data selection criteria were applied to remove events occurring in the NTD (instead of the crystal).



Edelweiss RED 30 Detector: HV Operation



- Heat only events (those not affected by NTL amplification) are the main source of backgrounds.
 - 10^6 DRU @ 10 eV_{ee}
 - 1.5×10^5 DRU @ 25 eV_{ee}
- Dominant limitation for >3 e- signals
- May hypothesis have been studied as to the origin. No single contributor has been found
 - These events are probably multiple sources.



($dru = event/day/keV/kg$)

Conclusions - Dark Matter

- The next decade will be very exciting for dark matter direct detection. Various G2 Experiments will come online, covering a lot of new parameter space.
- Although WIMPs remain a very interesting dark matter candidate, other scenarios are gaining traction in the theoretical community, while new ideas for direct searches have been proposed and are gaining momentum.
- Given the wealth of theoretical possibilities, a diversity of experimental designs and targets will be needed to constrain the theory and couplings of any discovered signal.

